REGULATION OF DROSOPHILA MIDGUT DEVELOPMENT AND HOMEOSTASIS BY DIETARY LIPIDS

by
Rebecca A. Obniski

A thesis submitted to Johns Hopkins University in conformity with the requirements for the degree of Doctor of Philosophy

Baltimore, Maryland
August, 2018

ABSTRACT

Tissue homeostasis involves a complex balance of developmental signals and environmental cues that dictate stem cell function. The second chapter of this dissertation describes how dietary lipids control enteroendocrine cell production from *Drosophil*a posterior midgut stem cells. By modulating the diet of newly eclosed flies, I found that dietary cholesterol influences new intestinal cell differentiation in an *Hr96*-dependent manner by altering the level and duration of Notch signaling. Exogenous lipids modulate Delta ligand and Notch extracellular domain stability and alter their trafficking in endosomal vesicles. Lipid-modulated Notch signaling occurs in other nutrient-dependent tissues, suggesting that Delta trafficking in many cells is sensitive to cellular sterol levels. These diet-mediated alterations in young animals contribute to a metabolic program that persists after the diet changes. A low sterol diet also slows the proliferation of enteroendocrine tumors initiated by Notch pathway disruption.

In the third chapter I contrast the regions of the larval and adult midgut, and describe how the adult midgut progenitors divide during pupation to create the foundation for the adult midgut. I induced a lineage mark at varying times during development, and then observed the developed clones later to show that midgut development occurs in an anterior to posterior manner. I also present preliminary data that demonstrates a role for the nuclear receptor and nutrient sensor, HNF4, in midgut development. These results provide a foundation for future work analyzing the role of other nutrients in midgut development.

This is the first study to identify a specific dietary nutrient that can modify a key intercellular signaling pathway to shift stem cell differentiation and cause lasting changes in tissue structure and physiology. This work further identifies a developmental window when the midgut is especially susceptible to influences by dietary metabolites, and demonstrates a way to use this developmental window to study the influence of metabolites on cell signaling pathways. An understanding how diet affects these pathways will be a critical asset in developing disease treatments and understanding the implications of metabolic disorders.

Readers

Allan C. Spradling (Thesis Advisor)
Adjunct Professor, Johns Hopkins Department of Biology
Staff Member, The Carnegie Institution for Science

Xin Chen
Associate Professor, Johns Hopkins Department of Biology

ABBREVIATIONS

EC	Enterocyte
EB	Enteroblast
ee	Enteroendocrine cell
ISC	Intestinal stem cell
CD	control diet
LD	lipid depleted diet
1xC	1x cholesterol supplemented diet
4xC	4x cholesterol supplemented diet
A2	Anterior 2 midgut region
P1	Posterior 1 midgut region
P3	Posterior 3 midgut region

TABLE OF CONTENTS

LIST OF TABLES

LIST OF FIGURES

Chapter 1

Chapter 2

Chapter 3

ACKNOWLEDGMENTS

I would like to begin with sincere gratitude to my advisor, Allan Spradling, who has been a source of fathomless patience and guidance from the time I first rotated in the lab. I'm especially grateful for the experience of the past year, writing a paper together, and learning how data becomes a story, and finally a part of collective scientific knowledge. Allan's contagious passion for research is surpassed perhaps only by his passion and commitment to seeing his "people" (the post docs, students, and technicians who work in the lab) succeed, and I consider myself very fortunate to have worked with him. I would also like to thank my thesis committee, Xin Chen, Joe Gall, and Chen-Ming Fan for their helpful suggestions and discussions through every step of my graduate career.

This project would not have developed the way it did without the advice and support of Matt Sieber. With Matt, no detail was too small, nor question too broad that he wouldn't stop everything to help you find the answer. Few people are as generous with their time and talents, and I'm grateful for all I've learned from him.

I've benefited tremendously from all of my labmates, but in particular want to thank my rotation mentor, JJ Sun, and my "roommates", Vicki Losick, Ming-Chia Lee, and Alexis Marianes. Vicki always challenged me to think about how every experiment fits into a larger story, and gave me the opportunity to teach a lab course with her at the NIH. Ming-Chia and Vicki both reminded me, during the unavoidable times of scientific

frustration, that there was life outside, and after, graduate school. Alexis performed the research that is the groundwork for this thesis, and gave me invaluable technical training when I first started working with the *Drosophila* intestine. I'd also like to thank Ethan Greenblatt for enriching the lab with his insights and persistent optimism.

The support of the Spradling lab exists beyond the walls of Carnegie, as I experienced at every Fly Meeting that I attended, and with every alumnus that I met. I am grateful again to Allan for building this community, and welcoming me as a part of it.

I received tremendous technical support at The Carnegie from Allison Pinder with RNA sequencing, Mike Sepanski for beautiful electron microscopy, and Mahmud Siddiqi and Zehra Nizami for confocal microscopy training. I also have to thank Dianne Williams, who keeps the lab, and me, running.

Lastly, I'd like to thank the friends and family who have given me endless encouragement, especially Andrea Lin, and William Supik.

CHAPTER 1

INTRODUCTION

Tissue homeostasis relies upon integrating environmental cues with an intrinsic genetic program. Nowhere is this more apparent than the organs of the digestive tract which integrate signals from the diet with complex stem cell regulation. The diversity of dietary nutrients and the varied requirements for them demand that the digestive tract process an array of molecules from ingested food including vitamins, minerals, sugars, proteins, and lipids. A diet with each of these nutrients in balance with the others is essential for optimal organismal function, but in the wild organisms rarely experience the optimal nutrient environment.

Nutrient imbalance, either from imposed environmental scarcity, or a consequence of behavior, can strongly influence cell signaling and gene expression which not only impacts development, but also disease susceptibility. Examples linking diet and pathology include the effect of caloric intake on longevity (Templeman and Murphy, 2017), ingestion of a high fat diet on colon cancer incidence and progression (O'Neill et al., 2016), and the anticonvulsant protection provided by a ketogenic diet in children with epilepsy (Millichap et al., 1964). Despite these many observations, the mechanisms by which diet exerts unprogrammed effects on tissues have been difficult to identify.

At the cellular level, however, researchers have identified ways intracellular and membrane lipids affect cell signaling, including the effect of phospholipid membrane composition on EGF and Notch signaling (Weber et al., 2003), and cholesterol-dependent membrane organization by lipid rafts (Lingwood and Simons, 2010). Furthermore, the mechanisms of lipid metabolism and catabolism are themselves modulated by intracellular lipid levels. While lipids could affect development through a previously unidentified mechanism, it is likely that biology has repurposed one of these strategies.

Cholesterol Metabolism

Cholesterol is essential for the structural and physiological integrity of all metazoan tissues. Cholesterol in subcellular and surface membranes can modulate the function of membrane proteins and impact membrane trafficking and transmembrane signaling (Egawa et al., 2015). Equally important, free cholesterol can be added to signaling molecules such as *Hedgehog* (Porter et al., 1996) or act as precursors to signal transducers such as bile acids and steroid hormones (van der Wulp et al., 2013).

Many tissues, such as the mammalian central nervous system, lack the ability to absorb circulating cholesterol from the blood stream, and must instead synthesize it *de novo*. Cholesterol synthesis occurs in the endoplasmic reticulum, and is highly dependent on the rate-limiting enzyme, 3-hydroxy-3-methylglutaryl (HMG) CoA reductase (HMGR; Vallett et al., 1996). The signaling and structural implications of cholesterol levels demand that its production be highly regulated. Interestingly, membrane HMGR is able to sense cholesterol levels in ER membranes. High membrane cholesterol triggers structural changes in the protein that allow binding by the ER membrane protein Insig-1. This complex is subsequently ubiquitinated and then degreaded by the proteasome (Gil et al., 1985; Ravid et al., 2000). This ubiquitination is mediated by the E3 ubiquitin ligase, gp78 (Song et al., 2005; Lee et al., 2006), which ubiquitinates Insig-1 instead of HMGR when sterol levels are low (Gong et al., 2006) thus providing multistep regulation of protein stability by cholesterol.

The transcription of HMGR is also tightly regulated by cholesterol. The transcription factor sterol response element binding protein (SREBP) was so named for its binding to sterol response elements (SRE) of the genome that are upstream of

cholesterol synthesis and uptake proteins such as HMGR and cholesterol transport proteins (Wang et al., 1994). When cholesterol levels are high, SREBP is held in the ER following its translation into the membrane (Hua et al., 1996). As cholesterol levels decrease, proteins that hold SREBP in the ER dissociate allowing it to be transported to the Golgi where it is cleaved, releasing a cytoplasmic DNA binding domain (DeBose-Boyd et al., 1999). This subunit can translocate to the nucleus and initiate changes in gene expression to increase cholesterol levels (Wang et al., 1994). In mammals, *SREBP-1c* regulates fatty acid and triacyl glyceride metabolism (Bennett et al., 1995; Briggs et al., 1993), while *SREBP2* induces cholesterol synthesis (Vallett et al., 1996). *Drosophila* have only one SREBP which is essential for fatty acid metabolism and TAG storage (Kunte et al., 2006). The role of SREBP in cholesterol metabolism has been speculated (Sieber and Thummel, 2012) but not been fully studied.

The mechanisms that control cholesterol synthesis illustrate two ways proteins with sterol sensing domains may be regulated by membrane cholesterol. In both cases, cholesterol sensing domains initiate changes in protein structure. In the first example with HMGR, cholesterol enables targeting by ubiquitin ligases allowing degradation by the proteasome. In contrast, SREBP undergoes structural changes that enable it to undergo vesicular protein transport leading to modifications/cleavage by organelle specific enzymes and proteases.

Lipid Mediated ERAD

To complete HMGR degradation, cells utilize a conserved protein quality control processes termed endoplasmic reticulum-associated protein degradation (ERAD)

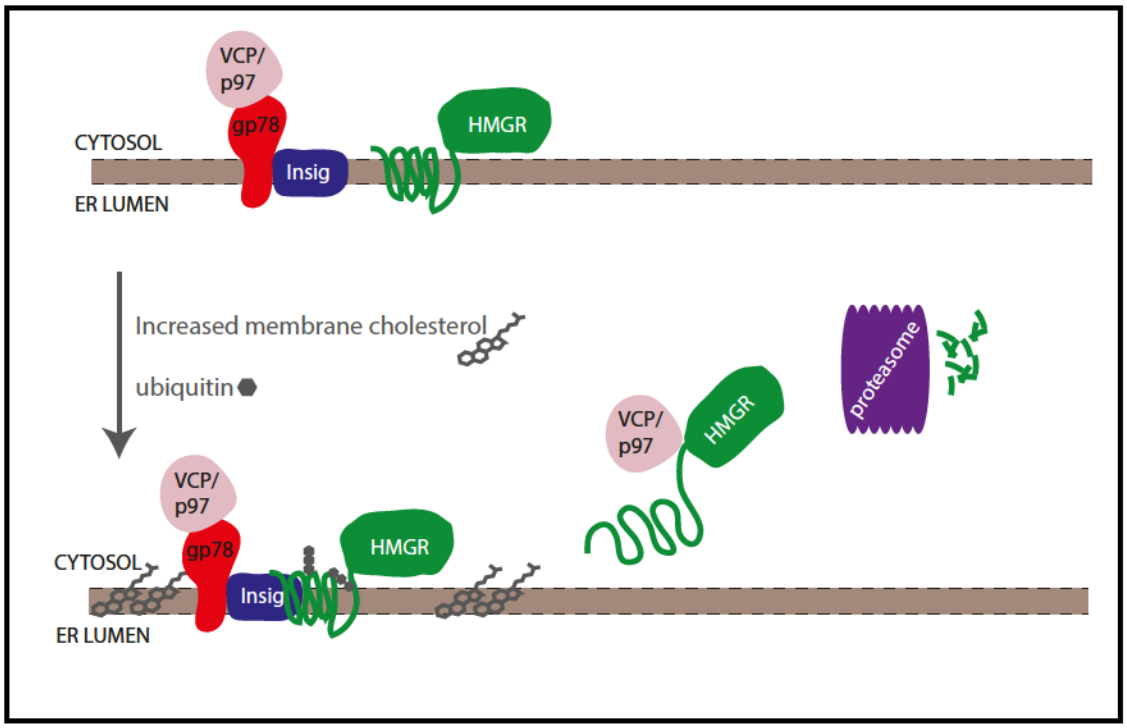

Figure 1. Modeling lipid-mediated ERAD. This cartoon summarizes the content of the section "Lipid Mediated ERAD". The top of the image shows HMGR (green) separate from its binding partner Insig-1 (blue). As membrane cholesterol increases (arrow) HMGR and Insig-1 bind. HMGR becomes ubiquitinated and is extracted from the membrane by VCP/p97. HMGR is then degraded by the proteasome (purple).

(modeled in Figure 1). Misfolded proteins previously labeled by cytoplasmic ubiquitin ligases are identified by ubiquitin-binding-factors that extract labeled proteins from the membrane to the cytoplasm by coupling translocation with ATPase activity (Ye et al., 2003; Lipson et al., 2008). Extracted proteins are then escorted by ATPase associated chaperones to the proteasome (Barthelme and Sauer, 2012; Raman et al., 2015). In humans, the valosin-containing ATPase (VCP/p97) associates with gp78 until it identifies labeled proteins to extract into the cytoplasm (Fang et al., 2001). VCP/p97 has been most well characterized for its role in protein quality control, but this same mechanism is recycled for cholesterol mediated degradation of HMGR (Song et al., 2005; Goldstein et al., 2006). It is unknown whether these mechanisms may also regulate the levels of signaling proteins, or indeed which signaling proteins have cholesterol response elements.

Regulation of Cholesterol Homeostasis by LXR Related Nuclear Receptors

Nuclear receptors (NRs) are one major mechanism cells use to respond to changing diets and subsequent changes in nutrient availability. NRs are ligand regulated transcription factors that recognize small lipophilic molecules, such as bile acids, fatty acids, and sterols, and mediate broad changes in gene expression to regulate development, homeostasis, and metabolism. The regulation of cholesterol metabolism, specifically, is a common target for NR regulation. Many NRs including CAR,PXR, FXR, and LXR have known roles in the regulation of specific aspects of cholesterol homeostasis (Wang and Tontonoz, 2018).

LXRα in particular is expressed specifically in the liver, intestine, and other digestive tissues. In response to high intracellular cholesterol, LXR induces the expression of cholesterol transport proteins such as ATP-binding cassette transporter A1 (ABCA1) and Nieman-Pick disease, type C1 and 2 (NPC1/2), stimulating cholesterol trafficking to the plasma membrane and decreasing the production of stored cholesterol esters (Janowski et al., 1996; Repa et al., 2002). *LXRalpha* mutants have high levels of circulating and stored cholesterol, indicating an impaired ability to sense cholesterol levels. In mammals, LXR expression also promotes reverse cholesterol transport, where stored cholesterol in non-hepatic tissues is transported back to the liver, and then excreted from the body (Lo Sasso et al., 2010; van der Veen et al., 2009). Interestingly, the liver may not be required for cholesterol excretion since 60% of excreted fecal sterols can come directly from the proximal intestine (van der Velde et al., 2007).

In *Drosophila,* a single LXR subfamily 1 ortholog, Hr96, is expressed in the intestine and fat body, and regulates xenobiotic detoxification, triglyceride metabolism and sterol metabolism (Bujold et al., 2010; Horner et al., 2009; Sieber and Thummel 2009). Strikingly, *Hr96* mutants accumulate excess cholesterol when cultured on wild type food, and die when given a low-cholesterol diet (Bujold, M., 2010), supporting a model that Hr96 serves to measure the amount of intracellular cholesterol, and initiate global changes in gene expression to promote cholesterol import and trafficking when cholesterol levels drop below a threshold level. These genes include a predicted cholesterol acetyltransferase (ACAT, *CG8112*), the NPC2 family genes, and lipases including the *LipA* homolog *magro* (Sieber and Thummel, 2009).

Cholesterol Metabolism in *Drosophila*

Drosophila lack several enzymes required to synthesize their own cholesterol, and thus rely on the absorption and conversion of dietary sterols for their survival (Sang, 1956). Integral to this process is the ability of cells to import sterols and transport intermediates between various cellular compartments. Bulk sterols are first imported into cells where they are trafficked through the ER and Golgi and then processed into lipid droplets before they are trafficked to the plasma membrane or released into the circulatory system for transport to other tissues. Steroids derived from cholesterol, mainly ecdysone and its derivative, 20-hydroxyecdysone (20E) are indispensable for *Drosophila* development and oogenesis. This hormone is produced mainly in the prothoracic gland of larva, and the ovary of adult females (Gilbert et al., 2002).

The import of sterol into cells is mediated by the Niemann-Pick type C1-like protein (NPC1L1) in mammals, and related *NPC1b* in *Drosophila* (Voght et al., 2007). However, while NPC1b is able to import cholesterol, *NPC1b* mutants have functionally similar cholesterol levels as their wildtype counterparts, indicating the existence of at least one other redundant, and currently unidentified, mechanism for cholesterol import. Interestingly, while *NPC1b* facilitates cholesterol absorption, the related *NPC1a* antagonizes this process, as *NPC1a* mutants have higher than normal rates of cholesterol absorption (Wang et al., 2010; Xie et al., 1999). Furthermore, *NPC1a* is critical for the uptake of cholesterol into the prothoracic gland, as larval *NPC1a* developmental defects can be rescued by feeding 20E, or tissue specific rescue of *NPC1a* (Fluegel et al., 2006).

The related *Drosophila* proteins, NPC2a-h, are predicted to assist in subcellular sterol trafficking. Germline mutants of two well studied members of this family, *NPC2a*

and *NPC2b* exhibit gross defects in neuronal structure, and die during larval development (Huang et al., 2007). Filipin staining for sterol-specific compounds in *NPC2a/b* mutant cells shows accumulating punctate subcellular sterol deposits suggestive of a block in cholesterol trafficking from the ER to the golgi (Huang et al., 2007). While the roles of *NPC2c-h* have not been identified, their conserved sequence and predicted structure with *NPC2a/b* suggest that they serve similar roles, perhaps in varied cell types, or subcellular compartments.

Cholesterol regulation of the Notch signaling pathway

Tissues throughout the animal kingdom recycle Notch signaling for various stages of development and the differentiation of multiple tissues. While the canonical Notch pathway is one of the most simplistic signaling pathways in design, its activation level can be tightly modulated, and its method of signaling provides a fast source of lateral inhibition making it a powerful player in cell differentiation. The core pathway consists of a transmembrane receptor able to interact with another transmembrane ligand on a contacting cell. Recognition of the ligand by the receptor initiates cleavage and release of the intracellular domain of the Notch receptor (NICD). This component can then translocate to the nucleus to initiate the transcription of a large cohort of Notch target genes. These genes vary widely from cell to cell and are dependent on the NICD partners available for binding as well as the epigenetic state of the Notch signal receiving cell. Notch pathway activation has no amplification step, and as such, the transcriptional response initiated by Notch signaling is dependent on the amount of NICD cleavage. This relationship between the amount of Notch activity and target gene activity generates a

wide variety of phenotypes when the pathway is genetically manipulated (Mohr, 1919; Lyman and Yedvobnick, 1995). While there are many Notch receptor-ligand combinations in mammals, *Drosophila* have only one receptor, and three ligands- Delta, Serrate, and Jagged (D'Souza et al., 2010), Only Delta is significantly expressed in the intestine.

After Notch cleavage, the extracellular domain (NECD) is trans-endocytosed into the ligand-expressing cell (Parks et al., 2010). Studies in sensory organ precursor cells (SOP) show that Notch ligands can be recycled to the plasma membrane or degraded, while the receptor is proteolytically cleaved, transported in endosomes, and degraded in a lysosome dependent manner (Coumailleau et al., 2009). NECD positive endosomes are asymmetrically segregated during cell division in SOP cells, which has generated hypotheses that the rate of Notch turnover can influence downstream response to the pathway.

It has been speculated that lipid rafts, may influence the speed and magnitude of Notch signal transduction (Simons and Toomre, 2000). The increased membrane fluidity caused by high concentrations of cholesterol may enable low concentrations of Notch receptor and ligand to reach each other more easily than in cholesterol depleted membranes. Additionally the activity of the Notch cleavage protein complex, gamma secretase, can be regulated by its lipid microenvironment in neurons, as the addition of soluble cholesterol, in culture, increased the cleavage of APP and Notch substrates (Osenkowski et al., 2008). Cholesterol may also influence the turnover of proteins by titrating the number of lysosomes since cells depleted of cholesterol had fewer lysosomes near the cell membrane (Hissa et al., 2012). Since this work has been done entirely in

cell culture, where cholesterol is manipulated by drug treatment, it is unknown whether dietary changes may be able to cause cellular cholesterol changes that influence the Notch signaling, or other signaling, pathways.

Gut Regionalization

Food digested by the intestine passes through successive regions that are similarly structured, but each uniquely capable of digesting and exporting particular nutrients. Specialization can be seen at the level of RNA expression (Buchon et al., 2013; Marianes and Spradling, 2013), differentially secreted peptides (Lee and Kaestner, 2004; Veenstra et al., 2008), cellular makeup (Schonhoff et al., 2004), and stored nutrients (Shanbhag and Tripathi, 2009; Mehta et al., 2009; Sieber and Thummel, 2009). In 2013, Marianes and Spradling provided a mechanism for these observations by showing that the regions of the *Drosophila* intestine are distinct in part because they are maintained by unique pools of self-renewing stem cells. Stem cell progeny can be mapped by initiating a permanent genetic mark during cell division. By carefully timing the induction of these marks, they showed that stem cells along five out of six borders tested did not generate progeny for their neighboring region, but only differentiated cells for the stem cell's region of origin.

This data suggests that intestinal stem cells of many regions are intrinsically different from each other, and may also respond uniquely to changes in cell signaling and stem cell regulation. A later study sequenced pools of sorted stem cells from 5 unique regions and confirmed that each pool expressed a unique transcriptional profile (Dutta et al., 2015). Interestingly, regions with a similar mitotic index (Anterior 2 and Posterior 1)

also shared more similarities in their transcriptional signature than the predicted cell cycle genes and regulators. These results are consistent with each region housing stem cells that each respond differently to local regulatory signals.

The Intestine is Maintained by Multipotent Stem Cells

Intestinal stem cells (ISCs) are found in every region of the midgut and can produce every epithelial cell of the midgut – stem cells, enteroblasts (EB)/transit amplifying cells, enteroendocrine cells (ee), and enterocytes (EC), in each region (Buchon and Osman, 2015). The ISC lineage was characterized by two groups (Ohlstein and Spradling, 2006; Michelli and Perrimon, 2006) who initially showed that a common progenitor (EB) can differentiate into either an ee or EC. Further characterization found that ISCs vary in the amount of intracellular Delta they contain, and that ISC daughters with high Delta concentrations produce ECs while those with lower concentrations produce ees (Ohlstein and Spradling, 2006; Ohlstein and Spradling, 2007). Additional studies have identified factors that promote ee or EC fate in initial progenitors, even before stem cell division. In particular, the Notch inhibitor, Numb, acts to promote ee fate within ee progenitor cells (Salle et al., 2017).

Recent work has suggested this differentiation paradigm is more complicated, and must account for creating multiple classes of ees (Beehler-Evans and Micchelli, 2015). Each class can be described by the region where the ees are found, as well as the hormones that they secrete. This variation may be accounted for in part by the many ways of generating ees that have been observed by lineage tracing (modeled in Figure 2): 1) ISCs may directly differentiate into ees without undergoing division (Zeng and Hou,

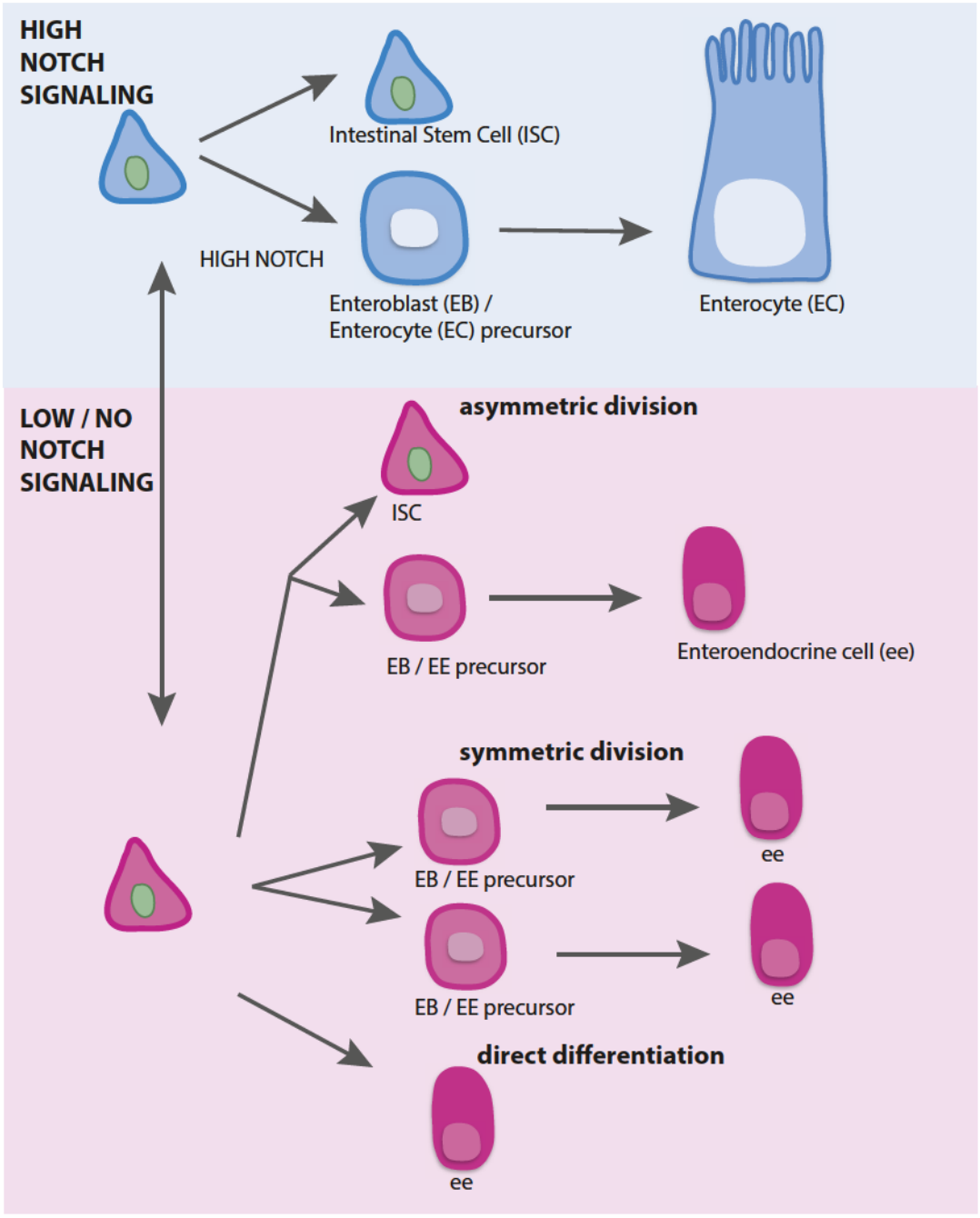

Figure 2. Intestinal cell differentiation is determined by Notch signaling.
Modeled after Figure 1 in Gervais and Bardin (2017).
This model summarizes the possible fates for intestinal daughter cells following stem cell division. When Notch is high, an enteroblast differentiates into an enterocyte. When Notch is low, daughter cells become ees through a variety of mechanisms.

2015), 2) The traditional stem cell paradigm characterized by Ohlstein and Spradling where upon ISC division one daughter cell differentiates along an ee fate, and the other remains an ISC with the marks of a stem cell, and can produce both ECs and other ees in the future, 3) Upon ISC division, both daughters generate ee cells (de Navascues et al., 2012). All of these methods, but particularly the third, may be corrupted by mutation to produce enteroendocrine tumors which will be discussed in a later section.

Differentiation of the adult *Drosophila* midgut

Immediately after pupal formation, larval enterocytes are histolyzed, and detach from the larval epithelial layer, moving into the lumen (Jiang and Edgar, 2009). From there they are surrounded by a layer of dying peripheral cells and a second layer of activating adult midgut precursor cells (AMPs), which migrate to form a new epithelial sheet (Takashima et al., 2011, Micchelli et al., 2011). Even before pupation, initial signaling has occurred to establish which of the AMPs will differentiate into stem cells (Mathur et al., 2010). By twelve hours after pupation, some of these stem cells begin a process of transient amplification to increase in number, and by twenty four hours into pupation (about 1/5 through metamorphonsis) BMP ligands from the muscle have established a pool of stem cells in the middle midgut which will divide to produce the cells of the copper region (Drive and Ohlstein, 2014).

There are no enteroendocrine cells in this early adult midgut until 48-54 hours after pupation, and arise from a wave of asymmetric divisions of the first ISCs (Takashima et al., 2011). During this first division, no enterocytes are produced, but following this initial wave, stem cells begin to express Delta, triggering an upregulation

in Notch signaling, and very few ees are produced until after eclosion (Takashima et al., 2011).

The adult midgut develops rapidly during pupation, but still begins adulthood about half of its final size. One explanation for this may be that because the pupal fly is protected from environmental influences until eclosion, it delays the final stages of development, until it can properly assess its new environment. This allows the midgut to become established as it begins digesting food and is newly populated by bacteria.

Regulation of Metabolism by Enteroendocrine (ee) Cells

The digestive tract has evolved to quickly respond to dietary changes, and in some cases is required to produce an appropriately scaled physiological response to diet. For example, ingestion of dietary glucose produces a larger insulin response, and thus a smaller change in blood glucose than the insulin response that proceeds injecting the same quantity of glucose directly into the blood stream (Elrick and Stimmler, 1964). This illustrates the essential role of the intestine in transmitting information from the diet to other organs, in this case the pancreas.

This type of inter-organ communication is facilitated by the endocrine system which transmits signals between different tissues in the body to accomplish homeostasis and regulate behavior. Within the digestive tract, communication occurs from a subset of this system, the enteroendocrine cells, which are located in the stomach, intestine, and pancreas, and secrete hormones that regulate digestion, the immune response and metabolism. In mammals, there are 10 types of intestinal ees, each restricted to a certain region of the intestine, and capable of expressing a subset of ee hormones (Moran et al.,

2008). K cells, for example, are interspersed within the epithelium of the duodenum and jejunum, where they secrete gastric inhibitory peptide, to regulate triglyceride storage (Parker et al., 2009).

Ees have chemoreceptors that sense various classes of nutrients on their apical, lumen-facing side, although it is not well understood which nutrients are sensed by which ee classes (Gutierrez-Aguilar and Woods, 2011). On the basal side, a large number of vesicles are polarized where they facilitate the excretion of hormones to enteric neurons and capillaries.

In *Drosophila* there are the nine prohormones: AstA, AstB, AstC, NPF, sNPF, TK, DH31, CCHamides1 and 2, which can be processed into 24 mature peptides that are secreted by ees (Song et al., 2014). While all ees express the marker Prospero, the expression of the other peptides is regional, and only occur in certain combinations. For example, AstA expression is largely limited to the posterior midgut (Veenstra et al., 2008).

Mammalian ees are rare, comprising <1% of the intestinal epithelial cell population (Buffa et al., 1978), while about 10% of epithelial cells in the *Drosophila* midgut are ee cells. Interestingly, in *Drosophila, Scute* loss-of-function mutants which prevent enteroendocrine cell differentiation still exhibit normal feeding and egg laying behaviors when kept on high nutrient food (Amcheslavsky, A., et al. 2014). However, while ee-less flies can survive under static conditions, the midguts of these animals are unable to modulate their size in response to diet, because the surrounding muscle fails to express insulin-like peptide 3, and they live approximately half as long as control animals (Amcheslavsky, A., et al. 2014). These results demonstrate an essential role for

enteroendocrine cells in nutrient sensing. Furthermore, the inability to sense nutrient availability may affect lifespan.

The decrease in lifespan observed in ee-less mutants may be caused in part by an inability to regulate lipid homeostasis. When flies are starved and nutrients are scarce, ees express significantly more TK which represses lipogenesis (Song et al., 2014), allowing stored lipids to be mobilized for fuel. Conversely, mutants unable to secrete TK have significantly more stored and circulating lipids than wildtype animals, indicating a misregulation in lipid metabolism (Song et al., 2014). More recent studies have gone on to show that amino acids, and not sucrose or triglycerides, promote polarization, and potentially activation in TK+ ees, while an uncharacterized population of ees was induced with high sucrose (Park et al., 2016).

Lipid metabolism in health and human disease

Since cell proliferation requires a supply of new phospholipids and cholesterol for the production of new membranes, it is not surprising that cancer cells thrive when lipids are readily available. Additionally, a high fat diet in general, and high cholesterol consumption in particular has been linked with an increased risk of gastrointestinal cancers in epidemiological studies (Jarvinen et al., 2001). Studies have also identified intestinal and colonic stem cells as the founding cells in cancer initiation, and that they are able to contribute to cancer progression (Barker et al., 2009). Furthermore, by manipulating the phospholipid-remodeling enzyme Lpcat3, researchers found that they could artificially induce high levels of cholesterol biosynthesis, producing high intracellular cholesterol specifically in intestinal stem cells. These mutant animals

exhibited increased stem cell proliferation, and enhanced tumorigenesis when combined with mutations for the tumor suppressor gene adenomatous polyposis coli (*Apc*) (Wang et al., 2018). In the future it will be interesting to see whether cholesterol drives cell division through a downstream sterol-related product, or by influencing signaling pathways. Dietary cholesterol has been shown to influence the proliferation of follicle stem cells in *Drosophila* by regulating the release of Hedgehog protein (Hartman et al., 2013), and a similar mechanism, be at work in the intestine. Recent studies have also shown that forcing the production of cholesterol rich lipid droplets by overexpressing enzymes that produce phosphatidylcholine blocks ER stress and subsequent cell death resulting in chemotherapy resistance in colon cancer cells (Cotte et al., 2018).

High intracellular cholesterol is also a marker of neurological disease. Researchers noticed that patients with Alzheimer's disease had an approximately 10% increase in plasma cholesterol relative to healthy individuals, but it was not known if this small increase had any biological effect (Popp et al., 2013). Recent work has shown that this small change is able to change the nucleation rate of amyloid-beta peptide into the insoluble aggregates that characterize Alzheimer's disease (Habchi, J. et al., 2018). This increased rate occurs in isolated vesicles, but it will be interesting to see if it occurs in cultured neurons, and *in vivo* tissue as well.

The *Drosophila* midgut as a model for studying metabolic disorders

Metabolic disorders in humans are difficult to study in part because of the complex nature of the pathways and gene networks that are required to regulate metabolism, and also because of the complications of regulating diet in humans.

Drosophila in contrast have a plethora of genetic tools available to study their development and physiology, and their diet can be easily manipulated. The use of *Drosophila* as a system for metabolic studies has been reviewed many times (Baker and Thummel, 2007; Kuhnlein, 2010; Cox et al., 2017). Importantly, work in *Drosophila* has foreshadowed important findings later identified in humans, such as the role of the *adipose* gene in regulating TAG levels (Doane, 1960; Lai et al., 2009). Because of their essential roles for growth and survival, the basic metabolic pathways, including glycolysis, gluconeogenesis, fatty acid beta-oxidation, the citric acid cycle, and the electron transport chain are nearly identical between flies and humans, making metabolism a particularly attractive area of study in *Drosophila.*

It is this system that I have used in this thesis to study how diet influences development, specifically how modulating lipid availability from the diet influences stem cell behavior in the *Drosophila* intestine. Knowing that the intestine undergoes massive growth during the first few days of adulthood, we predicted that any cell-level changes that may be inflicted by diet would be most visible during this transition time. While normally, the enterocytes of the intestine turnover in 7-10 days (Marianes and Spradling, 2013), the enteroendocrine cells turnover more slowly (Zeng and Hou, 2015), and turnover may also vary by region. However, the intestine grows uniformly after eclosion, so a dietary perturbation at this time could cause a large scale effect that would be readily identifiable. Interestingly, these effects not only change the cellular makeup of the intestine, but also cause long term effects such as changing the amount of cholesterol animals store when fed a rich diet, and the rate of tumor initiation and growth after an instigating mutation.

As part of this long term study, I performed a large scale RNA sequencing experiment that is outlined in Chapter 3. We sequenced RNA from an anterior and posterior segment of the female midgut in 10-14 day old flies, from animals fed a control, lipid depleted, and high cholesterol diet, as well as in to genetic backgrounds where cholesterol storage is disrupted. I have performed initial analysis to identify the metabolic genes that are significantly affected in these backgrounds. These results show that the regulation of many these genes is not transcriptional. Additionally, the transcriptional changes that were identified are different between the anterior and posterior midgut, further helping us characterize the differences between these two regions.

Chapter 3 also contains some characterization of the larval and pupal midgut. These studies were performed and published more extensively by other groups (Takashima et al., 2011; Driver and Ohlstein, 2014; Harrop et al., 2014; Jones et al., 2015). Finally, I include initial experiments characterizing the nuclear receptor, HNF4 as a regulator of adult midgut development. This thesis has shown that a single dietary metabolite is capable of influencing a signaling pathway to modulate differentiation. These changes in differentiation occur in particular region of the intestine, a region that metabolizes the nutrient that initiates these changes. It is likely then that metabolites that are processed in other regions (glucose/glycogen in the anterior, iron in the middle midgut, etc) may also influence the differentiation of cells in those regions. Furthermore, the techniques used here can be used to study other lipid species such as fatty acids, phospholipids, and triglycerides. Just as cholesterol induces changes in the activity of Hr96, long chain fatty acids can activate HNF4. It will be interesting in the future to study how fatty acid availability and HNF4 interact during development, early adult

midgut formation, and adult homeostasis. Continuing to characterize the connections between environmental nutrients and developmental signaling will contribute to understanding how tissues respond to stress, age, disease, and the presence of cancer, and how nutrition might be able to positively modulate those responses.

CHAPTER 2

DIETARY LIPIDS MODULATE NOTCH SIGNALING AND INFLUENCE ADULT INTESTINAL DEVELOPMENT AND METABOLISM IN DROSOPHILA*

Written by: Rebecca Obniski[1,3], Matthew Sieber[1,2,3] and Allan C. Spradling[1]

[1]Howard Hughes Medical Institute Research Laboratories
Department of Embryology, Carnegie Institution for Science
3520 San Martin Dr., Baltimore, Maryland 21218 USA

[2]Department of Physiology
University of Texas Southwestern Medical Center
5323 Harry Hines Blvd., Dallas, TX 75390-9040 USA

[3]These authors contributed equally

* This chapter is an edited replication of a manuscript *in press*, "Dietary lipids modulate Notch signaling and influence adult intestinal development and metabolism in *Drosophila*, published in Developmental Cell (Obniski et al., 2018). Edits have been made to accommodate formatting requirements, and clarifications, for this publication.

INTRODUCTION

Development is a unique partnership between a flexible genetic program and the environment. Major advances have occurred in recent years in understanding the genes and pathways that program embryo and tissue development, many of which are highly conserved among diverse invertebrate and vertebrate animals. In addition, numerous examples have been documented where environmental variables, nutrition in particular, exert or are believed to exert strong modulating effects on developmental outcomes and disease susceptibility (reviewed in Preston et al., 2018). Examples, include folate and neural tube closure (Imbard et al., 2013), cholesterol and heart disease (Orho-Melander, 2015), and caloric intake and longevity (Templeman and Murphy, 2018). Despite the great interest and importance of understanding how the environment modifies development, gaining a mechanistic understanding of these unprogrammed effects on animal form and function has proved much more difficult than deciphering the developmental program itself.

Diet is one of the most important and ubiquitous environmental variables impacting animal life cycles. A nutrient poor diet during embryonic development may establish a scarcity metabolic program in the offspring that can lead to metabolic syndrome (review: Ramakrishnan, 2004). Dietary intake of certain nutrients may also increase the risk of cancer. For example, there is a strong correlation between a high fat diet and colon cancer (Beyaz et al., 2016; O'Neill et al., 2016) raising the possibility that a high fat diet may influence developmental signaling pathways that promote cell proliferation. However, nutrients such as cholesterol can potentially affect cancer incidence in many ways, complicating our understanding of the connections between

dietary cholesterol intake and oncogenesis (Silvente-Poirot and Poirot, 2014; Kloudova et al., 2017).

Cholesterol uptake and utilization is controlled by mechanisms that are highly conserved between Drosophila and mammals. For example, intestinal enterocytes in both groups take up dietary cholesterol by endocytosis and vesicle trafficking into lysosomes. Subsequently, under control of Niemann-Pick type C genes *NPC1* and *NPC2*, cholesterol is moved from lysosomes to other organelles such as endoplasmic reticulum (ER) and mitochondria (Huang et al., 2005). Once in the ER a large portion of the cholesterol is esterified by acetylCoA cholesterol acyltransferase (ACAT), packaged into lipoprotein particles and transported to peripheral tissues. In mammals, cholesterol biosynthesis is controlled by the lipid-mediated regulation of protein stability in the endoplasmic reticulum (Goldstein and Brown, 1990). When cholesterol levels in enterocytes are high, the rate limiting biosynthetic enzyme, the membrane protein HMGCoA reductase, is destabilized by ubiquitination, dislocated out of the ER and degraded via the endoplasmic reticulum-associated degradation (ERAD) pathway. In contrast, in lipid-deprived cells, Insig-1, a key protein involved in HMGCoA turnover and in processing sterol regulatory element binding proteins (SREBPs), is degraded via ERAD. Even though Drosophila is a cholesterol auxotroph, mammalian lipid regulatory proteins expressed in Drosophila are still subject to sterol-regulated ERAD showing that lipid mediated control of protein stability in the ER via ERAD has been highly conserved (Faulkner et al., 2013).

The expression of genes mediating cholesterol uptake, as with many other dietary lipids, is mediated largely through nuclear receptors (NR). These ligand-regulated transcription factors recognize small lipophilic molecules and mediate broad changes in

gene expression to regulate development, homeostasis, and metabolism (Evans and Mangelsdorf, 2014). Cholesterol efflux in mammals is regulated primarily by NR subfamily 1 members LXRα and LXRβ. In response to high intracellular oxysterols, LXR induces the expression of cholesterol transport proteins thereby stimulating cholesterol trafficking from the peripheral tissues to the liver where it is eliminated in the form of bile (Kalaany and Mangelsdorf, 2006). In *Drosophila,* a single subfamily 1 ortholog, Hr96, is expressed in the intestine and the fat body, and is required for development in cholesterol-depleted environments (Horner et al., 2009). Consequently, NR1 members and their conserved target genes are strong candidates for mediating cholesterol-induced effects on intestinal development.

The *Drosophila* midgut is a powerful model system in which to analyze the relationship between diet and intestinal development at the cellular, molecular and functional levels, in part because nutrient processing is highly regionalized (Buchon et al., 2013; Marianes and Spradling, 2013). The activity within each gut sub-region is strongly impacted by distinct self-renewing intestinal stem cells (ISCs) (Micchelli and Perrimon, 2006; Ohlstein and Spradling, 2006) whose daughter cells, known as enteroblasts (EBs), differentiate in response to a high Notch signal into nutrient-processing enterocytes (ECs). In the presence of low intracellular Notch activity, ISCs produce enteroendocrine mother cells that differentiate into multiple types of hormone-secreting enteroendocrine cells (ee's) (Ohlstein and Spradling, 2007; Guo and Ohlstein, 2015). Notch signaling is largely regulated by its ligand, the transmembrane protein Delta, whose activity is influenced by factors that impact the trafficking, recycling and turnover within endosomal vesicles of both Delta and Notch itself (Seugnet et al., 1997;

Weber et al., 2003; Coumailleau et al., 2009; Conner, 2016). In the mammalian intestine, Notch signaling also specifies enterocytes and enteroendocrine cells (Demitrack and Samuelson, 2016). Abnormalities in Notch signaling are associated with increased cell proliferation in both *Drosophila* and mammals, including colon cancer (Suman et al., 2014).

We have found that dietary cholesterol influences intercellular Notch signaling and enteroendocrine cell differentiation in the adult midgut. Differences in enteroendocrine cell number established in young animals persist and appear to contribute to a metabolic memory, as flies raised initially under lipid deprivation later in life accumulate 18% more sterols on a standard diet than controls. Moreover, dietary lipid levels affect the progression of enteroendocrine tumors. Thus, our results reveal a specific and potentially widespread mechanism through which a dietary nutrient affects Notch intercellular signaling and cellular differentiation with possible consequences for adult metabolic programming and cancer susceptibility.

MATERIALS AND METHODS

Experimental Model and subject details

Drosophila melanogaster.

Normal and modified dietary treatments

To enhance uniformity, all diets were prepared from lipid-extracted ingredients. The lipid-depleted diet was prepared by extracting yeast extract and agar with chloroform at a 1:5 ratio by weight. Each component was extracted for 4 hours, separated with vacuum filtration, and then extracted for 1 hour with fresh chloroform. Both components were then allowed to dry for five days in a fume hood. Extracted yeast extract and agar were used to make a 1.0 SY diet according the following formula: 30g sucrose, 30g lipid-extracted yeast extract, 3g agar, 300 mL H_2O (Sieber and Thummel, 2009). The control diet consisted of a lipid-depleted 1.0 SY diet supplemented with fresh yeast paste and vehicle alone (1-4% ethanol) to control for the ethanol in the lipid-supplemented diets. Lipid supplemented diets (1X) consisted of the lipid-depleted 1.0 SY diet supplemented with free fatty acid (5 mg/ml stearic acid), triglyceride (5 mg/ml glycerol tristearate), cholesterol (5 mg/ml) or ergosterol (5 mg/ml) to a final concentration of 0.05% supplemental lipid. 4x cholesterol (high sterol diet) and 4x ergosterol were prepared to a final concentration of 0.2% supplemental sterol. Either pupae or 5-day old adult flies were transferred to vials with the diet of interest. Flies moved to a new dietary treatment were tested after an indicated period during which they were transferred to fresh vials containing the media every other day.

Mammalian cell culture

HEK293 cultures

Cultures of HEK293 cells grown petri dishes in Dulbecco's modified Eagle's medium (+10% FBS, 1x antibiotic) at 37˚C and 5% CO_2. Cultures were split at 80% confluency.

HCT116 cultures

HCT116 cells were cultured in petri dishes in McCoy's medium (+10% FBS, 1x antibiotics) at 37˚C and 5% CO_2. Cultures were split at 80% confluency.

Methods details

Drosophila melanogaster

Immunofluorescent staining

Midguts or ovaries were dissected in Grace's insect medium and fixed for 30 minutes at room temperature (or 15-18 hours at 4°C for midgut Delta staining) in antibody wash with 4% EM grade paraformaldehyde). Tissues were then washed three times for at least 2 hours and then blocked at room temperature in antibody wash +5% BSA for 4 hours. Primary antibodies were added to incubate overnight at 4°C at the following concentrations: anti-Prospero (Developmental Studies Hybridoma Bank MR1A;), RRID:AB_528440) (1:100), 1:100, anti-PH3, Ser10 (Millipore Sigma) 1:1000, (1:100), anti-Delta (DSHB C594.9B, RRID:AB_528194) (1:50), anti-NECD (DSHB C458.2H, RRID:AB_528408), anti-LpR2 (Parra-Peralbo E; PLoS Genet. 2011 Cat# LpR2, RRID:AB_2569135) (Parra-Peralbo and Culi, 2011), anti-Hindsight (DSHB 1G9, RRID:AB_528278) (1:100). Samples were washed for at least 9 hours. Secondary antibodies: Alexa-488, Alexa-568, and Alexa-596 incubated overnight at 4°C in antibody wash. Samples were then washed and counterstained with DAPI at 0.5 µg/ml. Tissue was

then mounted with Vectashield and imaged. Antibody wash used for guts contained 1xPBS + 0.3% Triton X-100 + 0.5% BSA. Antibody wash for ovaries contained 1xPBS + 0.1% Triton X-100 + 0.5% BSA. Tunel labeling was performed before incubation with secondary antibodies per manufacturer's instructions using The DeadEnd™ Fluorometric TUNEL System (Promega, G3250).

Analysis of enteroendocrine cell frequency

Physical characteristics of the *Drosophila* midgut described in Buchon et al., (2013) and Marianes and Spradling (2013) were used to identify anterior (A2, specifically) and posterior (either P1 or P3) midgut regions. Percent ee's were scored by counting the number of Prospero-labeled nuclei divided by the total number of DAPI positive cells. For each quantified intestine plotted in Figures 1, 2 and 6, three 2500μm^2 regions were averaged.

Fluorescence quantification

Quantified Delta and NECD fluorescence reported in Figure 3, 4 and 5 was measured using the integrated density measurement function in ImageJ. Corrected total cell fluorescence was calculated by subtracting mean fluorescent background from the same image. Each graphed point is the average of 3 cells within a 2500μm^2 region. At least 10 midguts were analyzed for each experiment.

Notch tumor induction

Notch knock-down was performed using UAS-N-RNAi; esg-GAL4; GAL80^{ts}, UAS-GFP flies raised at 18°C and then moved to 29°C upon eclosion. Knock-down flies with a supplemented diet were introduced to this diet at eclosion, and transferred to fresh media

every day. Notch$^{-/-}$ and FRT19A control clones were induced in 5 day old flies with one 30-minute heat shock at 37°C.

RNA sequencing

Female y^1 w^1 flies aged 10-12 days were dissected in cold Grace's insect medium. Anterior (a1-a3) and posterior regions(p1-p4) were identified morphologically and isolated using microdissection scissors. 30-50 cut regions per sample were transferred to 400 µl Tripure on ice. Each experimental condition was collected in triplicate. Collected midguts were homogenized and 600µL fresh Tripure added. After 10 min at room temperature 180µl chloroform was added, shaken briefly by hand and allowed to stand at room temperature for 10 minutes. Following centrifugation for 15 min at 12,000 rpm at 4°C, the aqueous layer was removed and RNA precipitated with 400 µl isopropanol. The pellet was recovered by centrifugation, re-suspended in 50uL nuclease free water and stored at -80°C. cDNA libraries were constructed from poly(A)-selected RNA using the llumina TruSeq RNA Library Prep Kit v2 and sequenced on an Illumina NexSeq 500.

Sequenced reads were analyzed using bcl2fastq v2.17.1.14 for base calling, Bowtie 2.2.9 for alignment to the dm6 Drosophila genome, TopHat 2.1.1 for alignment to transcripts defined by BDGP6 and Ensembl.85.gtf. Transcript and gene fpkm was calculated using Cufflinks 2.2.1 and fold change quantified with cuffdiff (v7). We analyzed genes whose expression was >2 FPKM and with a q-value <0.05. Genes reported as significantly changing had at least 2-fold increased or decreased expression levels.

qRT-PCR

RNAi knock-down efficiency reported in Figure S2P was measured in dissected midguts. RNA was collected as described for RNA sequencing and then 1µg of total RNA was reverse transcribed using Bio-Rad iScript Reverse Transcription Supermix. Quantitative PCR was performed using iTaq™ Universal SYBR® Green Supermix. Biological and technical triplicates were used for each genotype. Results were normalized to rp49.

Cholesterol Measurements

Cholesterol and cholesterol ester (cholesteryl) in single flies or in isolated intestines were measured exactly as described in Sieber and Thummel (2012). Single female flies or 25 midguts from female flies were dissected and rinsed in 1X PBS + 0.5% Triton X-100 (PBST). Tissue was homogenized in 250µl in PBST and the volume raised to 900µl. Samples were sonicated 3 x 30 seconds and split into two samples. 10µl cholesteryl esterase was added to one sample and both samples were incubated at 37°C for 18 hours. Samples were extracted with a 2:1 chloroform:methanol solution. Lipids were solubilized in 500µl PBST and then sonicated 3x 30 seconds. Cholesterol and cholesterol ester were measured using the Amplex Red Cholesterol Assay Kit and samples read per kit instructions.

NMS-873 Treatment

Ten 5-day-old female flies were put with an equal number of male flies in a vial containing 1.0 SY media. Flies were fed fresh yeast paste with either 15µM or 30µM NMS-873, or 30µM DMSO every other day. Lethality of the treatment was assessed every day for 7 days. Delta protein levels were observed by immunofluorescence after 4 days.

Mammalian cell culture

Treatment of HEK293 cells with GW3965

Samples were collected from parallel cultures of HEK293 cells and treated with 2 μM GW3965 or DMSO vehicle for 16hrs.

Treatment of HCT116 cells with Simvastatin

HCT116 cells were cultured with 5μM activated Simvastatin or 5μM ethanol in McCoy's medium (+10% FBS, 1x antibiotic) for 48 hours, with fresh media and Simvastatin/ethanol added after 24 hours. Simvastatin was activated according to manufacturer's instruction by dissolving 1.4mg Simvastatin in 100μl of ethanol and incubating the resulting solution with 150μl of 0.1 N NaOH at 50 ˚C for 2 hours. The final stock concentration was adjusted to a pH of 7.0 with HCl and brought to a final concentration of 4 mg/ml.

HCT116 Immunofluorescent Staining

Cells were cultured as described on round coverglass. Prior to fixation, cells were rinsed 3x with 1X PBS and then incubated with freshly diluted 4% paraformaldehyde for 10 minutes at room temperature. Cells were rinsed again 3x with PBS and then incubated with 1 ml of 1.5 mg glycine/ml PBS for 10 minutes at room temperature. Samples were either immediately stained with 1ml of filipin (0.05 mg/ml in PBS) for 2 hours at room temperature or blocked with 5% NGS in 0.1% PBS + Triton X-100 for 1 hour. Following block, samples were incubated overnight at 4 ˚C with anti-Notch1 (1:500) and anti-sec61 (1:2000) in blocking solution. Samples were washed the next day 3x5 minutes with PBS and then incubated with secondary antibodies at 1:1000 for 1 hour at room temperature.

Samples were washed again for 3x5 minutes with PBS, incubated with 1µg/ml DAPI for 10 minutes, and mounted with Prolong Gold Antifade Reagent.

Western Blot for Tubulin and DLL4

HEK293 and HCT116 cells were collected in cold PBS and combined with an equal volume of 2x Laemmli Sample Buffer. Cells were sonicated for 10 seconds and incubated at 70 ˚C for 10 minutes. 15µl sample was loaded into 4–15% Mini-PROTEAN® TGX™ Precast Protein Gels and proteins separated at 100V for 90 minutes. Proteins were then transferred onto nitrocellulose membrane at 10mA constant current for 18 hours. The membrane was blocked with Odyssey Blocking Buffer for 1 hour and then incubated overnight at 4˚C with 0.1% Tween-20 and primary antibodies anti-DLL4 (1:500) and anti-alpha tubulin (1:1000). Appropriate IRDye secondary antibodies were incubated for 1 hour at room temperature at 1:20,000 in Odyssey Blocking Buffer with 0.1% Tween-20. Membranes were washed 3x5 minutes with 1x TBS after primary and secondary antibody incubation.

Quantification and statistical analysis

The significance of experimental treatments relative to matched controls were determined using Students t-tests (single-tailed) using GraphPad, as described in Figure legends. Significance levels are shown on the Figures using the following code: * = $p<0.05$; ** = $p<0.01$; *** = $p<0.001$.

Data and Software availability

"*The RNAseq data described have been deposited in the NIH GEO archive under ID codes GSE111057* ."

RESULTS

Dietary sterols influence adult midgut enteroendocrine cell number

The *Drosophila* midgut completes development shortly after adult eclosion, (Ohlstein and Spradling, 2006; Takashima et al., 2013; Marianes and Spradling, 2013) like the mammalian intestine, which develops rapidly after birth. Delayed differentiation is proposed to allow intestinal metabolism to adapt to an individual's nutrient environment (reviewed in Reynolds et al., 2015). We observed a delay in the appearance of intestinal SREBP signaling activity (Figure 1A-B), a key pathway in the regulation of lipogenesis (Brown and Goldstein, 1997; Kunte et al., 2006). Only sparse, low level activity is present in the intestine of newly eclosed flies (Figure 1A), consistent with previous studies (Reiff et al., 2015). In contrast, the pathway is highly activated in the posterior midgut of 5-day old flies (Figure 1B). Consequently, we investigated whether midgut differentiation in young adults is influenced by the lipid content of their initial diet. We collected late stage pupae and allowed these animals to eclose and feed on either a control or lipid-depleted diet for 10 days. We then dissected these flies and stained both the anterior and posterior midgut with markers to assess their cellular composition (Figure 1C).

We examined the distribution of midgut cell types in adult animals fed a lipid-depleted diet, and observed a significant decrease in posterior ee cells (recognized by Prospero staining) relative to controls (Figure 1D-E). This reduction was not observed in the anterior midgut (Figure 1H,I). To confirm that the absence of dietary lipids caused the

Figure 1. Dietary sterols influence adult midgut enteroendocrine cell number. (A-B) Midguts from 6-12 hour old (A) or 5 day old (B) adult females. SREBP reporter (green) DAPI (blue). Scale bar = 400μm. (C) Experimental strategy to test the effects of diet on differentiation. (D-K) Posterior (D-G) or Anterior (H-K) midgut regions from animals fed a control diet (CD) (D,H), lipid-depleted diet (LD) (E, I), or lipid-depleted diet supplemented with 1X cholesterol (1X C, Fig. S1B) or 4X cholesterol (4X C) (F, J). DAPI (blue); Prospero (red). Scale bar = 40μm. (G, K) % enteroendocrine (ee) cells (Prospero$^+$) relative to total posterior (G) or anterior (K) cells. Circles show individual values color-coded for diet as indicated (N = 20 for all samples). Bar = Average value; *** = $p < 0.005$ (t-test). (L-O) Notch signaling reporter *GBE-Su(H)-GAL4* driving *UAS-mCD8::GFP* in posterior midgut. Animals were fed on CD (L), LD (M) or 4X C (N), for 10 days prior to analysis. DAPI (blue); GFP (green). Inset scale bar = 10μm. (O) % of total cells with Notch signaling (GFP$^+$) in a 5000 μm^2 field. GFP$^+$ cells were subdivided by ploidy based on nuclear size and DAPI intensity: blue (< 4C), red (4C-8C), green (>8C).

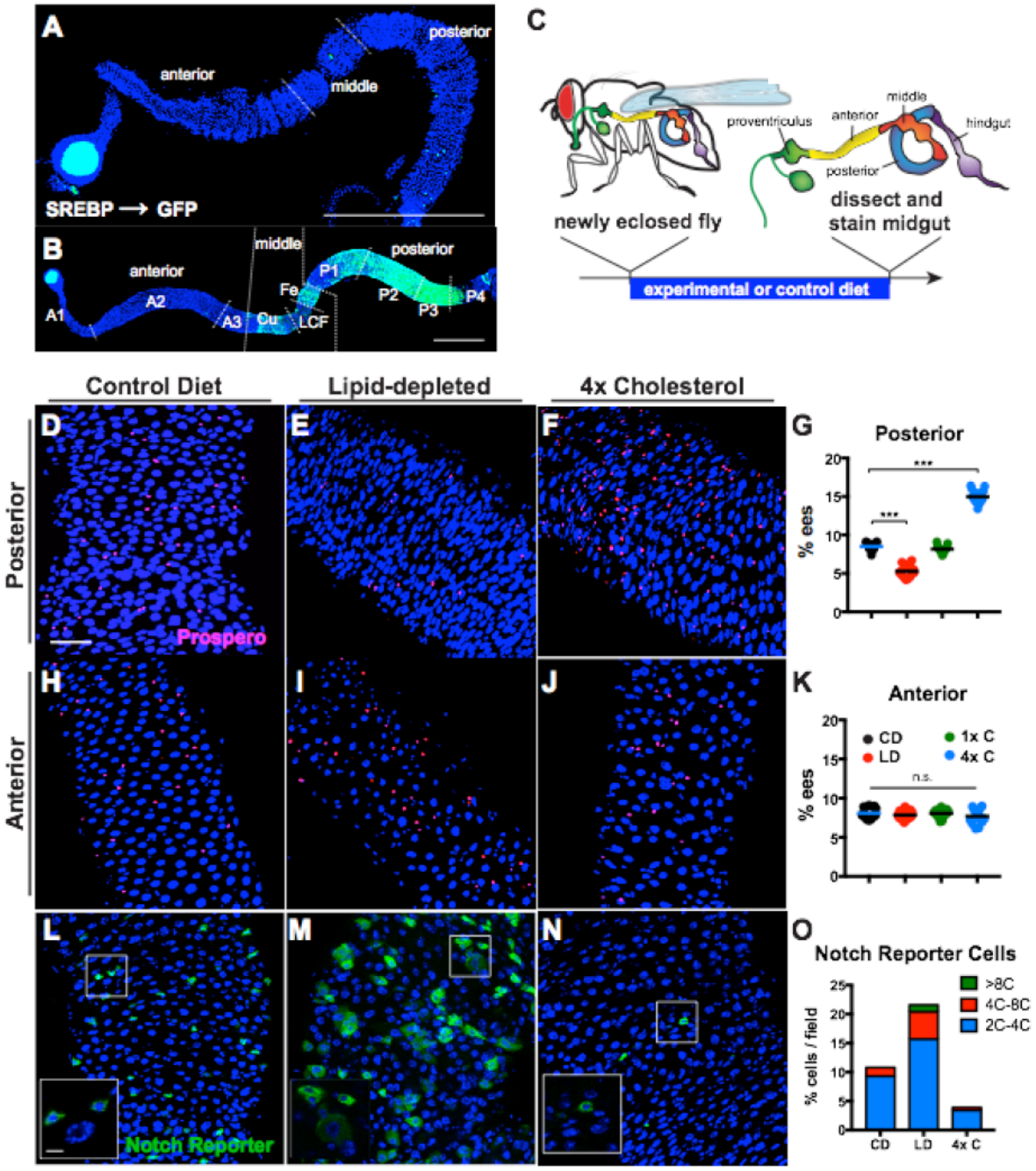
A
anterior
middle
posterior
SREBP → GFP
B
anterior
middle
posterior
A1
A2
A3
Cu
Fe
LCF
P1
P2
P3
P4
C
proventriculus
anterior
middle
posterior
hindgut
newly eclosed fly
dissect and stain midgut
experimental or control diet
Control Diet
Lipid-depleted
4x Cholesterol
Posterior
Anterior
D
E
F
G
Posterior
% ees
***
***
H
I
J
K
Anterior
CD
LD
1x C
4x C
n.s.
L
M
N
O
Notch Reporter Cells
% cells / field
>8C
4C-8C
2C-4C
CD
LD
4x C
Prospero
Notch Reporter

reduction in ee number, we fed newly eclosed flies a lipid-depleted diet supplemented with a single lipid species in the form of cholesterol, fatty acid, or triglyceride, and found that providing these dietary metabolites prevented the reduction in ee number (Figure1G, Figure S1B,E-H). The effect was specific to the period of initial adult gut development, because flies shifted to a lipid-depleted diet after one week on control media did not show a significant change in ee number 10 days post-shift (Figure S1D).

To determine whether elevated dietary lipid levels could likewise affect ee number, we supplemented a lipid-depleted diet with high levels of specific lipid species. Increasing the concentration of dietary fatty acid resulted in death within a week of feeding, however, animals fed a high cholesterol diet are viable and fertile. In newly eclosed animals fed a diet with four times the amount of cholesterol in a control lab diet the frequency of posterior ee cells was significantly increased (Figure 1F). When cholesterol supplementation commenced one week after eclosion, this increase did not occur, even after 14 days of high cholesterol feeding (Figure S1D). We found that, as expected, growth on a lipid-depleted or 4X cholesterol diet significantly changed the levels of intestinal cholesterol and cholesterol ester (Figure S1C). Since *Drosophila* are sterol auxotrophs, we fed newly eclosed flies on lipid-depleted media supplemented with 4x ergosterol, the major yeast sterol and observed a similar increase in the percentage of ee cells in the posterior midgut (Figure S1G-I). Cholesterol supplementation or depletion does not act by altering rates of ISC division, because the effects of these treatments on the mitotic index (ISC divisions) did not correlate with ee production (Figure S1K). Furthermore, ee's did not change in frequency due to altered death rates, because the number of TUNEL-positive cells per midgut was unchanged following cholesterol

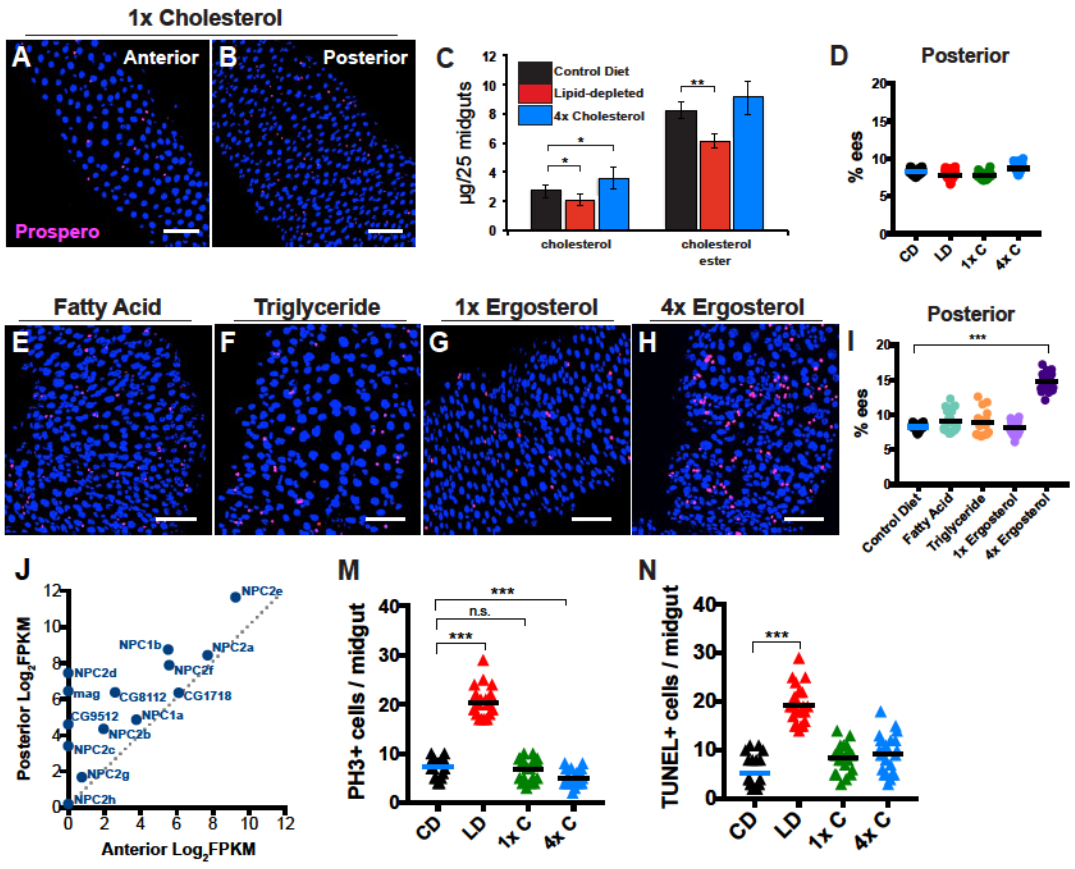

Supplemental Figure S1. Dietary sterols, specifically, mediate changes in posterior midgut differentiation. Anterior (A) or posterior (B) midguts from animals fed a lipid-depleted diet supplemented with 1X cholesterol (1X C). DAPI (blue), Prospero (red). C) cholesterol or cholesterol ester per 25 midguts for animals raised on the indicated diets. Bars = +/- SD, * = $p < 0.05$, ** = $p < 0.01$ (t-test). D) % ee cells relative to total posterior cells for animals fed a control diet for ten days after eclosion, and then switched to the indicated diets for ten days. Circles show individual values color-coded for diet: control diet (CD, black), lipid-depleted diet (LD, red), 1X cholesterol diet (1X C, green), 4X cholesterol (4X C, blue). Bar = Average value. N = 15 for all samples. (E-H). Posterior midguts from animals fed on diets supplemented with fatty acid (E); triglyceride (F); 1x ergosterol (G), 4x ergosterol (H). DAPI (blue); Prospero (red); Scale bar =40 µm. (I) % enteroendocrine (ee) cells relative to total posterior cells for animals raised on the indicated diets (E-H). Circles show individual values color-coded for diet as indicated (N = 15 for all samples). Bar = Average value; *** = $p < 0.001$ (t-test). J) Average gene expression values for the indicated NPC genes from the triplicate RNAseq from posterior (y-axis) vs anterior midgut (x-axis) showing higher expression of most in posterior. (K-L) Number of phospho-histone H3 (PH3) positive cells (K) or TUNEL positive (L) cells per posterior midgut from animals raised on the indicated diets. Triangles show individual values color-coded for diet as indicated (N = 18 for all samples). Bar = Average value; *** = $p < 0.001$, n.s. = not significant, (t-test).

supplementation and cell death increased rather than decreased following lipid depletion (Figure S1L).

Notch signaling regulates the differentiation of ISCs into enterocytes or enteroendocrine cells. To determine whether Notch pathway activation is affected by dietary lipids, we used a reporter for Notch signaling, *GBE-Su(H)-GAL4*, and found that animals fed a low cholesterol diet had significantly more midgut Notch signaling activity than animals fed a control diet (Figure 1L,M). Moreover, a lipid-depleted diet caused Notch signaling activity in enteroblasts to remain high for an extended period as they developed into enterocytes as seen by poyploidization (Figure 1M,O). In contrast, animals fed a 4X cholesterol-supplemented diet had significantly fewer cells with Notch reporter activity (Figure 1N,O). This suggests that increasing or reducing dietary cholesterol levels decreases or increases the level and kinetics of Notch signaling during differentiation, and hence increases or reduces enteroendocrine cell production, respectively.

Hr96 mediates cholesterol-dependent control of enteroendocrine cell number

Physiological effects of dietary cholesterol on enteroendocrine cell number would require cholesterol uptake and cellular utilization, pathways regulated by the nuclear hormone receptor Hr96 (Horner et al., 2009). Consequently, we analyzed $Hr96^{1}$ null mutant animals, fed a control diet. $Hr96^{1}$ midguts contained significantly fewer ee's compared to heterozygous controls in the posterior region (Figure 2A-B), and also throughout the midgut (Figure S2A-H). In the posterior this reduction strongly resembles

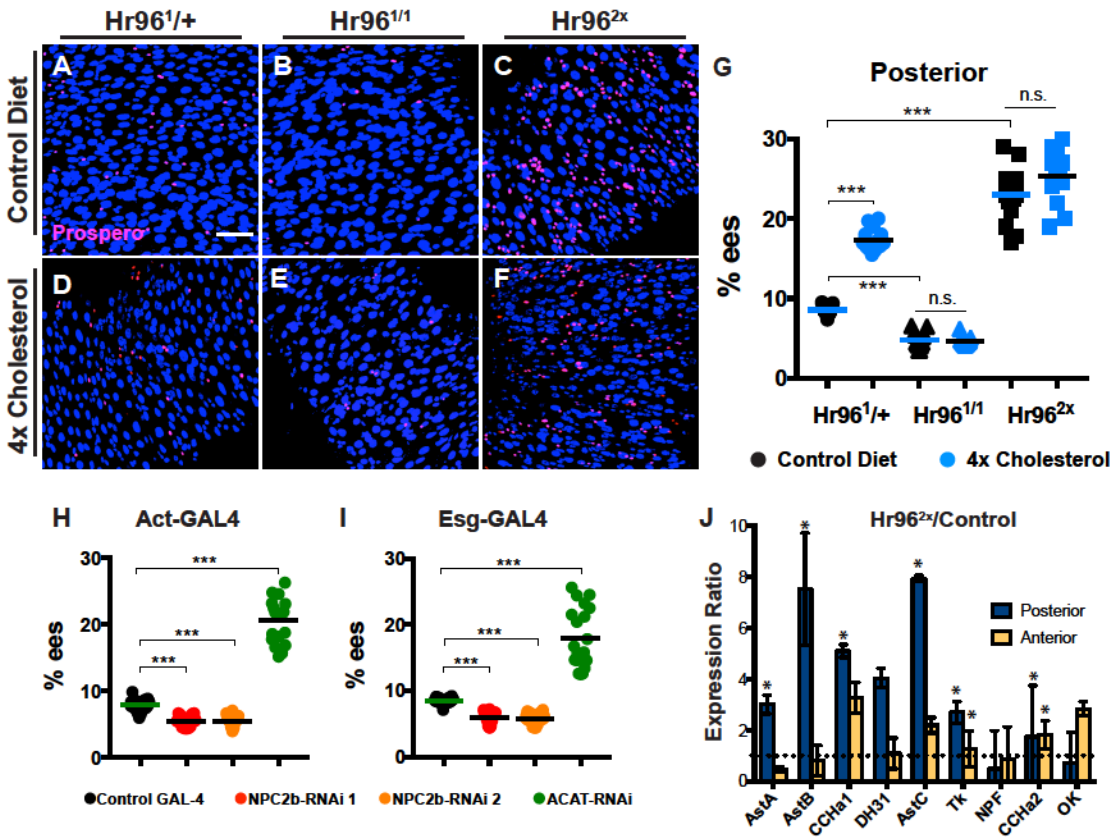

Figure 2. Hr96, NPC2b and ACAT mediate sterol availability and enteroendocrine cell number. (A-F) Posterior midguts from animals of the indicated genotypes following culture on the indicated diets. (A,D) *Hr96*^{1} / + (as a control); (B,E) *Hr96*$^{1/1}$; (C,F) *Hr96*^{2X}. Animals were fed a control diet (A-C) or 4X cholesterol-supplemented diet (D-F) for 10 days prior to analysis. DAPI (blue); Prospero (red); scale bar = 40µm. (G) % ee cells relative to total posterior cells. Data points show individual values shape-coded for genotype and color-coded for diet as indicated (N = 15 for all samples). Bar = Average value; *** = $p < 0.005$ (t-test), n.s. = not significant. (H-I) % ee cells relative to total midgut posterior cells for animals expressing the indicated RNAi constructs driven in enterocytes by Act-GAL4 (H) or in ISCs and enteroblasts by esg-GAL4 (I) and raised on a control diet. Midgut images for these experiments are in Fig. S2L-O: RNAi control is in Fig. S2P. (J) The relative expression based on triplicate RNAseq in anterior (yellow) or posterior (blue) midguts of the nine known enteroendocrine peptide hormone genes from *Hr96*^{2X} animals (elevated ee number) compared to controls. * = Significant increases compared to control (t-test), p-value < 0.05. bars - standard deviation.

the effects of a lipid-depleted diet on young wild type adults, since ee differentiation during early adulthood in this region will be affected when cholesterol levels are reduced either via diet or *Hr96* mutation. Most ee differentiation in the anterior and middle midgut occurs prior to adult eclosion, which explains the insensitivity of this region to adult dietary cholesterol restriction (Fig. 1K), but its sensitivity to *Hr96* mutation, which would effectively reduce cholesterol and influence Notch signaling during ee differentiation both before and after adulthood.

We investigated whether the normal gene dosage of *Hr96* is rate-limiting for sterol utilization by examining midguts from animals carrying two tandem copies of *Hr96* on each homolog ($Hr96^{2X}$) (Sieber and Thummel, 2009). $Hr96^{2X}$ flies contained significantly more enteroendocrine cells in the posterior midgut (Figure 2C) and also in middle and anterior regions (Figure S2C,G), as expected if $Hr96^{2X}$ increases ee differentiation both before and after eclosion. Interestingly, a 4X sterol diet did not further increase ee number in $Hr96^{2x}$ animals beyond the levels observed on a control diet (Figure 2C,F-G). Over-expressing *Hr96* in enterocytes using *Myo1A-GAL4* was sufficient to increase ee number relative to controls (Figure S2I-K). This suggests that increased dietary sterols taken up and processed by the over-expressing enterocytes may be transferred to ISCs/EBs where they would depress Notch signaling and enhance ee cell differentiation.

Drosophila has two NP1 class C genes, and eight NP2 class C genes, and several of these genes are regulated by *Hr96* (Horner et al., 2009). These include *Npc1b* which is required for dietary cholesterol absorption (Voght et al., 2007), and at least two *Npc2* class genes involved in intracellular cholesterol trafficking, *Npc2a* and *Npc2b*

Supplemental Figure S2. Hr96 affects the production of ee cells throughout the midgut. Hr96 affects the production of ee cells in the Anterior (A-D) and middle (E-H) midguts from animals of the indicated genotypes: (A,E) $Hr96^{1/+}$ (control); (B,F) $Hr96^{1/1}$; (C,G) $Hr96^{2X}$. (D,H) % ee cells relative to total anterior (D) or middle cells (H) for animals of the indicated genotypes. Individual values are shape-coded by genotype (N = 10 for all samples). Bar = Average value; *** = $p < 0.001$ (t-test). (I-K) Posterior midguts from animals raised on a control diet in which myo1A-GAL4 alone (control) (I) or myo1A-GAL4::UAS-Hr96 (J) were expressed in enterocytes. (K). % ee cells for animals shown in I, J. (N = 10 for all samples). Bar = Average value; *** = $p < 0.001$ (t-test). (L-O) Posterior midguts of control diet raised animals expressing either Npc2b-RNAi (L,N) or ACAT-RNAi (M) driven by either act-GAL4 (L,M) or esg-GAL4 (N,O). (P) qPCR verification that the RNAi lines (color coded as in Fig. 2H,I) reduce midgut RNA levels. DAPI (blue); Prospero (red); Scale bar =40 μm. Q) The relative expression based on triplicate RNAseq from posterior midguts of $Hr96^{1/1}$ compared to controls ($Hr96^{+/1}$) of a panel of genes known to function genetically in Notch signaling. * = Significant fold change.

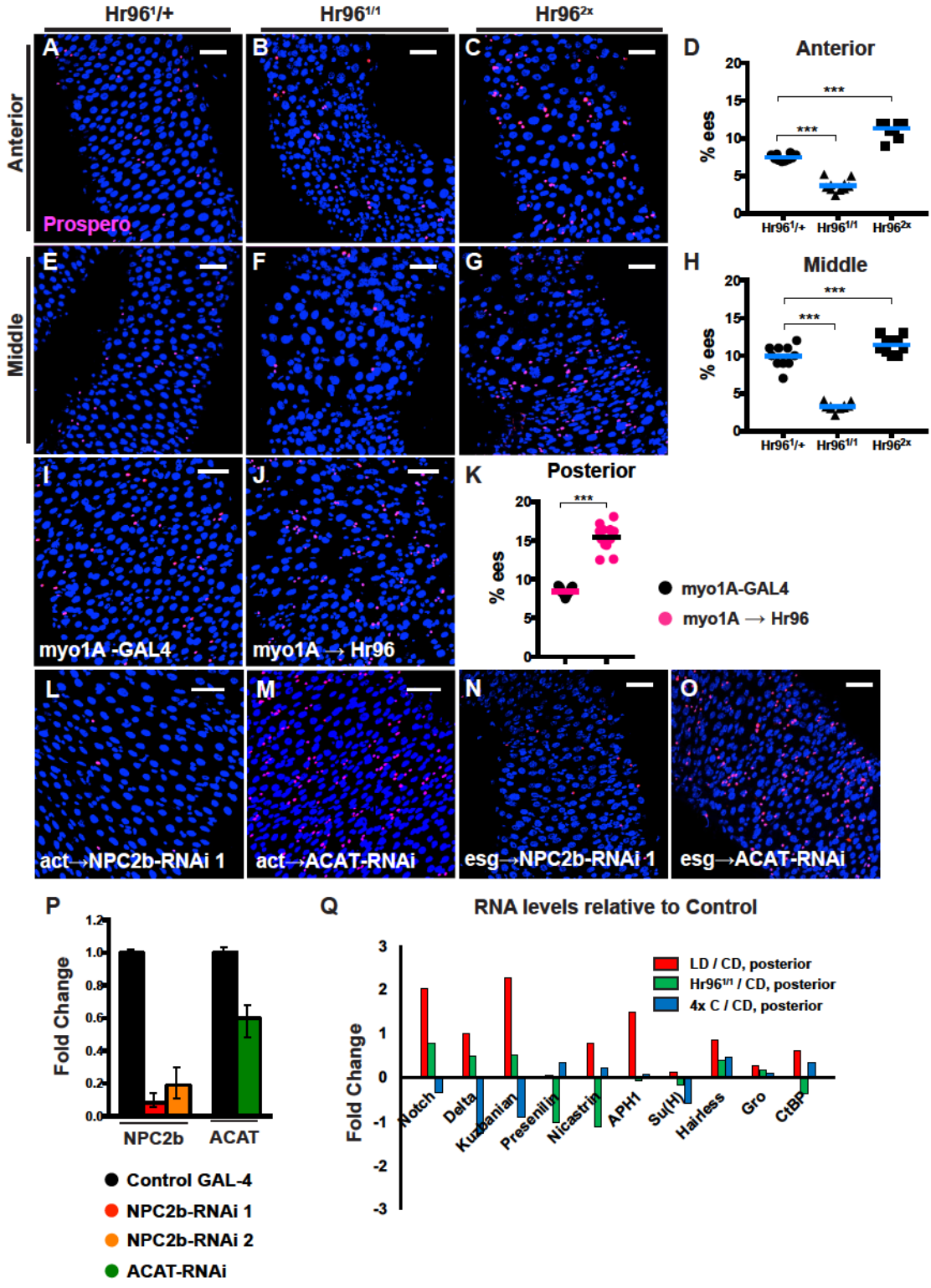
Hr96¹/+
Hr96¹/¹
Hr96²ˣ
Anterior
Middle
A
B
C
Prospero
D
Anterior
% ees
***
***
Hr96¹/+
Hr96¹/¹
Hr96²ˣ
E
F
G
H
Middle
% ees
***
***
Hr96¹/+
Hr96¹/¹
Hr96²ˣ
I
J
myo1A -GAL4
myo1A → Hr96
K
Posterior
% ees
***
myo1A-GAL4
myo1A → Hr96
L
M
N
O
act→NPC2b-RNAi 1
act→ACAT-RNAi
esg→NPC2b-RNAi 1
esg→ACAT-RNAi
P
Fold Change
NPC2b
ACAT
Control GAL-4
NPC2b-RNAi 1
NPC2b-RNAi 2
ACAT-RNAi
Q
RNA levels relative to Control
Fold Change
LD / CD, posterior
Hr96¹/¹ / CD, posterior
4x C / CD, posterior
Notch
Delta
Kuzbanian
Presenilin
Nicastrin
APH1
Su(H)
Hairless
Gro
CtBP

(Huang et al., 2005; 2007). To examine whether *Hr96* acts on ee number by controlling sterol transport genes, we used two different RNAi lines to suppress the *Hr96* target gene *Npc2b* in the adult flies (Fig. S2R). The posterior midguts of animals expressing either RNAi construct contained fewer ee's compared to controls (Figure 2H; Figure S2L-M).

This was similar to the behavior of animals on a lipid-depleted diet, consistent with the predicted inability of *Npc2b* mutant animals to take up and utilize sterols. Interestingly, knocking down *Npc2b* only in stem cells and undifferentiated cells using esg-GAL4 in the intestine still reduced ee number (Figure 2I; Figure S2O-P). Thus, altering cholesterol transport and availability only in undifferentiated cells is sufficient to influence the differentiation of intestinal stem cell daughters.

Another important and conserved gene required for steroid metabolism in mammals and *Drosophila* is ACAT, which mediates sterol esterification, transport and storage. We used RNAi to silence the expression of *CG8112*, the Drosophila *ACAT* homolog (Fig. S2R; Horner et al., 2009), and found a subsequent increase in the percentage of ee's in the midgut, similar to the effects of high dietary cholesterol (Figure 2H-I, Figure S2N,Q). This is consistent with the expectation that ACAT knock-down will increase free intracellular sterols. These experiments strongly support the view that the *Hr96* and *Npc2b*-dependent uptake of dietary sterols in the midgut influences the differentiation of enteroendocrine cells in young adults.

To address the autonomy of *Hr96* function, we generated $Hr96^{1}$ homozygous ISC clones and stained them for a clonal marker and Delta (Figure 2K-L). Clonal mutant cells showed higher Delta immunofluorescence and a greatly increased frequency of

Delta persistence in pairs (Fig. 2L), as expected if *Hr96* function is required cell autonomously.

Dietary lipids increase the abundance of diverse posterior enteroendocrine cell types

Enteroendocrine cells comprise multiple subtypes expressing different peptide hormones that are organized regionally along the anterior-posterior midgut axis, presumably in response to transcription factor differences (Marianes et al., 2013; Veenstra and Ida, 2014). All these ee subtypes are generated from ISCs and their differentiation is influenced by Notch signaling in a similar manner. If dietary lipids modulate ee differentiation primarily through changes in Notch signaling, then the production of all classes of ee cells in posterior regions should be affected. In contrast, only one or a few subclasses of ee's might be affected if dietary lipids only stimulate cells that function in concert with lipid-metabolizing enterocytes. To assess the diversity of ee subtypes following dietary or genetic treatments, we performed RNAseq in triplicate on anterior and posterior midguts from wild type animals fed a control, lipid-depleted, or cholesterol-supplemented diet. Parallel studies were done on anterior and posterior midguts from $Hr96^{1}$ and $Hr96^{2X}$ mutants.

The results of these studies strongly support the view that dietary lipids affect the differentiation of all subclases of ee cells by altering Notch signaling. Since $Hr96^{2X}$ animals contain the largest increase in enteroendocrine cells, approximately three-fold in the posterior, we examined the expression levels of known enteroendocrine hormone genes in $Hr96^{2X}$ midguts to query which ee subtypes were likely to have increased. Six of the seven enteroendocrine hormone genes known to be expressed in posterior ee cells

(Marianes et al., 2013; Veenstra and Ida, 2014) were significantly increased 3-8 fold in posterior midguts from *Hr96*^{2X} animals compared to controls (Fig. 2J). The bHLH transcription factor Dimmed, which mediates peptide secretion via the large dense core vesicle pathway used by ee cells (Beehler-Evans et al., 2015), was also significantly increased (1.27 +/- 0.18 vs 0.76 +/- 0.26 $p<0.05$, t-test) in *Hr96*^{2X} posterior midguts, consistent with the overall increased number of functional, neuropeptide-secreting ee cells. Expression of RNAs encoding two enteroendocrine hormones, AstC and Orcokinin, also rose in the anterior midgut of *Hr96*^{2X} animals (Figure 2J). An enteroendocrine cell subtype expressing these hormones has been described in both the anterior and middle midgut (Veenstra and Ida, 2014).

Dietary sterols modulate Delta levels and trafficking

A lipid-depleted diet only produced modest increases in Notch pathway gene expression (Fig. S2Q). Consequently, to better understand the dramatic changes in Notch signaling induced by such a diet (Fig. 1L-O) we immunostained the Notch ligand Delta to visualize its expression and subcellular localization in the posterior midguts of 10-day old animals fed various diets. Delta was found in cytoplasmic vesicles in control animals within scattered diploid cells that correspond to ISCs (Figure S3A; Ohlstein and Spradling, 2006). ISCs from animals fed a lipid-depleted diet consistently stained more strongly for Delta compared to controls (Figure S3B,D). Moreover, in these animals Delta staining could be readily detected within daughter enteroblasts, generating pairs of Delta-labeled cells (Figure S3B). Since posterior midgut size did not increase as a result of lipid depletion, these cell pairs were likely caused by reduced Delta turnover in

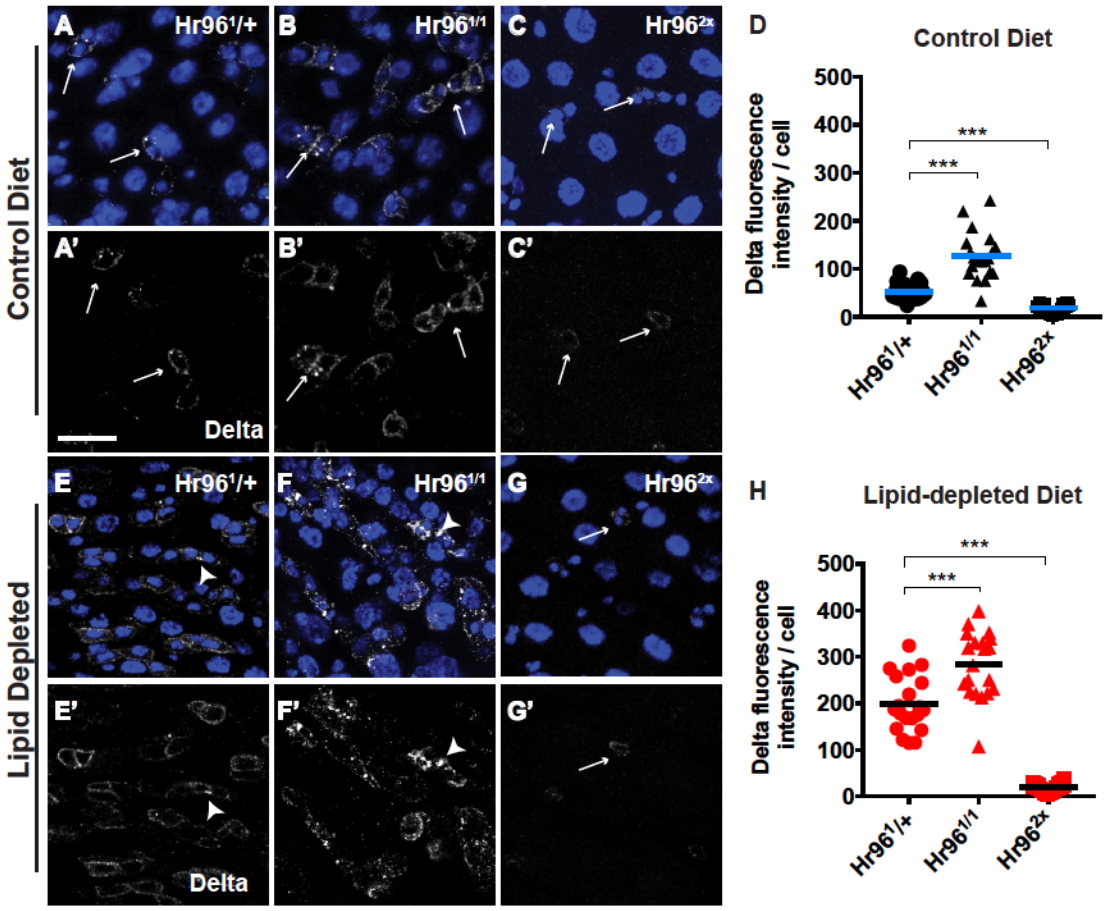

Figure 3. Hr96-mediated sterol metabolism regulates Delta protein levels and trafficking. Posterior midguts are shown from (A,E) *Hr96*$^{1/+}$ (B,F) *Hr96*$^{1/1}$ and (C,G) *Hr96*^{2X} animals fed a control diet (A-C) or a lipid depleted diet (E-G) for 10 days prior to analysis. DAPI (blue) and Delta (white). arrows: ISCs (A,C); ISC-enteroblast pairs (B). (D,H) Corrected fluorescence intensity per Delta^{+} cell is plotted in arbitrary units from animals of the indicted genotypes and is comparable between all 6 experiments. Individual values are shape-coded for genotype as indicated. N = 15 (D); N = 20 (H). Bar = Average value; *** = $p<0.005$; (t-test). Scale bar = 20µm for all images. (I-J) Flies were raised on food containing 30µM vehicle (I) or NMS-873 (J) and after four days posterior midguts were analyzed for Delta expression. (K) Integrated Delta fluorescence (arbitrary units) of cells from I, J showing 4-fold increase in Delta staining by the p97 inhibitor. (L) Survival plot of control flies or *Hr96*^{1} mutant flies treated with the indicated concentrations of NMS-873.

Supplemental Figure S3. Hr96 cell autonomously regulates the lipid-dependent accumulation of Delta protein. (A-C) Posterior midguts stained for Delta (white) from wild type animals raised on the indicated diets: (A) control; (B) lipid-depleted; (C) 4X cholesterol; DAPI (blue); A'-C' (Delta channel alone). Scale bar =5 μm. D) Delta fluorescence per cell from the animals in A-C. Circles show individual values color-coded for diet as indicated (N = 20 for all samples). Bar = Average value; ** = $p < 0.01$, *** = $p < 0.001$ (t-test). (E-H) Posterior midguts stained for Delta (white) from animals with RNAi-induced knockdown of Npc2b or ACAT in enterocytes and raised on control diets: (E) act-GAL4 control; (F) NPC2b-RNAi 1; (G) NPC2b-RNAi2; (H) ACAT-RNAi; DAPI (blue); E'-H' (Delta channel alone). Scale bar =10 μm. arrows: A, C, E, H (ISCs); B, F,G (ISCs and downstream cells). I) Delta fluorescence per cell from the animals in E-H. Circles show individual values color-coded for diet as indicated (N = 20 for all samples). Bar = Average value; ** = $p < 0.01$, *** = $p < 0.001$ (t-test). Control (J) and $Hr96^{1/1}$ homozygous (K) MARCM clone (stained for Delta (J',K') and clonal marker (green). arrowhead (J,J') shows and ISC-EB pair with little Delta in EB; arrowhead in (K,K') shows a 2-cell clone with increased and persistent Delta staining. Arrow in (K,K') shows single, wild type ISC with normal Delta staining. Scale bar = 20 μm. L) Quantitation of the increased frequency of cell pairs in Hr96 mutant clones. M) Delta fluorescence per cell in controls vs Hr96 clones from J,K.

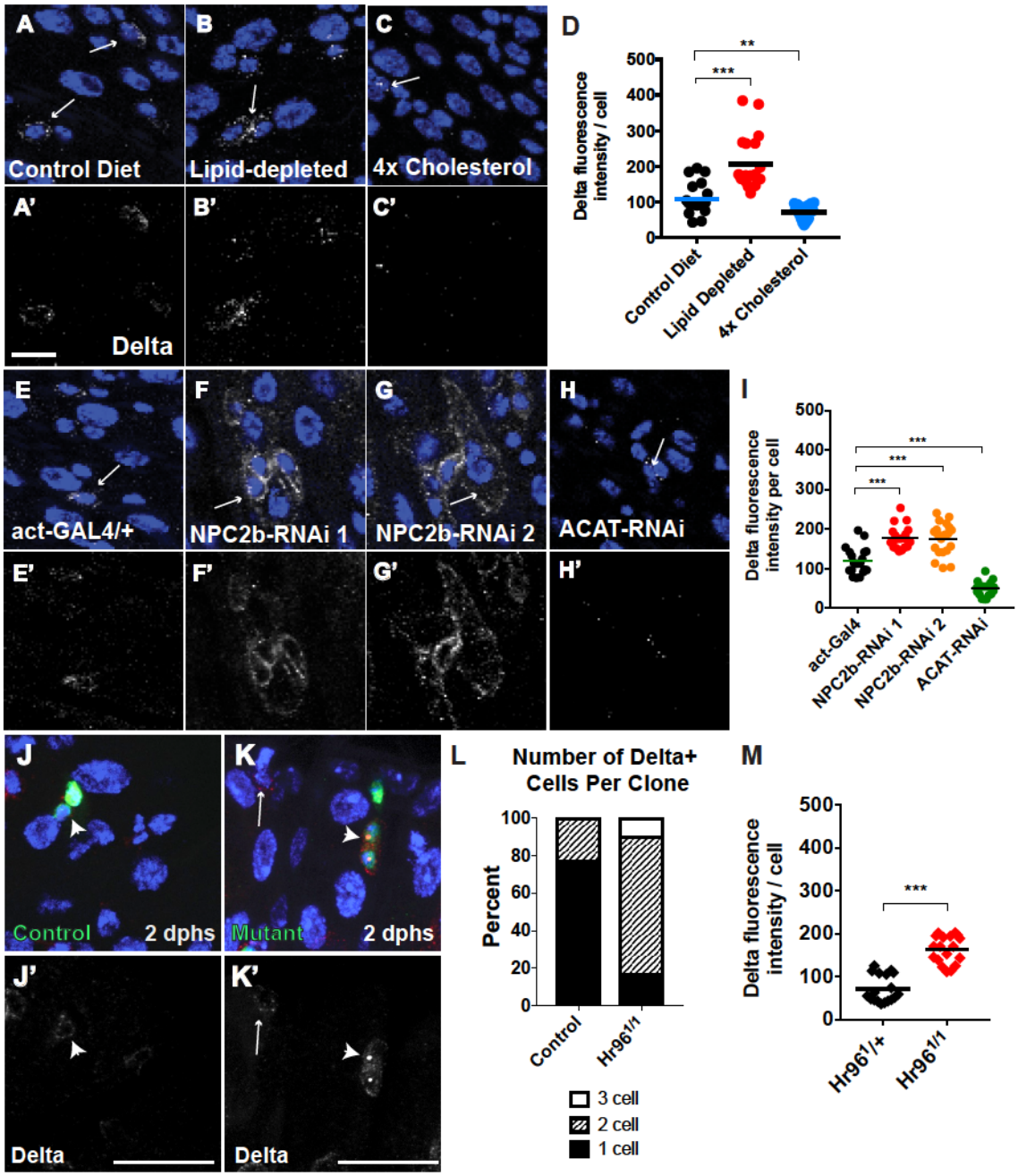
A
Control Diet
B
Lipid-depleted
C
4x Cholesterol
A'
Delta
B'
C'
D
Delta fluorescence intensity / cell
500
400
300
200
100
0
**
***
Control Diet
Lipid Depleted
4x Cholesterol
E
act-GAL4/+
F
NPC2b-RNAi 1
G
NPC2b-RNAi 2
H
ACAT-RNAi
E'
F'
G'
H'
I
Delta fluorescence intensity per cell
500
400
300
200
100
0
***
***
***
act-Gal4
NPC2b-RNAi 1
NPC2b-RNAi 2
ACAT-RNAi
J
Control
2 dphs
K
Mutant
2 dphs
J'
Delta
K'
Delta
L
Number of Delta+ Cells Per Clone
Percent
100
80
60
40
20
0
Control
Hr96^1/1
3 cell
2 cell
1 cell
M
Delta fluorescence intensity / cell
500
400
300
200
100
0
***
Hr96^1/+
Hr96^1/1

enteroblasts under lipid-deprived conditions rather than stem cell amplification divisions (O'Brien et al., 2011). Conversely, feeding young animals a high sterol diet reduced the level of Delta staining within ISCs (Figure S3C-D).

We examined Delta levels in animals mutant for cholesterol uptake genes to verify that these changes in Delta content depended on physiological lipid uptake. *Hr96*^{1} mutants on a normal diet showed elevated levels of Delta in ISCs compared to controls (Figure 3A-B). When these animals were grown on lipid-depleted media, the levels of Delta were further increased and abundant Delta-rich cytoplasmic vesicles were now readily apparent (Figure 3E-F). In contrast, Delta levels were scarcely detectable and foci were rare in *Hr96*^{2x} animals, even when fed a lipid-depleted diet (Figure 3C,G). *NPC2b* mutant animals, which like *Hr96*^{1} mutants are defective in cholesterol incorporation and mimic wild type animals on a lipid-depleted diet, showed higher levels of cytoplasmic Delta staining compared to control (Figure S3E-G). Like *Hr96*^{1}, in *Npc2b* RNAi animals, Delta protein expression persisted in enteroblasts and young enterocytes (Figure S3F-G), like control animals on a lipid-depleted diet (Figure 3E).

Taken together, these observations show that when lipids including cholesterol are low due to diet or a genetic defect, ISCs continue to proliferate but turn over Delta more slowly than normal. This change in Delta persistence matches the increased Notch signaling activity previously observed on lipid-depleted diets (Figure 1M) and is likely to favor EC over ee production from ISCs. Conversely, *Hr96*^{2x} animals on a control diet (Figure 3C) or *ACAT RNAi* animals on a control diet (Figure S3H) showed reduced Delta expression. This is similar to wild type animals fed a high sterol diet (Figure S3C) and is consistent with reduced Notch signaling activity (Figure 1N), a condition likely to favor

ee over EC production. These data strongly suggest that gut lipid uptake and utilization influences endomembrane lipid composition, and that these changes influence Delta abundance through their effects on Delta subcellular localization, trafficking and turnover.

Given that lipid-stimulated-ERAD requires the activity of p97 to facilitate the turnover of target proteins we hypothesized that p97 inhibition would mimic elevation of Delta levels seen in the intestine of *Hr96* mutants and in animals fed a lipid-depleted diet. Consistent with this prediction, treating flies with the allosteric p97-inhibitor, NMS-873, stimulated Delta protein accumulation, indicating that p97-mediated protein turnover regulates Delta protein levels (Figure 3I-K). Moreover, these data are consistent with the model that altering lipid levels in the intestine induces an ERAD-like degradation of Delta protein similar to what has been observed with proteins like HMG-CoA reductase (DeBose-Boyd, 2008). Consistent with the fundamental nature of this relationship between sterol metabolism and p97-mediated protein turnover we observed that, while control animals showed no defects in survival upon p97 inhibition, Hr96 mutants showed a pronounced sensitivity to decreases p97 activity (Figure 3L). This synthetic interaction between *Hr96* and p97 supports the idea that sterol homeostasis and p97 converge to regulate Delta, and potentially many other proteins, in the intestine.

Notch is also modulated by lipid uptake and utilization

We investigated whether the abundance and trafficking of Notch is also affected by dietary lipid utilization. Proper recycling of the Notch extracellular domain (NECD) is crucial for accurate Notch activation or suppression and is thought to couple to Delta

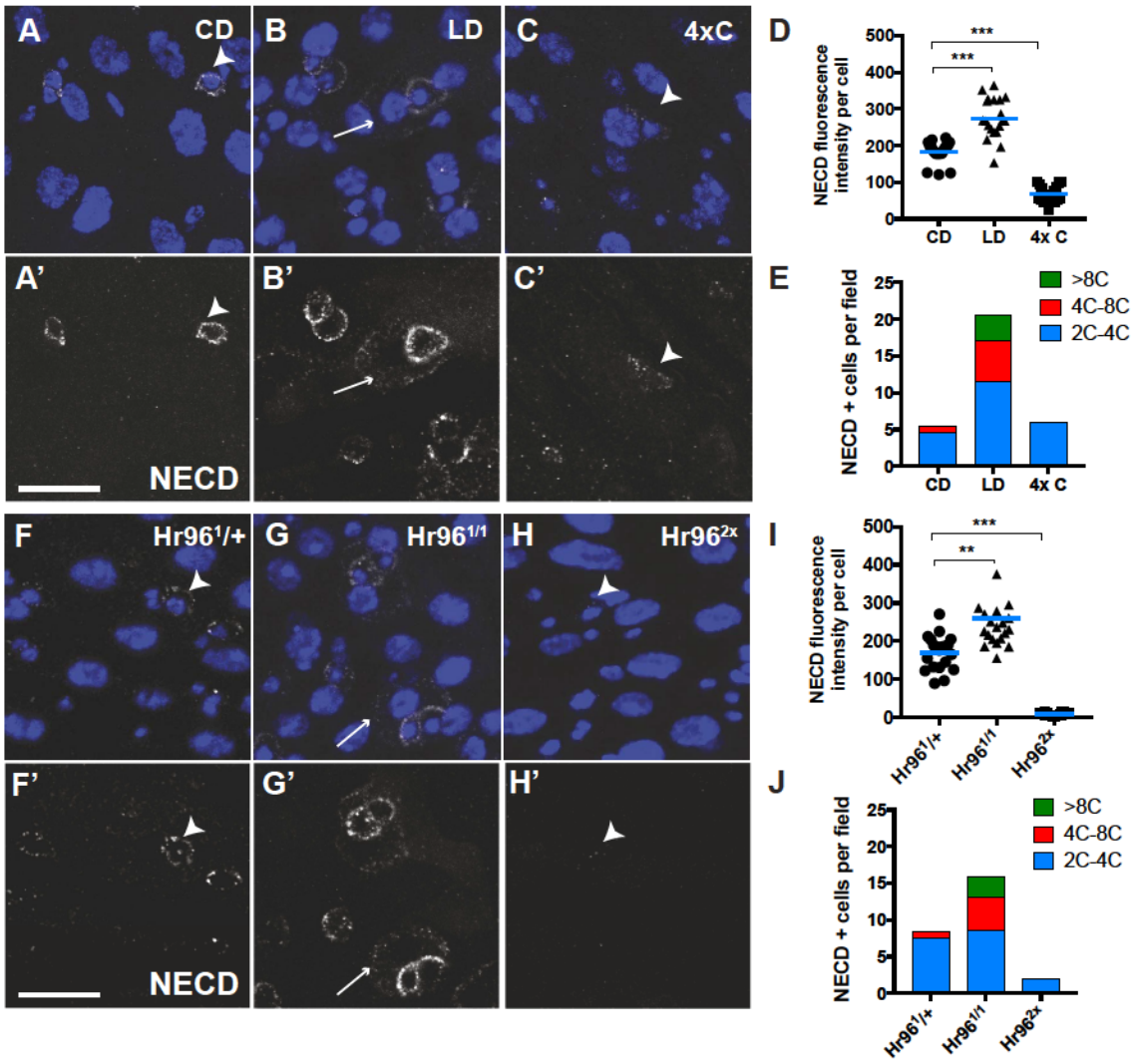

Figure 4. Diet and Hr96 regulate Notch extracellular domain (NECD) protein levels and trafficking. (A-C) DAPI (blue) and NECD (white) is shown in posterior midguts of wild type animals raised on a control (A, A'), lipid-depleted (B, B') or 4X cholesterol (C,C') diet, or from *Hr96*$^{1/+}$ (F) *Hr96*$^{1/1}$ (G) or *Hr96*^{2X} (H) animals raised on a control diet. (D,I) Corrected fluorescence intensity per NECD^{+} cell is plotted in arbitrary units from animals of the indicted diets or genotypes and is comparable between all 6 experiments. Individual values are shape-coded for genotype as indicated. N = 15 (D); N = 20 (I). Bar = Average value; *** = $p<0.005$; (t-test). (E,J) The % NECD-positive cells per field in the experiments plotted in (D,H) is shown according to ploidy, as colored coded. Scale bar = 10 μm for all images.

turnover (Coumailleau et al., 2009). If lipid depletion impairs Delta endosomal recycling or degradation, we reasoned that the NECD may also display aberrant turnover and trafficking. Using antibodies against the NECD we examined the intestines of flies fed a lipid-depleted diet and the intestines of *Hr96* mutants, and found that NECD staining was present in putative ISC-EB cell pairs (Figure 4B,E). In contrast, NECD was only detectable in single cells in control animals (Figure 4A,E). Furthermore, NECD-positive cells had less antibody staining in high sterol or Hr96 overexpression animals (Figure 4C,H). Taken together, these data further support the finding that cellular sterol levels strongly influence the trafficking and turnover of Notch pathway proteins, including Delta and Notch NECD. As with Delta protein, these results with NECD were paralleled by altering cholesterol metabolism with *Hr96* mutation (Figure 4F-G,I-J) or duplication (Figure 4H-J).

To regulate productive Notch signaling, cells internalize Delta and Notch proteins from the plasma membrane into early endosomes and then either send them back to the plasma membrane for another chance at activation, or retain them for progression into multivesicular bodies/late endosomes and then lysosomes where they are degraded (Fortini and Bilder, 2009). To investigate whether increased levels of Delta protein in lipid-depleted intestines were undergoing normal trafficking, we looked for colocalization of Delta and the late endosomal marker, Rab7 (Ghigo et al., 2005). We performed image analysis on particles of GFP tagged Delta and Rab7+ particles, and observed an increased fraction of rab-7 endosomes co-staining for Delta (Figure S4) in enterocytes of flies fed a lipid-depleted diet. However, vesicle trafficking within

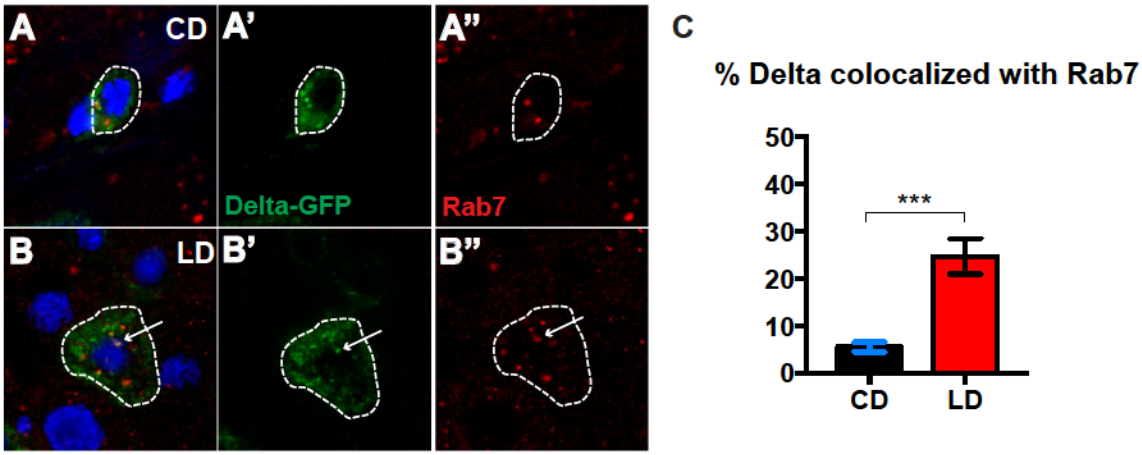

Supplemental Figure S4. Co-localization of Delta and Rab7 in midgut enterocytes from animals cultured on different diets. Midguts stained with Delta-GFP and Rab7 from animals (A) on a control diet (CD) and B) on a lipid-depleted diet (LD). C) % of cellular vesicles with Delta and Rab7 co-localized in ISCs from animals on a control diet (CD) or a lipid-depleted diet (LD). Scale bar = 10 μm. *** = $p < 0.001$ (t-test).

developing enterocytes appeared to be more abundant and complicated than in previous studies of Notch and Delta trafficking in neuroblasts or peripheral nervous system precursors, so no reliable insights into the mechanism of action of cholesterol could be deduced from these preliminary studies.

Sterol regulation of Delta is also observed in the ovary and in human cells

To investigate whether the relationship between cellular sterol levels and Notch signaling described above for the Drosophila midgut also applies to other tissues, we examined the Drosophila ovary. Oogenesis is highly dependent on efficient nutrient processing, since proteins, lipids, and carbohydrates, all initially processed by the midgut, are accumulated in a tightly regulated, stepwise manner to support the growing oocyte (Sieber and Spradling, 2015). Like midgut enterocytes and enteroendocrine cells, the follicle cells of the ovary also rely on Notch signaling to induce follicle cell differentiation at the mitotic-endocycle (ME) transition, and to coordinate somatic and germline development (Sun and Deng, 2005). Diet strongly influences the rate of follicle development and passage through checkpoints (Drummond-Barbosa and Spradling, 2001), so we used genetic manipulation of sterol metabolism to look for connections to Notch signaling.

Delta was present on membranes at only low levels in wild type mid-stage follicles (Figure 5A), consistent with previous reports (Bender et al., 1993). However, significantly more Delta was present on membranes from similarly staged *Hr96*^{1} mutant follicles (Figure 5B). Furthermore, large cytoplasmic Delta foci were observed in *Hr96*^{1} mutant follicles (Figure 5D), but not in controls (Figure 5C), reminiscent of the Delta foci

Figure 5. Delta and NECD levels and trafficking are specifically modulated by lipids in the ovary and in mammalian cells. Notch (A-D), NECD (F-G), or Lpr2 (I-J) immuofluorescence is shown in *Drosophila* ovarian follicles from $Hr96^{1/+}$ (A,C,F,I) or $Hr96^{1/1}$ (B,D,G,J). C and D show Delta expression in a large polyploid nurse cell. DAPI (blue), Delta (red). Scale bar = 50μm. (E) Corrected Delta fluorescence intensity is plotted in arbitrary units (R.F.U) from Control ($Hr96^{1/+}$) $Hr96^{1/1}$ or *NPC2b-RNAi* (Fig. S5B) follicles. ** = $p<0.01$; (t-test). (H) Corrected NECD fluorescence intensity is plotted in arbitrary units (R.F.U) from Control ($Hr96^{1/+}$) $Hr96^{1/1}$ or *NPC2b-RNA*i (Fig. S5D) follicles. ** = $p<0.01$; (t-test). (K-L) show HCT116 cells treated with vehicle (K), or Simvastatin (L) and stained with the fluorescent cholesterol-binding agent filipin, Scale bar = 25μm. (M,N) show HCT116 cells treated with vehicle (M), or Simvastatin (N) and stained for Notch1-ECD. Scale bar = 10μm. O. Integrated fluorescence per cell from M,N. *** = $p<0.001$.

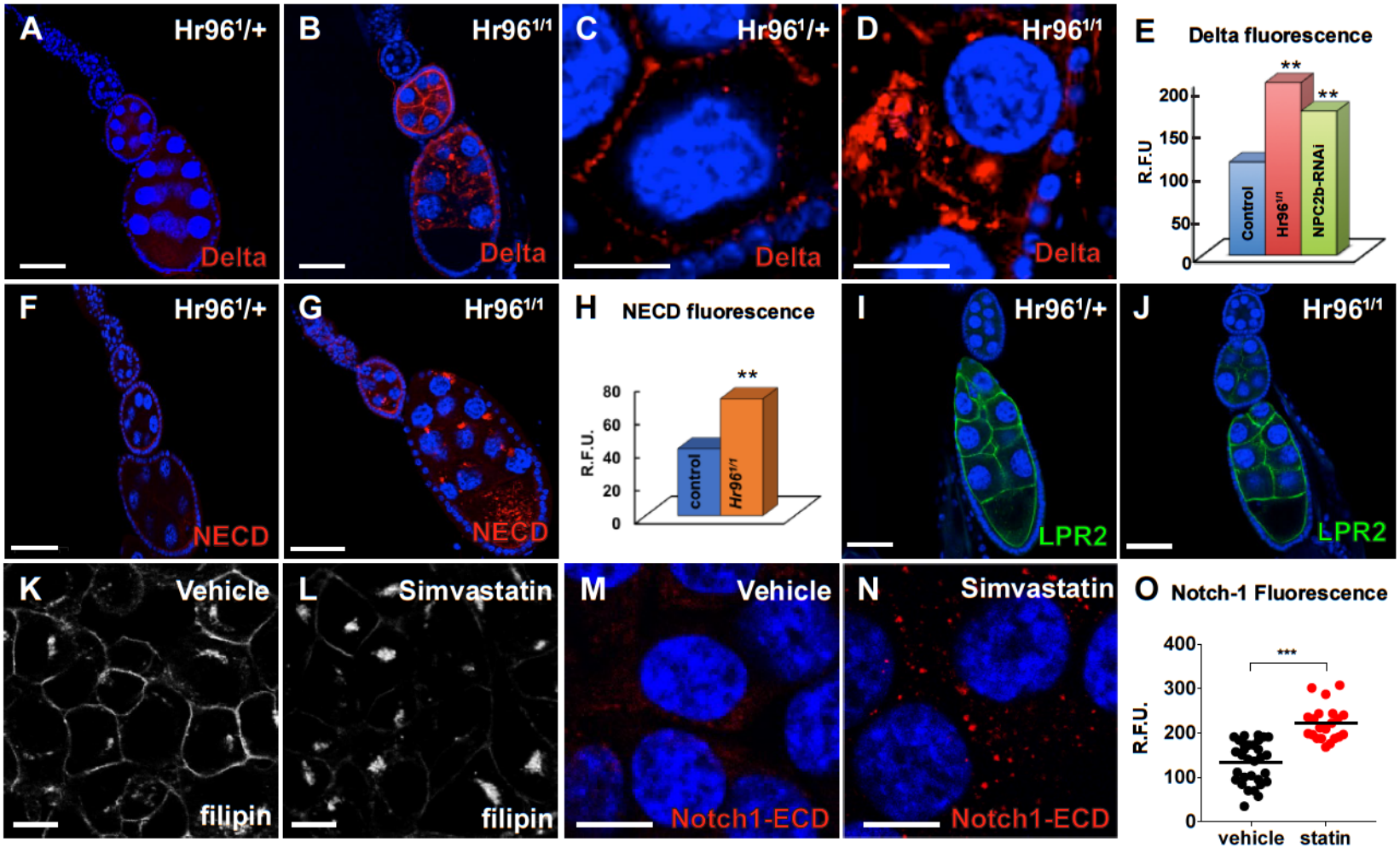
A
Hr96¹/+
Delta
B
Hr96¹/¹
Delta
C
Hr96¹/+
Delta
D
Hr96¹/¹
Delta
E
Delta fluorescence
R.F.U
200
150
100
50
0
**
**
Control
Hr96ⁱⁿ
NPC2b-RNAi
F
Hr96¹/+
NECD
G
Hr96¹/¹
NECD
H
NECD fluorescence
R.F.U.
80
60
40
20
0
**
control
Hr96¹/¹
I
Hr96¹/+
LPR2
J
Hr96¹/¹
LPR2
K
Vehicle
filipin
L
Simvastatin
filipin
M
Vehicle
Notch1-ECD
N
Simvastatin
Notch1-ECD
O
Notch-1 Fluorescence
R.F.U.
400
300
200
100
0
***
vehicle
statin

Supplemental Figure S5. Sterols regulate Notch signaling in cells with high metabolic demands. (A,B) Ovariole containing several ovarian follicles stained for Delta from control (A) or Npc2b-RNAi (B). (see quantitation in Fig. 5E.) (C,D). Ovariole containing several ovarian follicles stained for NECD from control (C) or Npc2b-RNAi (D). General and membrane staining is strongly increased. (E-H) Follicle cells stained with DAPI from an $Hr96^{1/+}$ (control) (E,G) or $Hr96^{1/1}$ (F,H) stage 10 (E,F) or stage 14 (G,H) follicle. Yellow arrows in (H) indicate excess nuclei that have degenerated. (I) The average number of follicle cells per visible side is greater in $Hr96^{1/1}$ compared to control. ** $p<0.01$ t-test. (J) % of ovarioles with PH3 staining is increased in $Hr96^{1/1}$ mutants. ** $p<0.01$ t-test. (K,L) (M,N). Ovariole containing several ovarian follicles stained for Hindsight (red) from $Hr96^{1/+}$ (control) (K) or $Hr96^{1/1}$ (L). DAPI (blue). Scale bar = 50□m. Similar levels of Sec61 expression in HCT116 cells treated with vehicle (M) or Simvastatin (N). Scale bar = 20μm. Western blot assaying Delta-like ligand 4 (DLL4) levels vs tubulin in HCT116 cells treated with vehicle (Veh.) or Simvastatin. Lanes are from independent assays. (P) Quantitation of O showing a significant increase in DLL4 expression relative to tubulin. (bars = average +/- SD) * = $P<0.05$ (t-test). Q. DLL4 staining relative to tubulin in HEK293 cells treated with vehicle alone or LXR agonist. Lanes are from independent assays. R) Quantitation of Q showing that average DLL4 levels relative to tubulin decreased significantly (bars = average +/- SD). ** = $P<0.01$ (t-test).

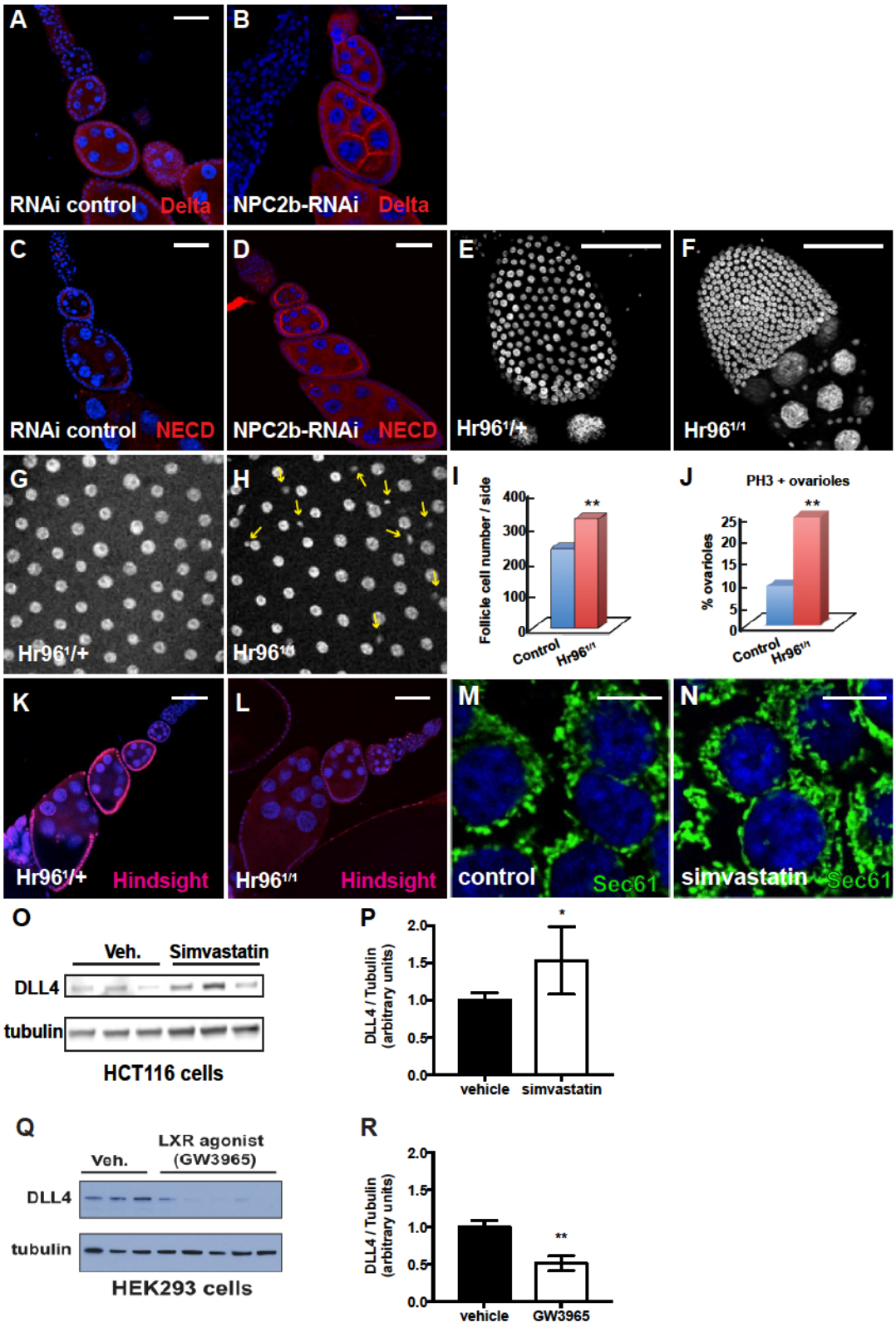
A
RNAi control Delta
B
NPC2b-RNAi Delta
C
RNAi control NECD
D
NPC2b-RNAi NECD
E
Hr96¹/+
F
Hr96¹/¹
G
Hr96¹/+
H
Hr96¹/¹
I
Follicle cell number / side
400
300
200
100
0
**
Control
Hr96¹/¹
J
PH3 + ovarioles
% ovarioles
25
20
15
10
5
0
**
Control
Hr96¹/¹
K
Hr96¹/+ Hindsight
L
Hr96¹/¹ Hindsight
M
control Sec61
N
simvastatin Sec61
O
Veh.
Simvastatin
DLL4
tubulin
HCT116 cells
P
DLL4 / Tubulin (arbitrary units)
2.0
1.5
1.0
0.5
0.0
*
vehicle
simvastatin
Q
Veh.
LXR agonist (GW3965)
DLL4
tubulin
HEK293 cells
R
DLL4 / Tubulin (arbitrary units)
2.0
1.5
1.0
0.5
0.0
**
vehicle
GW3965

in midgut ISCs and developing enterocytes. Similarly, we found *Hr96*^{1} ovaries displayed increased levels of NECD (Figure 5F) relative to controls (Figure 5E). Large NECD aggregates were present in stage 9-10 follicles of *Hr96*^{1} mutants (Figure 5F), but not controls (Figure 5E). Corresponding increases in membrane Delta and NECD were observed in ovaries from *NPC2b-RNAi* animals as well (Figure S5A-D). To determine whether these effects on protein levels and aggregation were specific to components of the Notch pathway, or affected other transmembrane proteins, we stained control and *Hr96*^{1} mutant follicles with an antibody against the LDLR homolog LpR2 and found no significant change in LpR2 levels or localization (Figure 5I-J). These observations argue that sterol levels have similar effects on Notch signaling components in ovarian cells as in the midgut.

Notch signaling regulates the ME transition in follicle cells during stage 5-6 of oogenesis (Sun and Deng, 2007). Late stage follicles in *Hr96*^{1} mutants had significantly more follicle cells than similarly staged controls (Figure S5E-F,I), indicating that the Notch-induced ME transition had been delayed. Moreover, *Hr96*^{1}-mutant stage 14 follicles (Fig. S5H) contained follicle cell nuclei that had been extruded from the follicular layer (arrows), further suggesting that a delayed or incomplete switch to the endocycle resulted in excess follicle cells (Figure S5G-H). Normally, the Notch-regulated gene *hindsight* (*hnt)* is expressed in follicle cells after the ME transition (Figure S5K). In contrast, *Hr96* mutants expressed Hnt slightly earlier than normal, but Hnt levels remained lower than in control follicles (Figure S5L) suggesting that altered Notch signaling ultimately delayed rather than accelerated normal follicle development. This

defect in Notch signaling may stem from the fact other sterol dependent pathways such as ecdysone signaling also function to regulate the M/E transition.

Since all the components linking intracellular sterol levels to Notch signaling are highly conserved between *Drosophila* and mammals, we investigated whether human cells show similar responses. We identified a human colon cancer cell line, HCT116, that responds to the statin Simvastatin by losing membrane cholesterol and accumulating it in internal vesicles (Fig. 5K-L), without altering the amount of ER (Fig. S5M-N). Simvastatin treated HCT-116 cells accumulated Notch1-ECD internally (Fig. 5M-O). Levels of the Delta-like Notch ligand 4 (DLL4) also increased following Simvastatin treatment (Fig. S5P-Q).

We identified another human cell line, HEK293, that expresses the cholesterol regulator LXR, as well as DLL4 and asked whether promoting intracellular reverse cholesterol transport with the LXR agonist GW3965 would affect DLL4 protein levels. DLL4 protein levels were consistent in cells treated with vehicle alone, but after treatment with the LXR agonist, DLL4 protein decreased significantly in 5 independent experiments (Figure S5Q-R). The results with both cell lines suggest that intracellular sterol levels act in a conserved manner on Notch ligand stability and Delta-Notch signaling in at least some mammalian cells.

Early lipid depletion reduces posterior ee numbers and establishes a scarcity metabolic state

Our observation that dietary lipids and cholesterol in particular enhance Notch signaling in the midgut and ovary raises the question of how such a connection affects

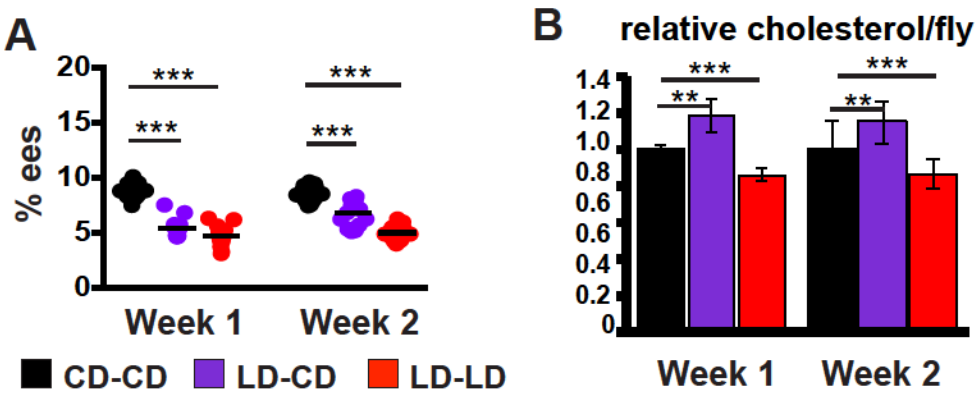

Figure 6. A lipid-depleted diet generates a persistent scarcity metabolic state. (A) A lower percentage of ee's is present in the posterior midgut of flies raised on a lipid-depleted diet for 7d and then shifted to control diet for 1 or 2 additional weeks (LD-CD: purple), than in flies raised continuously on a control diet (CD-CD, black). Flies raised and maintained on an LD diet (LD-LD, red) also differed. (N = 10); (B) Total body cholesterol per fly (relative to CD-CD values as 1.0) is greater in LD-CD treated animals. bars - standard deviation. ** = $p<0.01$, *** = $p<0.005$ (t-test).

animal physiology. For example, do changes in ee number mediated by dietary lipids during early adult life persist and influence the animal's response to a different dietary regime? To determine whether nutrients in the early diet influence metabolism after the diet has changed, we raised young flies on lipid-depleted food for one week to increase Notch signaling and decrease posterior ee number. We then transferred the flies to normal yeast food and observed that the reduction in posterior ee number persisted for at least two additional weeks (Figure 6A). Interestingly, flies raised initially on lipid-depleted media, during one week back on normal yeast food, accumulated 18% more whole body cholesterol per fly than animals that had eaten a normal diet beginning at eclosion (Figure 6B). This suggests that low lipid levels early in development generate a scarcity metabolic phenotype that parallels the reductions in ee number, and that persists and programs sterol storage in the subsequent week under normal dietary conditions. When tested two weeks after switching from a lipid-depleted to a normal diet, the animals still had fewer posterior ee cells and still stored 14% more whole body cholesterol than controls that were never lipid-deprived (Figure 6A-B). Thus, the cellular and metabolic effects of nutrient starvation early in adult life can persist for a significant period in the absence of the original stimulus.

Dietary lipids influence enteroendocrine tumor development

When Notch signaling is strongly reduced in ISCs they give rise to a rapidly proliferating neoplasia composed of ISC-like and enteroendocrine-like progenitors (Micchelli and Perrimon, 2006; Ohlstein and Spradling, 2006; Patel et al., 2015). Strikingly, these "enteroendocrine tumors" preferentially form in lipid-rich regions of the

Figure 7. A lipid-depleted diet blocks enteroendocrine tumor growth. (C-H) Posterior midguts from (C) control (Esg::GFP) or (D-G) Notch-RNAi (Esg::N-RNAi) fed (D-E) a control (CD) or (F-G) a lipid-depleted (LD) diet for 9 days. DAPI (blue); GFP (green); Prospero (red, nuclear) and Delta (red, cytoplasmic). Scale bar = 40μm. (H) Plot quantitating reduced tumor burden of flies on LD compared to CD. (I-M) Posterior midguts from animals fed the indicated diets and showing individual MARCM clones marked with GFP for controls (I-J) or $N^{-/-}$ cells (K-L) 9 days after induction. Scale bar = 10μm. (M) Mean clone size from experiment in (I-L) showing significant reduction in $N^{-/-}$ tumor clone size on LD food. ***$p<0.001$ (t-test).

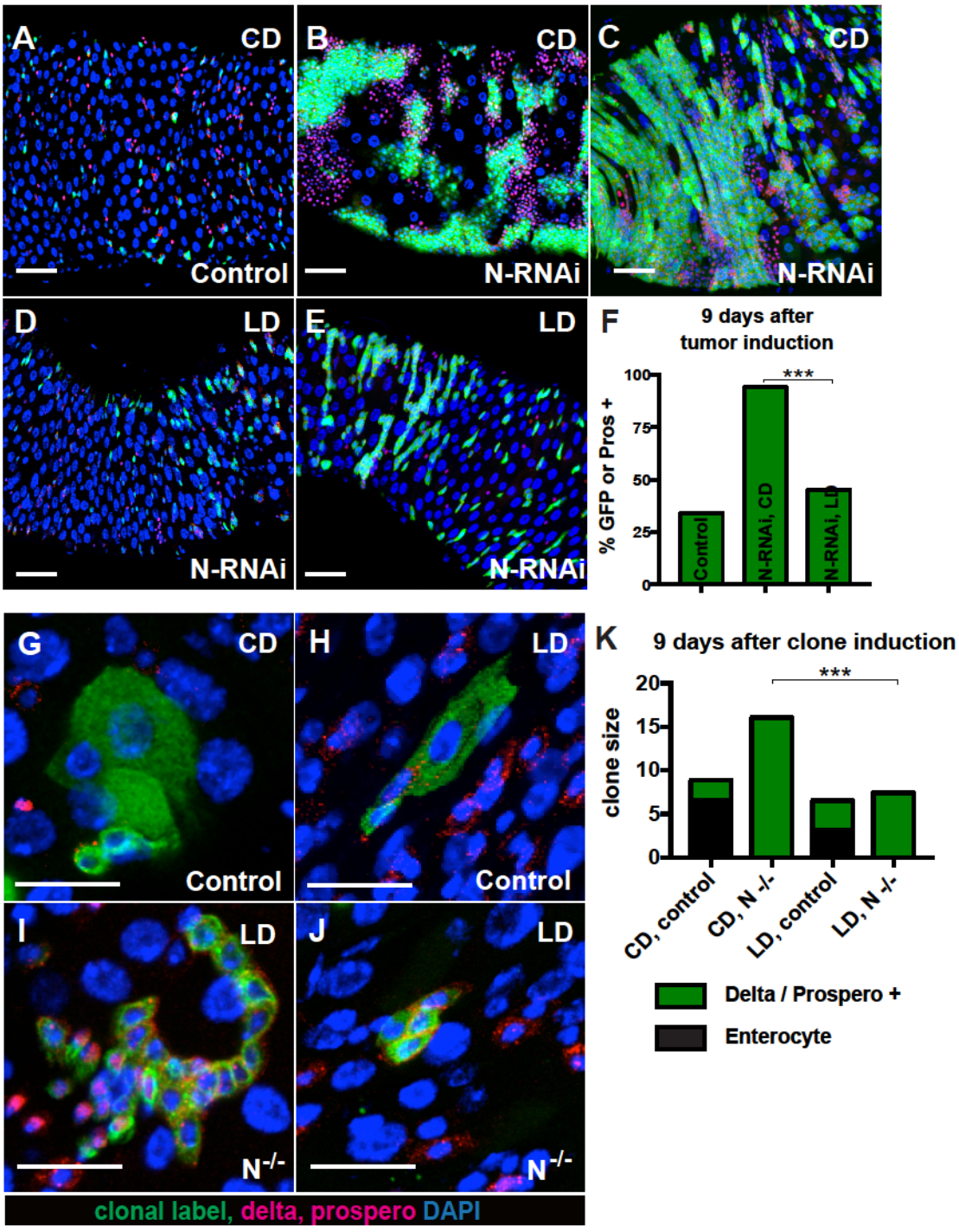
A
CD
Control
B
CD
N-RNAi
C
CD
N-RNAi
D
LD
N-RNAi
E
LD
N-RNAi
F
9 days after
tumor induction
***
% GFP or Pros +
100
75
50
25
0
Control
N-RNAi, CD
N-RNAi, LD
G
CD
Control
H
LD
Control
I
LD
N-/-
J
LD
N-/-
clonal label, delta, prospero DAPI
K
9 days after clone induction
***
clone size
20
15
10
5
0
CD, control
CD, N -/-
LD, control
LD, N -/-
Delta / Prospero +
Enterocyte

intestine, which are mostly located in the posterior midgut (Marianes and Spradling, 2013). Our finding that elevated dietary sterol downregulates Notch signaling suggests an explanation for the preferential development of enteroendocrine tumors in lipid-rich midgut regions. ISCs in lipid-rich zones would likely contain elevated levels of membrane cholesterol and other lipids that would further depress Notch signaling by the mechanism described here, enhancing the effect of genetic lesions in the Notch pathway. Thus, tumor formation might represent another adult characteristic affected by diet.

If increased dietary lipids suppress Notch signaling in stem cells and thereby promote enteroendocrine tumors, we reasoned that a lipid-depleted diet, which increases Notch signaling, might slow tumor development. We induced tumor formation by expressing *Notch RNAi* in progenitor cells throughout the intestine using *esg-GAL4*, and tracked tumor development quantitatively by counting the number of clustered tumor cells that were labeled using *UAS-GFP* and Prospero staining. By 9 days after tumor induction, animals on control diets had large to massive tumors (Fig. 7B-C), while animals fed lipid-depleted food had tumor burdens ranging from scarcely detectable to moderate (Figure 7D-F). To further analyze the effects of diet we induced ISC clones lacking Notch and counted clone size as a function of diet (Figure 7G-J). Nine days after induction, Notch mutant clones were significantly smaller in animals on a lipid-depleted diet than in animals on a control diet (Figure 7K).

DISCUSSION

Nutrient regulation of development

Both unicellular organisms and metazoans maximize their utilization of scarce environmental resources such as sterols. Mechanisms for optimizing cholesterol uptake, biosynthesis, transport and excretion evolved early and are widely shared throughout unicellular and metazoan animals and plants. Perhaps because lipid uptake inherently involves endocytosis and vesicle trafficking, and affects membrane lipid composition, regulatory mechanisms controlling lipid utilization in animals are centered on the stability of key regulatory endosomal membrane proteins (Brown and Goldstein, 1990).

Our experiments imply that this ancient system extends beyond nutrient homeostasis and metabolism to encompass tissue development and maintenance. As the locus of nutrient uptake, the intestine is the tissue most directly responsible for bringing environmental nutrients into balance with organismal requirements, both in the short term and by anticipating future needs. The Notch signaling pathway controls the differentiation of enterocytes and enteroendocrine cells downstream from intestinal stem cells that are among the most active in the body. Thus, linking sterols to Notch signaling provides a pathway for these nutrients to rapidly modulate the cellular machinery controlling both their immediate and long-term utilization. The ovary makes great metabolic demands on females by abundantly producing nutrient-laden oocytes surrounded by follicle cells. In Drosophila, ovarian germline and somatic cells, like intestinal cells, arise from adult stem cells and differentiate under the influence of Notch

signaling. Thus, sterol-mediated regulation of ovarian cell differentiation potentially provides a control on the tissue making the largest demand for sterol production.

Not all tissues that require Notch are affected by alterations is steroid availability. Unless a significant number of new cells are being generated, altered Notch signaling may have little effect on a tissue's cellular composition. We observed no defects in wing vein patterning or bristle development in the *Hr96* mutant. Even sensitive tissues have limits to the degree of modulation. When Hr96 is overexpressed, the accumulation of additional ee cells could not be increased further by a high sterol diet (Fig. 2G). In the absence of all Hr96 function in null mutant animals a low level of ee cells was still produced regardless of diet. This suggests that the regulation of Notch signaling by environmental lipids has natural limits that maintain at least a basal level of tissue function even under extreme dietary circumstances. This ensures at a minimum that the tissue will still be able to respond if the nutrient environment becomes more favorable.

Mechanism of dietary influence on Notch signaling

We have found that endosomal trafficking of the Notch pathway membrane proteins Notch and Delta is lipid sensitive, like other key membrane regulators of nutrient utilization and metabolism. Delta (and NECD) localization changed dramatically on a lipid-depleted diet or in the *Hr96* mutant, appearing in more vesicles and larger vesicles spread throughout the cytoplasm, and at higher levels associated with the plasma membrane. These changes, amounting to 3-6 fold increased integrated Delta immunofluorescence per cell (Figure 3), may result partly from small (~2X) increases in Delta mRNA, but mostly from reduced Delta turnover (modeled in Figure 8). The

greater stability of Delta was the likely explanation for its increased perdurance downstream from the stem cell in the enterocyte lineage. Normally only ISCs have high Delta levels, but in flies starved for cholesterol or bearing an *Hr96* mutation, Delta remained at high levels in enteroblasts and in differentiating enterocytes up to and including cells with 8c genomes. This implies that Delta persistence under lipid-starved conditions increases from perhaps an hour in normal enteroblasts to more than the 48 hours needed for an enteroblast to develop into an 8c enterocyte. Conversely, under conditions of excess lipids or *Hr96* duplication, Delta levels were reduced 2-3 fold based on fluorescence measurements.

Since the effects of dietary lipids on Notch signaling and ee production depended on the *Drosophila* LXR homolog Hr96, changes in cholesterol homeostasis in the membrane compartments of the affected cells are likely involved. Many studies have shown that a high-fat diet induces ER stress and stimulates ER associated protein degradation (ERAD). Moreover, the changes in Delta cytoplasmic distribution are exactly those expected for an alteration in stability within endosomes. However, the substantial changes in Delta and NECD stability we observed did not affect all membrane proteins and mostly likely result from regulatory mechanisms that target these proteins specifically. Classical studies have shown that cholesterol levels can control the turnover of specific cholesterol biosynthetic enzymes like HMG-CoA reductase (Goldstein and Brown, 1990; DeBose-Boyd, 2008; Nakanishi et al., 1988). Low cholesterol conditions stimulate ER protein trafficking of SREBP proteins (Wang et al., 1994) and can result in different proteins, such as the ER regulatory protein Insig-1, being targeted for ERAD

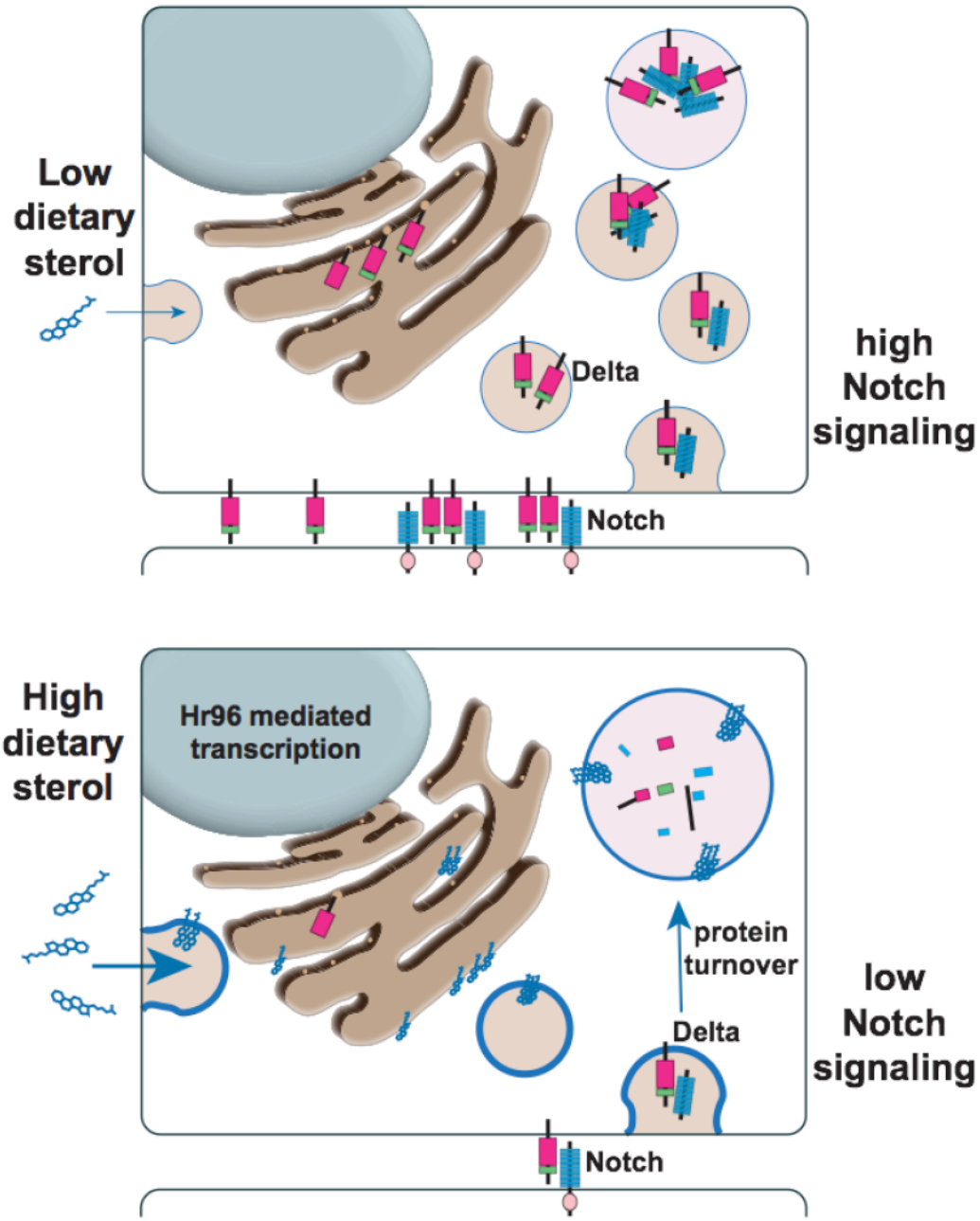

Figure 8. Model of dietary sterol-mediated regulation of Notch signaling via changes in Delta and Notch trafficking and stability in the ER. When cells import low levels of dietary cholesterol (lipid-depleted diet or *Hr96* mutant) there is a resultant low level of cholesterol on membranes (thin blue lines). As a result, Notch and Delta proteins are retained in the ER and endosomes. When cells can import high levels of sterols, membranes become sterol rich (thick blue lines). ER protein regulation occurs normally, and, post-signaling Delta/Notch is degraded.

(Gong et al., 2006). Strong evidence that high sterol levels trigger Delta turnover via an ERAD-like process was provided by the effects of inhibiting the key ERAD enzyme p97, and by the synergistic effects of *Hr96* mutation and p97 inhibition, which caused lethality.

Dietary sensitivity of Notch signaling causes midgut adaptation

Our experiments provide new insight into how specific nutrients early in life influence intestinal structure and metabolic programming. Dietary cholesterol early in adult life influences ee production in a direction likely to better adapt the organism to its initial nutrient environment. In mammals, after birth crypts begin to develop, new cell types emerge, and certain regional characteristics are formed (Carulli et al., 2014; Hudry et al., 2016). Many studies (Bates et al., 2006; Rakoff-Nahoum et al., 2015) have suggested that these postnatal effects on development may stem from seeding the intestinal flora. However, given that these later events in epithelial development occur when the animal begins to feed it is also likely that dietary nutrients play a major role in the maturation of the adult intestine in mammals.

Although altered Notch signaling may affect metabolism in multiple ways, changes in the abundance of at least some types of ee's have the potential to significantly influence nutrient utilization. The enteroendocrine hormone AstA, which increased threefold under conditions of high cholesterol utilization, regulates feeding (Chen et al., 2016). In the brain AstA controls production of adipokinin and insulin, whose levels influence the amount of lipid stored in the fat body (Hentze et al., 2015). We also

observed an increase in Tk, an enteroendocrine hormone that negatively regulates lipid biosynthesis in the intestine and transport throughout the body (Song et al., 2014).

Lipid-deprivation-mediated reductions in ee number persisted for at least two weeks after the animals were shifted to a rich diet. Lower ee numbers may explain in part our observation that 18% more whole body cholesterol was stored under these conditions, than in flies that had been raised continuously on rich medium. Persistent changes in tissue cellular composition represent an attractive model for understanding metabolic adaptations in mammals. Mammalian development is strongly dependent on the mother's nutrition, and children born to malnourished mothers often begin life with a low birth weight (Lechtig et al., 1975). These individuals are more likely to become obese later in life if nutrients are not restricted (Ramakrishnan, 2004). Low nutrient exposure early in life appears to trigger metabolic changes that enhance nutrient scavenging by the developing fetus. After birth, these resets become a permanent state that puts individuals at risk for metabolic syndromes in a normal nutritional environment (Reusens et al., 2011).

Dietary sterols, Notch signaling and cancer

The connection between sterol metabolism and Notch signaling has potentially strong implications for cancer etiology and therapeutics. Mutations in the Notch signaling pathway have been associated with cancer deriving from many tissues in the digestive tract including the liver, pancreas and the colon. Furthermore, Notch signaling has been a common therapeutic target for these types of cancer. However, drugs and therapies targeting Notch signaling commonly have severe side effects throughout the body

complicating their use with patients. We found that stimulating reverse cholesterol transport using LXR agonists in human embryonic kidney cells (HEK293) caused a dramatic and highly reproducible decrease in DLL4 protein levels. This suggests that sterol metabolism may have a highly conserved role in the regulation of Notch signaling that could be exploited for therapeutic purposes. For example, sterol regulating drugs such as LXR agonists may provide a way to alter Notch signaling in a tissue-directed manner for adjuvant therapy and as a means to reduce cancer risk in genetically susceptible patients. Inhibiting DLL4 is sufficient to reduce tumor growth and initiation in mice and humans (Hoey et al., 2009).

Numerous studies have shown that consuming a high-fat diet increases susceptibility to several specific types of cancer (Huang et al., 2012; Tang et al., 2012; Beyaz et al., 2016). High-fat diets have been proposed to increase chronic inflammation in tissues including liver and intestine (Ding et al., 2010; Miyagi et al., 2010; van der Heijden et al., 2015). Our study provides a specific mechanism to explain these connections. Large quantities of dietary lipids, particularly sterols, may directly inhibit tumor suppressor pathways, such as Notch signaling, and increase cancer susceptibility in a manner that synergizes with inflammation. In contrast, consuming a low-fat diet has been suggested to protect against multiple types of cancer. Consistent with this idea we found that feeding flies a diet low in sterols suppresses enteroendocrine tumor growth and tumor size. Taken together our work suggests that dietary lipid levels play a central role in dictating cancer risk for digestive track tumors and that dietary intervention in conjunction with the use of cholesterol modulating drugs may provide an effective strategy for reducing cancer risk in genetically predisposed patients. In sum, our work

reveals new connections between environmental nutrients and developmental signaling. Further characterizing these connections will help reveal how environmental nutrients can positively impact tissues that have become stressed due to age, disease or the presence of cancer.

ACKNOWLEDGMENTS AND CONTRIBUTIONS

We thank Steve DeLuca, Ethan Greenblatt, Chenhui Wang, and members of the Spradling lab for discussion and valuable comments on the manuscript. We are very grateful to Joseph Tran for his assistance with the mammalian cell culture experiments. RO is a student in the Cellular, Molecular and Developmental Biology graduate program of Johns Hopkins University. MS was a fellow of the Jane Coffin Childs Memorial Fund. RO, MS and ACS designed experiments and wrote the manuscript. RO and MS performed research.

CHAPTER 3

ESTABLISHMENT OF REGIONALIZTION IN THE *DROSOPHILA* MIDGUT

INTRODUCTION

There are many common and well-studied disorders of lipid metabolism, and many of them are caused or influenced by lipid absorption from dietary lipids in the intestine. As such, understanding how lipids absorptive regions are established, and how they function in the context of whole animal metabolic processes is of great significance.

To study the adult *Drosophila* midgut it is important to understand how it develops. The larval midgut is unique in its development that it is specified by two populations of endodermal progenitors in the embryo. These cells migrate, merge, and undergo a mesenchymal-epithelial transition to form the larval midgut (Campos-Ortega and Hartenstein, 1985; Tepass and Hartenstein, 1994). A subset of these cells remain undifferentiated becoming the adult midgut progenitors (AMPs), while the remainder become post mitotic and differentiate into ees or endocycle becoming ECs. During the 3rd Larval instar, AMPs begin proliferating creating enough cells to create a new a new epithelial layer around the dying larval ees and ECs termed the ”yellow body” (Denton et al., 2009). It was thought that the metabolites that make up the larval gut are histolyzed to serve as nutrients and building blocks for the pupa and developing adult midgut. However, blocking autophagy in the larval midgut does not prevent adult midgut formation (Lee, 2002), suggesting that the developing adult midgut is an independent organ that does not receive nutrient or instructional cues from the previous larval midgut.

These results do not imply that nutrient sensors are not important for adult midgut development. On the contrary, large amounts of nutrients must be imported, likely from the fat body, and nutrient availability, as well as genetic programming likely dictates how

the adult midgut develops. One known nutrient sensor is the nuclear hormone receptor, HNF4. This ligand regulated transcription factor, when bound to long chain fatty acids, initiates changes in gene expression to regulate beta oxidation, lipolysis, and the starvation response (Palanker, 2009).

This chapter outlines the larval regions that house the AMPs which become the adult midgut, and how those AMPs divide during pupation to generate the adult midgut. It further continues to explore how a nutrient sensor, HNF4, may influence adult midgut development and physiology, and closes with an exploration of the transcriptional changes that follow changes to lipid availability in the adult diet.

MATERIALS AND METHODS

Normal and modified dietary treatments

To enhance uniformity, all diets were prepared from lipid-extracted ingredients. The lipid-depleted diet was prepared by extracting yeast extract and agar with chloroform at a 1:5 ratio by weight. Each component was extracted for 4 hours, separated with vacuum filtration, and then extracted for 1 hour with fresh chloroform. Both components were then allowed to dry for five days in a fume hood. Extracted yeast extract and agar were used to make a 1.0 SY diet according the following formula: 30g sucrose, 30g lipid-extracted yeast extract, 3g agar, 300 mL H_2O (Sieber and Thummel, 2009). The control diet consisted of a lipid-depleted 1.0 SY diet supplemented with fresh yeast paste and vehicle alone (1-4% ethanol) to control for the ethanol in the lipid-supplemented diets. Lipid supplemented diets (1X) consisted of the lipid-depleted 1.0 SY diet supplemented with free fatty acid (5 mg/ml stearic acid), triglyceride (5 mg/ml glycerol tristearate), cholesterol (5 mg/ml) or ergosterol (5 mg/ml) to a final concentration of 0.05% supplemental lipid. 4x cholesterol (high sterol diet) and 4x ergosterol were prepared to a final concentration of 0.2% supplemental sterol. Either pupae or 5-day old adult flies were transferred to vials with the diet of interest. Flies moved to a new dietary treatment were tested after an indicated period during which they were transferred to fresh vials containing the media every other day.

Immunofluorescent staining

Midguts or ovaries were dissected in Grace's insect medium and fixed for 30 minutes at room temperature (or 15-18 hours at 4°C for midgut Delta staining) in antibody wash with 4% EM grade paraformaldehyde). Tissues were then washed three times for at least 2 hours and then blocked at room temperature in antibody wash +5% BSA for 4 hours. Primary antibodies were added to incubate overnight at 4°C at the following concentrations: anti-Prospero (Developmental Studies Hybridoma Bank MR1A;), RRID:AB_528440) (1:100), 1:100, anti-PH3, Ser10 (Millipore Sigma) 1:1000, (1:100), anti-Delta (DSHB C594.9B, RRID:AB_528194) (1:50), anti-NECD (DSHB C458.2H, RRID:AB_528408), anti-LpR2 (Parra-Peralbo E; PLoS Genet. 2011 Cat# LpR2, RRID:AB_2569135) (Parra-Peralbo and Culi, 2011), anti-Hindsight (DSHB 1G9, RRID:AB_528278) (1:100). Samples were washed for at least 9 hours. Secondary antibodies: Alexa-488, Alexa-568, and Alexa-596 incubated overnight at 4°C in antibody wash. Samples were then washed and counterstained with DAPI at 0.5 µg/ml. Tissue was then mounted with Vectashield and imaged. Antibody wash used for guts contained 1xPBS + 0.3% Triton X-100 + 0.5% BSA. Antibody wash for ovaries contained 1xPBS + 0.1% Triton X-100 + 0.5% BSA. Tunel labeling was performed before incubation with secondary antibodies per manufacturer's instructions using The DeadEnd™ Fluorometric TUNEL System (Promega, G3250).

RNA sequencing

Female y^1 w^1 flies aged 10-12 days were dissected in cold Grace's insect medium. Anterior (a1-a3) and posterior regions(p1-p4) were identified morphologically and isolated using microdissection scissors. 30-50 cut regions per sample were transferred to

400 µl Tripure on ice. Each experimental condition was collected in triplicate. Collected midguts were homogenized and 600µL fresh Tripure added. After 10 min at room temperature 180µl chloroform was added, shaken briefly by hand and allowed to stand at room temperature for 10 minutes. Following centrifugation for 15 min at 12,000 rpm at 4°C, the aqueous layer was removed and RNA precipitated with 400 µl isopropanol. The pellet was recovered by centrifugation, re-suspended in 50uL nuclease free water and stored at -80°C. cDNA libraries were constructed from poly(A)-selected RNA using the llumina TruSeq RNA Library Prep Kit v2 and sequenced on an Illumina NexSeq 500.

Sequenced reads were analyzed using bcl2fastq v2.17.1.14 for base calling, Bowtie 2.2.9 for alignment to the dm6 Drosophila genome, TopHat 2.1.1 for alignment to transcripts defined by BDGP6 and Ensembl.85.gtf. Transcript and gene fpkm was calculated using Cufflinks 2.2.1 and fold change quantified with cuffdiff (v7). We analyzed genes whose expression was >2 FPKM and with a q-value <0.05. Genes reported as significantly changing had at least 2-fold increased or decreased expression levels.

RESULTS

Identification of larval midgut regions

To better understand the origin of AMPs, we looked to characterize the regions of the larval midgut. We performed electron microscopy throughout the length of the larval midgut, taking sections every 100 microns. We analyzed the structural changes that arise from the anterior to the posterior of the midgut and identified 10 regions of interest (Figure 1A-J). These regions are similar in structure and function to the regions of the adult midgut (Figure 1K-L), though vary in their organization. We identified AMPs in every region of the larval midgut, and identified GAL-4 drivers, and protein traps that are specifically expressed in a subset of regions.

Characterizing the development of adult midgut regions

Larval and adult midgut regions perform similar functional tasks, but vary in their order along the anterior to posterior axis. We wondered if AMPs may migrate before or after they begin amplification during pupation, to their corresponding adult midgut region, or if instead AMPs divide to establish the midgut along an anterior to posterior gradient, similar to the method of development used by other tissues.

To investigate this question we performed successive clonal induction by heat shock (Figure 2) of larval and pupal wild type flies. We dissected and analyzed clonal populations arising from these heat shocks at the same time for all samples, 2 days after eclosion. By performing the analysis at this time point we were prevented from definitively identifying the region clones were induced, but could say with certainty whether they were in the Anterior, Middle, or Posterior of the midgut based on

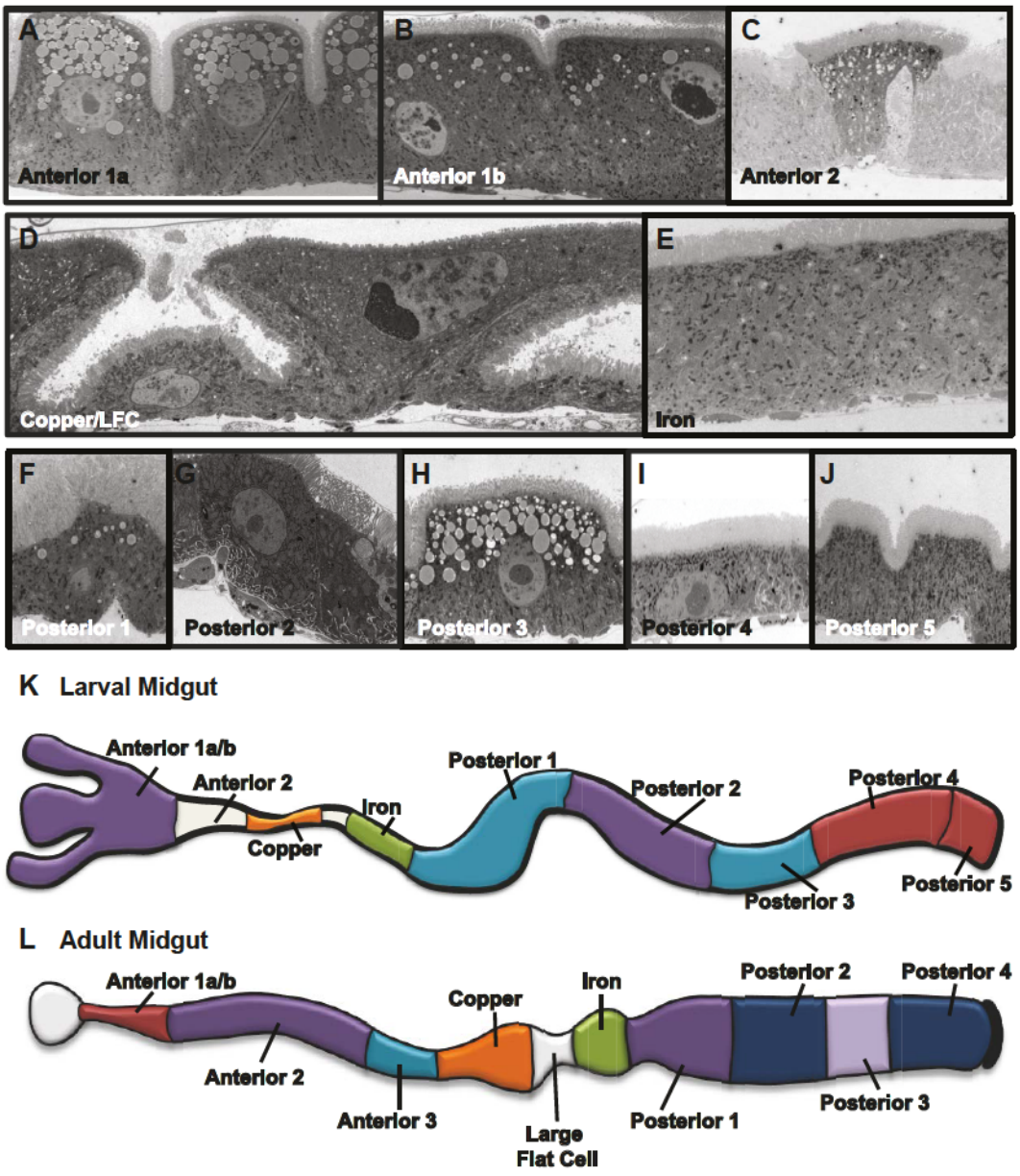

Figure 1. The larval *Drosophila* midgut contains comparable nutrient processing regions as the adult midgut.

(A-J) Electron micrographs from larval midgut enterocytes along the anterior-posterior axis from stage L-3. A) Anterior 1a, B) Anterior 1b, C) Anterior 2, D) Copper/LFC (structurally identical), E) Iron, F) Posterior 1, G) Posterior 2, H) Posterior 3, I) Posterior 4, J) Posterior 5. (K-L) Cartoon representations of the larval (K) and adult (L) midgut structure and regions. The cartoon of the adult midgut was used with permission from A. Marianes. Regions are color coded based on nutrients processed: purple = lipids, maroon = glycogen, orange = copper, green = iron, blue = unknown nutrients. Gray regions are structurally similar

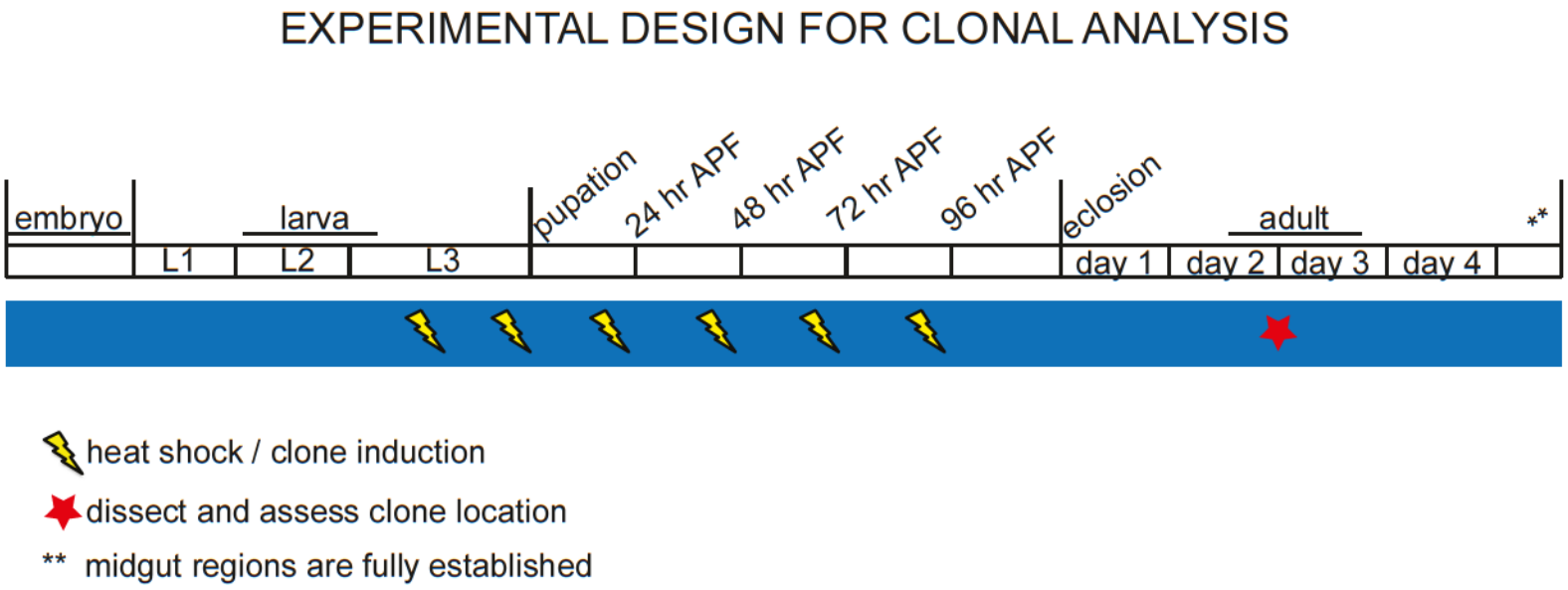

Figure 2. Experimental paradigm for labeling adult midgut progenitors and their progeny. Chart is made to scale for the approximate time required for each developmental stage when cultured on rich media at 25 °C.

sterotypical physiological constrictions of the midgut that are established during pupation. We titrated the amount of heat shock to ensure that the statistical likelihood of more than one clone being induced during heat shock was very low. Because of this, sometimes more than half of the analyzed midguts contained no clones, so we can be sure that the labeled cells that are seen are from one inciting labeling event. No clones were found in midguts that did not undergo heat shock.

Rather than identifying clones that spanned multiple regions, or migrating clones, we found that clones induced during development remain contiguous (data not shown). Furthermore, AMP division follows a stereotypical progression along the anterior to posterior of the developing midgut. While clones induced during the pre-pupal stage are equally likely to be found in the anterior, middle or posterior of the adult gut. Clones induced during later time points follow a more specific pattern. The raw data for this analysis can be found in Table 1. In brief, most of the clones induced at 24 hrs APF are found in the anterior adult midgut, clones induced at 48 hrs APF are found in the middle adult midgut, and clones induced at 72 and 96 hrs APF are found in the posterior adult midgut.

Consistent with our observation that the adult midgut develops in an anterior to posterior manner, we saw that cells undergoing S-phase which can be stained with a PH3 antibody, were found in higher number in the anterior at 24 hrs APF, the middle at 48 hrs APF, and the posterior from 72hrs onward (Figure 3).

	Anterior	Middle	Posterior	Total Guts
3rd Instar	18/45 (40.00%)	19/45 (42.22%)	8/45 (17.78%)	60
0 hr APF	37/96 (38.54%)	36/96 (37.50%)	23/96 (24%)	60
24 hr APF	14/23 (60.87%)	1/23 (4.35%)	8/23 (34.78%)	45
48 hr APF	6/34 (17.65%)	17/34 (50.00%)	11/34 (32.35%)	60
72 hr APF	4/46 (8.70%)	5/46 (10.87%)	37/46 (80.43%)	54
96 hr APF	11/60 (18.33%)	7/60 (11.67%)	42/60 (70.00%)	75

Table 1. Summary of the results of clonal analysis completed as per Figure 2. Shaded boxes indicate the time when most clones were induced: Most anterior clones were induced at 24 hours APF, most clones found in the middle midgut were induced at 48 hours APF, and posterior clones were found in equal measure when clones were induced at 72 hours and 96 hours APF. Total Guts indicates number of intestines that underwent heat shock at that time. Denominator of each experimental sample indicates the number of intestines from that sample set that had a productive heat shock that induced a clone. For example: clones were induced in 45 out of 60 of the 3rd Instar larvae that underwent heat shock. Of these 45 animals with clones, 18 had clones in the anterior, 19 had clones in the middle, and 8 had clones in the posterior of the adult midgut.

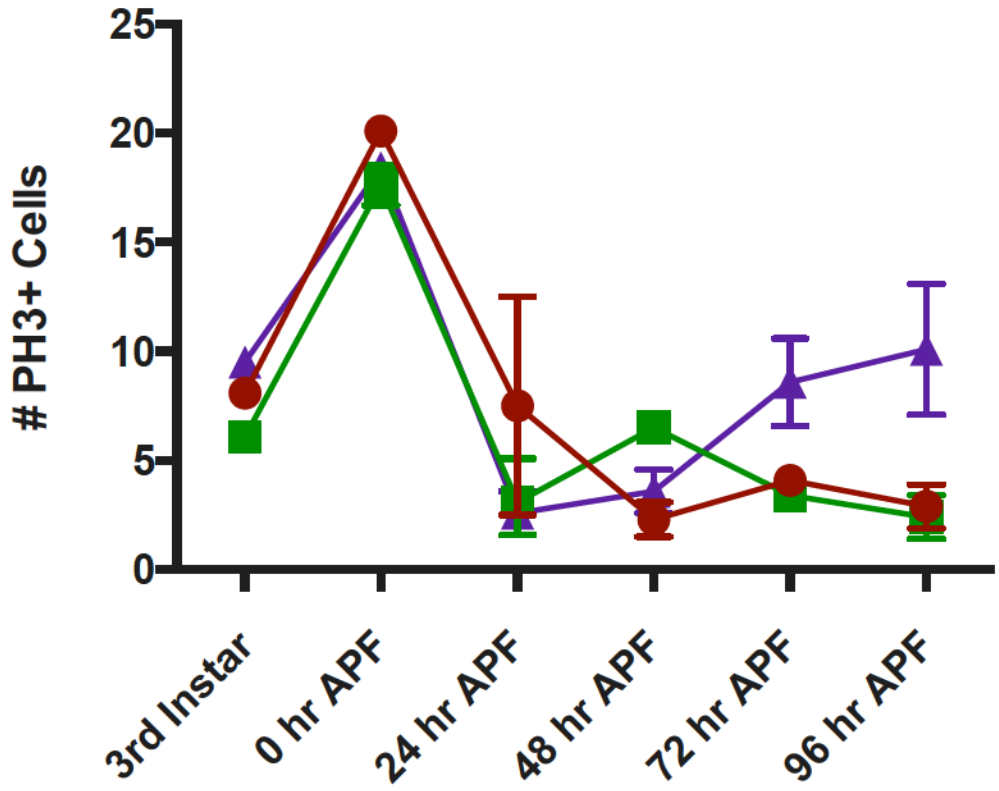

Figure 3. PH3 staining replicates clonal analysis demonstrating the anterior to posterior development of the adult midgut.
Graph summarizing the average number of PH3+ cells per midgut in flies of varying ages. Error bars show +/- standard deviation between 10 midguts analyzed per time point. Colors indicate the larval or pupal midgut region that was scored: anterior midgut (maroon), middle midgut (green), posterior midgut (purple).

HNF4 is expressed during adult midgut development, and under starvation conditions

HNF4 was named for its role in hepatocyte specification, but is also required cell autonomously for the embryonic development of the mouse colon, and the specification of some intestinal cells (Morrisey et al., 1998; Garrison et al., 2006). *HNF4* in *Drosophila* is known to regulate multiple metabolic pathways, and mediates endoderm specification in the embryo. To determine if *HNF4* may play a role in *Drosophila* midgut development, we first characterized its expression pattern with an antibody against the DNA binding domain provided by C.S. Thummel. We found that HNF4 has a regionally restricted expression pattern in the pre-pupal midgut (Figure 4A-B), expressing in the proventriculus, gastric caeca, Region A1b, the copper and iron region, a few cells in P1, and extensively in P5 and the hindgut. HNF4 is also expressed in P5 AMPs, denoted by their proximity to peripheral cells (Figure 4B).

HNF4 is expressed in a subset of diploid cells throughout the length of the pupal midgut by 24 hrs APF (Figure 4C), and in all cells at 72hrs APF (Figure 4D). The expression of the HNF4 protein becomes very restricted by 96 hrs APF, however, only expressing at the midgut-hindgut junction (Figure 4E).

We failed to see any HNF4 protein by antibody stain in the adult midgut. However, when we transferred wild type flies to starvation media, providing PBS-1x with agar alone, we saw nuclear HNF4 protein after 36 hours under starvation conditions (Figure 4F-G). Taken together, this data suggests that *HNF4* is important either as a

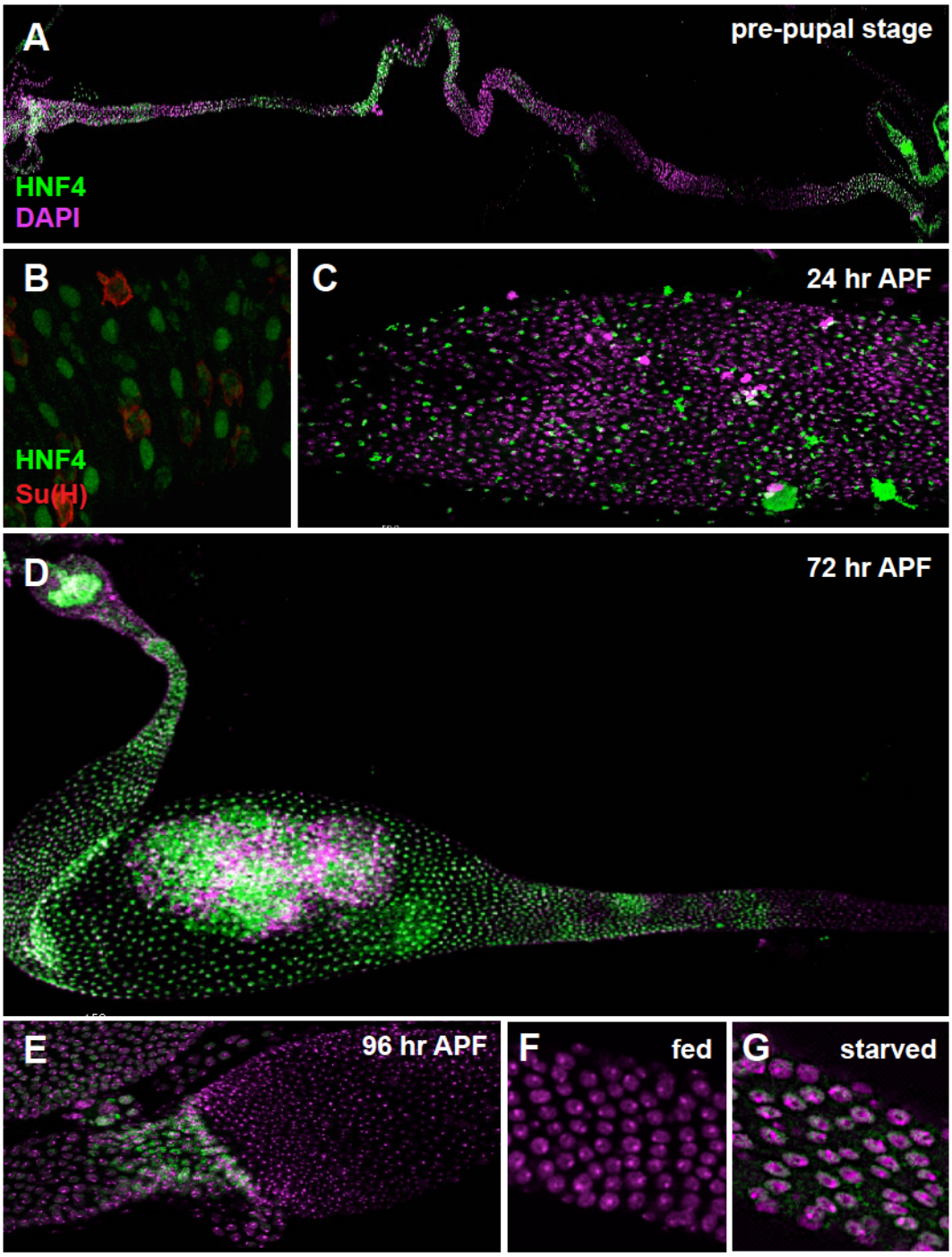

Figure 4. HNF4 is expressed during adult midgut development, and is also expressed under starvation conditions. (A) pre-pupal midgut; HNF4 antibody (green), DAPI (magenta) (B) cells from the posterior 5 region of the pre-pupal midgut; HNF4 (green), Su(H) identifying peripheral cells (red) (C) midgut, 24 hours APF, (D) midgut, 72 hr APF, (E) midgut, 96 hr APF; HNF4 (green), DAPI (magenta). (F-G) anterior midgut from adult female fed a control diet (F) or PBS-1x only (G); HNF4 (green), DAPI (magenta).

developmental or metabolic regulator during development, but is not required for adult midgut homeostasis. Instead, *HNF4* switches to its role mediating the starvation response in the adult midgut.

HNF4 is required for adult midgut development

Most *HNF4* mutants are die during embryogenesis, but a trans-heterozygote can be generated that produces very little functional protein (Palanker et al., 2009). These animals undergo development more slowly than wildtype, and about 50% die during eclosion. We compared the structure of the surviving adult *HNF4* mutant flies to flies that had one mutant copy of *HNF4*. We found that surviving *HNF4* mutants have a malformed proventriculous, an undefined middle midgut and were significantly shorter than their wild type counterparts (Figure 5A-C). Additionally, *HNF4* mutants are more susceptible to bacterial infection, identifiable by DAPI staining. This could either arise from a failure of the immune system to respond to infectious bacteria, or perhaps a failure to establish regionality that supports certain bacterial communities.

We performed antibody staining to identify the midgut cell types in the mutant and wildtype intestines, and counted the number of enterocytes, ees (prospero+) and stem cells (Delta+) in the anterior and posterior midgut (further regional identification was not possible since the physical character of the mutant midguts was altered). Previous studies have shown that different regions of the midgut have different ratios of ees, ISCs, and ECs (Marianes and Spradling, 2013). We found that the cell type ratios were unaltered throughout the midgut, and most resembled the ratios found in P1 of wildtype midguts (Figure 5D).

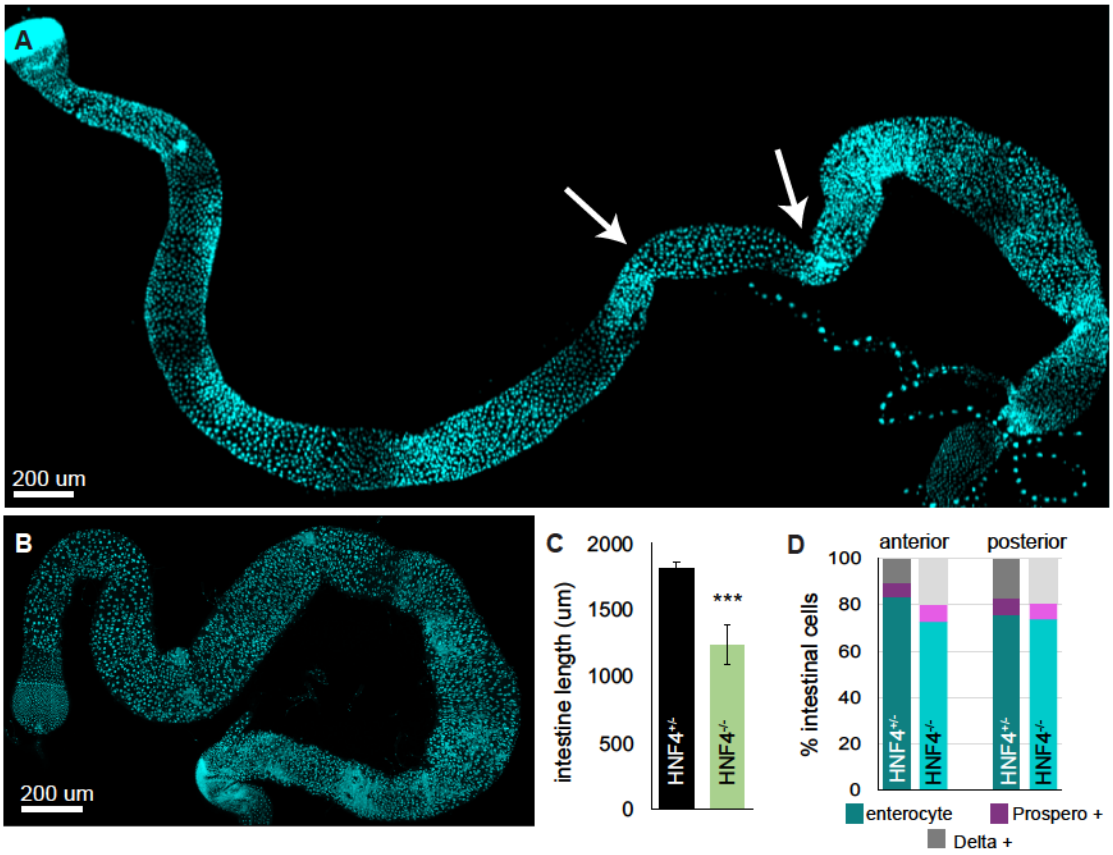

Figure 5. HNF4 is required for adult midgut development. (A-B) 5 day old adult female midgut from $HNF4^{+/-}$ (A) and $HNF4^{-/-}$ (B), DAPI (teal). Arrows identify stereotypical constrictions in the normal adult midgut surrounding the middle copper region. (C) Average length of wild type (black) and *HNF4* mutant (green) intestines. Scale bars +/- standard deviation from 10 midguts per sample; *** = $p<0.005$ (t-test). (D) Percent of Delta+ (gray), Prospero+ (magenta) and enterocytes (teal) in the anterior and posterior regions of wild type and *HNF4* mutant midguts.

Modulating lipid availability influences metabolism related genes in the posterior midgut.

We performed extensive RNA sequencing, to understand how modulating lipid levels in the diet affects the transcriptional character of midgut regions. We acquired RNA transcripts from triplicate samples of y^1w^1 flies fed a CD, LD or 4xC diet, as well as *Hr96* mutants, and overexpression animals. We found that the genes significantly modified by the experimental treatments varied significantly with each treatment, but were consistent across biological replicates (Figure 6A). We performed GO analysis to identify gene families significantly regulated by dietary changes, and found that the three most highly regulated gene families were proteolysis, transmembrane transport, and lipid metabolism, all categories that we expected based on the nutrient changes (Figure 6B).

We used cuffdiff to identify the fold change between experimental and control samples, imposing a 2 fold cutoff, with a p value of significance < 0.01. We then compared the list of significantly regulated genes to a list of genes involved in metabolism in *Drosophila* and summarized the results (Figure 6C). We found that some of the significantly regulated genes did overlap between samples (Figure 4D).

Knowing most significantly regulated genes were involved in metabolism, we compared the fold change between LD, 4xC, and *Hr96* mutant posterior midguts (Figure 6E). We found that changes in sterol genes and fatty acid metabolism genes in *Hr96* mutants strongly resembled changes caused by feeding a high sterol diet. Conversely, genes involved in proteolysis and protein transport had similar changes in *Hr96* mutant and under a lipid depleted diet. These results confirm that changing lipid availability strongly influences the expression of metabolism genes, but does not appear to regulate

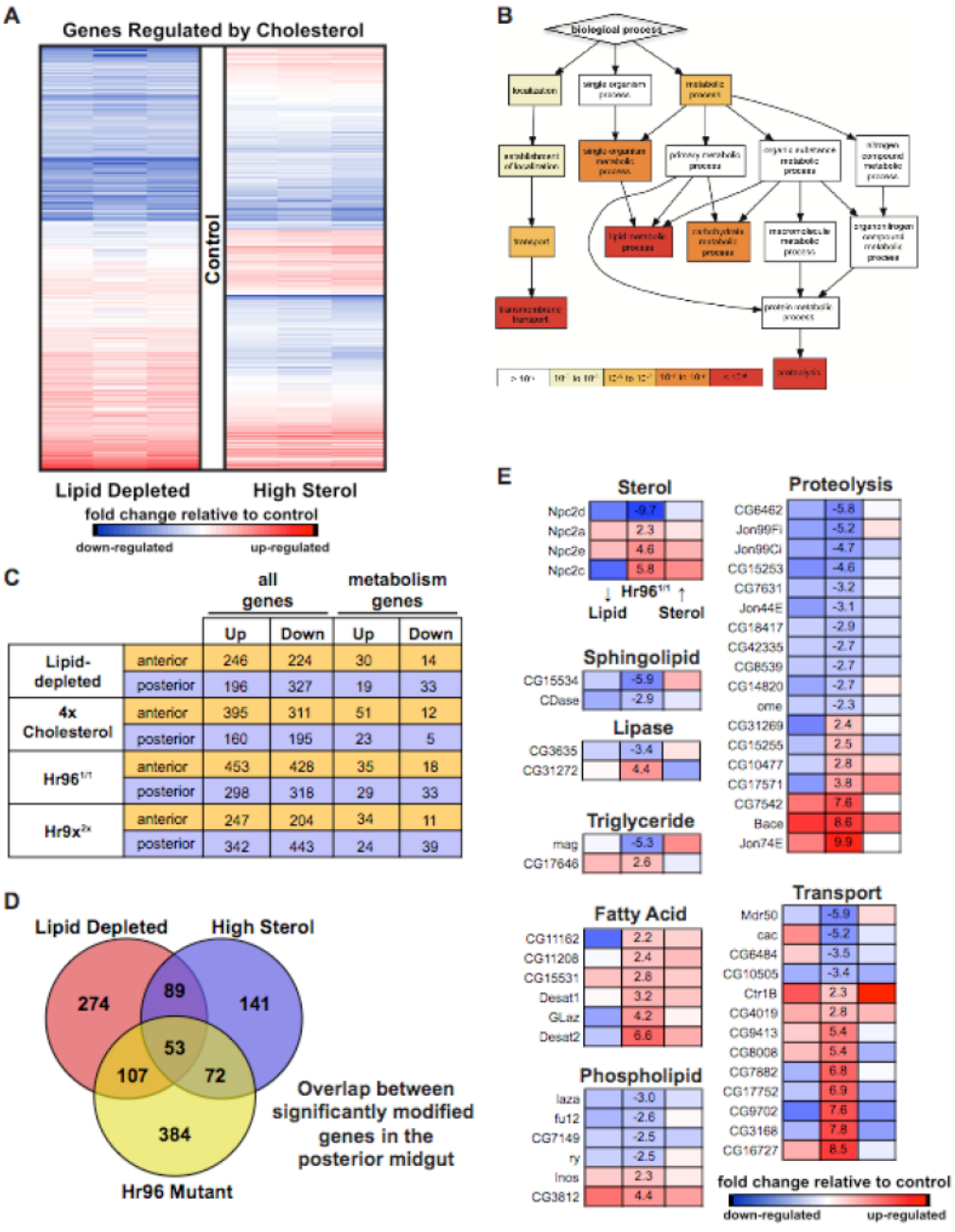

Figure 6. Modulating lipid availability influences metabolism related genes in the posterior midgut. (A) Heat map showing color coded fold change of triplicate samples from sequenced RNA from animals fed either a LD or 4xC diet, relative to control. (B) Gene ontology groups that were significantly regulated by modulating lipid levels in the diet. Significance is color coded as indicated. (C) Number of genes significantly up or down-regulated in different sample conditions. (D) Overlap of significantly modified genes between samples. (E) Fold change of metabolism genes significantly changed in experimental sample relative to control in the posterior midgut. Genes shown had significant fold changes in at least two samples.

signaling pathways, an immune response, or other regulatory pathways. This implies that developmental or signaling changes we see as a result of these nutritional changes are caused by translational or post translational regulation, or as a result of the direct interaction between proteins.

Modulating dietary lipids evokes regional specific changes in gene expression.

We were intrigued by the result that differentiation of the posterior midgut was strongly influenced by lipids from the diet, while the anterior was not as strongly affected (Chapter 2). And so, we simply compared the genes significantly regulated by lipid depletion or a high sterol diet in the anterior midgut vs. the posterior. We found that the number of genes overlapping between these samples was very significantly, and much higher than what would be expected by chance based on the sample sizes (Figure 7A). The majority of genes upregulated by lipid depletion in the anterior and posterior were involved in carbohydrate metabolism and transmembrane protein transport, while genes downregulated were often proteases (Figure 7B). We also performed gene ontology analysis on genes differentially regulated in the anterior or posterior midgut following a dietary change, but not in both regions (Figure 7C). We found some unique genes were up-regulated in the anterior that are involved in innate immunity, sphingolipid metabolism, and lipid biosynthesis. The gene lists produced by this analysis are available in the Appendix of this thesis.

A

up-regulated genes						down-regulated genes					
Lipid Depleted			High Sterol			Lipid Depleted			High Sterol		
Anterior	Posterior	overlap	Anterior	Posterior	overlap	Anterior	Posterior	overlap	Anterior	Posterior	overlap
246	133	69 p < 6e-95	395	160	93 p < 7e-114	224	327	114 p < 2e-142	311	195	90 p < 3e-108
Anterior			Posterior			Anterior			Posterior		
Lipid Depleted	High Sterol	overlap	Lipid Depleted	High Sterol	overlap	Lipid Depleted	High Sterol	overlap	Lipid Depleted	High Sterol	overlap
246	395	96 p < 1e-95	196	160	47 p < 9e-55	224	311	79 p < 5e-83	327	195	64 p < 5e-63

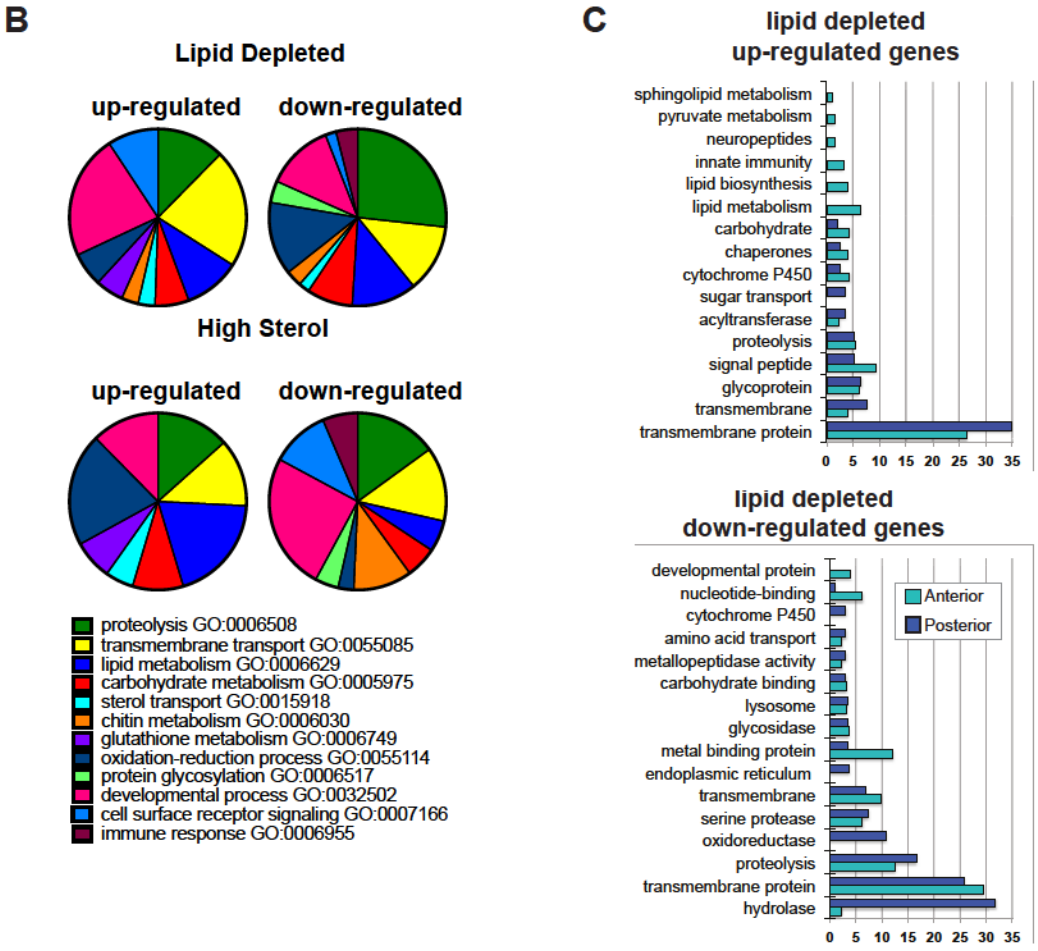

Figure 7. Modulating dietary lipids evokes regional specific changes in gene expression. (A) Number of overlapping genes, and significance of the overlap relative to total genes in the genome. (B) weighted representation of categories of genes that are significantly regulated by diet in both the posterior and anterior midgut. (C) weighted representation of categories of genes that are significantly regulated by diet in either the anterior or posterior midgut, but not both.

DISCUSSION

The anatomical differences between the larval and adult midgut may be a result of differences in their feeding habits. Larvae utilize mouth hooks to ingest solid food continuously to sustain rapid growth, even resorting to cannibalism during times of stress and starvation (Vijendravarma, 2013). In contrast, adult flies intermittently ingest liquid nutrients through their proboscis. A major site of digestion in the larval midgut are four gastric ceca in the anterior midgut. These small epithelial regions are lipid dense, and absorb a large portion of ingested nutrients (Nation, 2002). This feeding differences may be reflected in the order of the regions characterized here, namely that the first larval midgut region is responsible for a bulk of lipid processing. Interestingly, but the larval and adult midgut have a lipid rich region immediately following an acid producing region. This suggests that metal processing, or acid secretion may be important for processing lipids from the diet to aid their absorption in later regions.

We identified several GAL4 drivers and other tools that may be useful for further studies in the pupal midgut. However, our analysis of AMPs and adult midgut establishment suggest that migration does not occur, and that rather than being patterned in the larval midgut, AMPs receive new waves of signals during pupation from a primitive mesoderm that informs their differentiation decisions. This is consistent with results published within the last few years studying the pupal midgut (Takashima et al., 2011; Driver and Ohlstein, 2014). We found that the adult midgut is established using the same method many other tissues have adopted throughout evolution, an anterior to posterior progression.

Perhaps the most interesting area for further study is the analysis using the *HNF4* mutant alleles begun in this chapter. We found that approximately 30% of *HNF4* mutants survive to adulthood, but that they have a malformed midgut, and are susceptible to bacterial infection. Interestingly, the cell type ratios of the anterior *HNF4* mutant midgut resembles that of the posterior wildtype midgut. Conversely, the posterior mutant midgut ratios were unchanged compared to wildtype. Since *HNF4* is required for endoderm specification and gut development in mammals, it is possible that it serves a similar developmental role in *Drosophila*. Perhaps *HNF4* has two roles, first as a developmental regulator during pupation, and then a starvation sensor in adulthood. It would hardly be unique if it did so, since biology often recycles signaling molecules and pathways, and then context of development provides a much different environment than adult life.

If *HNF4* does have a developmental role, it might act to specify the anterior, and possibly middle midgut as distinct from the posterior, since all regions resembled the posterior in their cellular makeup. Since *HNF4* mutants lack the constrictions that neighbor the proventriculous and middle midgut, it is possible that *HNF4* acts in the endoderm to regulate signals to the mesoderm the provide the stereotypical muscle constrictions seen in wild type midguts. In sum, this data suggests that *HNF4* is an important player in adult midgut development and homeostasis.

Finally, this chapter presents the initial analysis of an RNA sequencing data that is the first of its kind to compare multiple regions of the same tissue, dietary perturbations, and a genetic mutant with a similar phenotype evoked by that diet.

APPENDIX

The following tables were compiled from sequencing data presented in Chapters 2 and 3. These lists highlight the specificity of transcriptional changes caused by dietary changes in *Drosophila*, and may be a helpful reference for research exploring the regional effects caused my changes in dietary lipids. The tables contain lists of genes involved in metabolism that are affected by diet.

The final table contains a reference list of genes currently known to be involved in metabolic pathways in *Drosophila melanogaster* at the time of this analysis. These lists were compiled using data from FlyBase which is freely accessible at www.flybase.org, and supported by the National Human Genome Research Intitutute at the U.S. National Institutes of Health, the British Medical Research Council, and the Indiana Genomics Initiative.

Metabolism genes upregulated by lipid depletion relative to control: Anterior		
Gene Name	Fly-Base ID	Metabolic Pathway
CG31075	FBgn0051075	aa catabolism
Hn	FBgn0001208	aa catabolism
CG14630	FBgn0014903	b-oxidation
Mal-A3	FBgn0002571	carb breakdown
Men	FBgn0002719	citric acid cycle
mt:ND3	FBgn0013681	electron transport
Pepck	FBgn0003067	gluconeogenesis
CG14205	FBgn0031034	glucose
CG10960	FBgn0036316	glucose transport
CG1208	FBgn0037386	glucose transport
ImpL2	FBgn0001257	insulin/TOR

Thor	FBgn0261560	insulin/TOR
Lip3	FBgn0023495	lipase
NinaE	FBgn0261244	lipase
CG15531	FBgn0039755	lipid metabolism
CG12512	FBgn0031703	lipid metabolism
CG9743	FBgn0039756	lipid metabolism
Cyp6a8	FBgn0013772	lipid metabolism
Fad2	FBgn0029172	lipid metabolism
bgm	FBgn0027348	lipid metabolism
eloF	FBgn0037762	lipid metabolism
CG3812	FBgn0030421	lipid synthesis
CG15533	FBgn0039768	sphingolipid catabolism
CG15534	FBgn0039769	sphingolipid catabolism
CG31414	FBgn0051414	sphingolipid metabolism
CG31148	FBgn0051148	sphingolipid metabolism
Npc1b	FBgn0261675	sterol traffic
Npc2a	FBgn0031381	sterol traffic
Npc2e	FBgn0051410	sterol traffic
Hr96	FBgn0015240	transcription

Metabolism genes downregulated by lipid depletion relative to control: Anterior		
Gene Name	Fly-Base ID	Metabolic Pathway
CG8112	FBgn0037612	cholesterol metabolism
Acon	FBgn0010100	citric acid cycle
Indy	FBgn0036816	citric acid cycle
slif	FBgn0037203	insulin/TOR
bmm	FBgn0036449	lipase
Yp2	FBgn0005391	lipase
Yp3	FBgn0004047	lipase
CG1718	FBgn0031170	lipid metabolism
fu12	FBgn0026718	lipid synthesis
laza	FBgn0037163	lipid synthesis
LpR1	FBgn0066101	lipoprotein transport

Zw	FBgn0004057	pentose PO4 shunt*
Cerk	FBgn0037315	sphingolipid metabolism
sug	FBgn0033782	transcription

Metabolism genes upregulated by ectopic cholesterol relative to control: Anterior		
Gene Name	Fly-Base ID	Metabolic Pathway
CG31075	FBgn0051075	aa catabolism
CG17597	FBgn0032715	b-oxidation
AcCoAS	FBgn0012034	b-oxidation
Acox57D-p	FBgn0034628	b-oxidation
CG1041	FBgn0037440	b-oxidation
CG2107	FBgn0035383	b-oxidation
CG4594	FBgn0032161	b-oxidation
CG8925	FBgn0038404	b-oxidation
CG9547	FBgn0031824	b-oxidation
yip2	FBgn0040064	b-oxidation
CG14630	FBgn0014903	b-oxidation
whd	FBgn0261862	b-oxidation
Mal-A2	FBgn0002569	carb breakdown
Mal-A3	FBgn0002571	carb breakdown
Mal-A7	FBgn0033296	carb breakdown
Mal-A8	FBgn0033297	carb breakdown
Men	FBgn0002719	citric acid cycle
ATPCL	FBgn0020236	citric acid cycle
Idh	FBgn0001248	citric acid cycle
CG1774	FBgn0039856	fatty acid synthesis
CG3523	FBgn0283427	fatty acid synthesis
fbp	FBgn0032820	gluconeogenesis
CG14205	FBgn0031034	glucose
CG1208	FBgn0037386	glucose transport
CG11208	FBgn0034488	glyoxylate catabolism
Thor	FBgn0261560	insulin/TOR
CG5966	FBgn0029831	lipase
Lip3	FBgn0023495	lipase
CG17292	FBgn0032029	lipase

CG3635	FBgn0032981	lipase
CG6295	FBgn0039471	lipase
CG12512	FBgn0031703	lipid metabolism
CG3961	FBgn0036821	lipid metabolism
Desat1	FBgn0086687	lipid metabolism
CG2781	FBgn0037534	lipid metabolism
CG9743	FBgn0039756	lipid metabolism
bgm	FBgn0027348	lipid metabolism
CG11426	FBgn0037166	lipid synthesis
CG4729	FBgn0036623	lipid synthesis
LpR1	FBgn0066101	lipoprotein transport
CG32250	FBgn0052250	peroxisome
Cat	FBgn0000261	peroxisome
Pex14	FBgn0037020	peroxisome
Pdk	FBgn0017558	pyruvate dehydrogenase
CG15534	FBgn0039769	sphingolipid catabolism
CG31148	FBgn0051148	sphingolipid metabolism
Npc1b	FBgn0261675	sterol traffic
Npc2e	FBgn0051410	sterol traffic
Hr96	FBgn0015240	transcription
sug	FBgn0033782	transcription
CG1315	FBgn0026565	urea cycle

Metabolism genes downregulated by ectopic cholesterol relative to control: Anterior		
santa-maria	FBgn0025697	fatty acid synthesis
CG10960	FBgn0036316	glucose transport
Ilp3	FBgn0044050	insulin/TOR
InR	FBgn0283499	insulin/TOR
CG31089	FBgn0051089	lipase
CG31091	FBgn0051091	lipase
Yp2	FBgn0005391	lipase
Yp3	FBgn0004047	lipase
laza	FBgn0037163	lipid synthesis
wun2	FBgn0041087	lipid synthesis

CG3376	FBgn0034997	sphingolipid catabolism
CDase	FBgn0039774	sphingolipid catabolism
CG15533	FBgn0039768	sphingolipid catabolism

Metabolism genes upregulated by lipid depletion relative to control: Posterior		
CG3790	FBgn0033778	b-oxidation
Mal-A7	FBgn0033296	carb breakdown
mt:ND4	FBgn0262952	electron transport
mt:ND5	FBgn0013684	electron transport
mt:ND6	FBgn0013685	electron transport
ACC	FBgn0033246	fatty acid synthesis
Pepck	FBgn0003067	gluconeogenesis
CG6484	FBgn0034247	glucose transport
ImpL2	FBgn0001257	insulin/TOR
Lip3	FBgn0023495	lipase
CG15531	FBgn0039755	lipid metabolism
CG9747	FBgn0039754	lipid metabolism
CG17646	FBgn0264494	lipid metabolism
CG3812	FBgn0030421	lipid synthesis
CG31414	FBgn0051414	sphingolipid metabolism
CG31413	FBgn0051413	sphingolipid metabolism
Npc2a	FBgn0031381	sterol traffic
Npc1b	FBgn0261675	sterol traffic
Npc2e	FBgn0051410	sterol traffic

Metabolism genes downregulated by lipid depletion relative to control: Posterior		
CG8665	FBgn0032945	aa catabolism
Gdh	FBgn0001098	aa catabolism
CG4630	FBgn0033809	b-oxidation
Acox57D-d	FBgn0034629	b-oxidation
Fatp	FBgn0267828	b-oxidation
Mal-A3	FBgn0002571	carb breakdown
CG8112	FBgn0037612	cholesterol metabolism
CG10960	FBgn0036316	glucose transport
CG7882	FBgn0033047	glucose transport

Glut1	FBgn0264574	glucose transport
Gpdh	FBgn0001128	glycolysis
slif	FBgn0037203	insulin/TOR
CG31089	FBgn0051089	lipase
CG2772	FBgn0031533	lipase
CG3635	FBgn0032981	lipase
Yp1	FBgn0004045	lipase
Yp2	FBgn0005391	lipase
Yp3	FBgn0004047	lipase
CG1718	FBgn0031170	lipid metabolism
CG5853	FBgn0032167	lipid metabolism
bgm	FBgn0027348	lipid metabolism
CG4753	FBgn0036622	lipid synthesis
fu12	FBgn0026718	lipid synthesis
laza	FBgn0037163	lipid synthesis
Pdk	FBgn0017558	pyruvate dehydrogenase
CG3376	FBgn0034997	sphingolipid catabolism
CG15534	FBgn0039769	sphingolipid catabolism
CDase	FBgn0039774	sphingolipid catabolism
Cerk	FBgn0037315	sphingolipid metabolism
Npc2c	FBgn0037783	sterol traffic
Npc2g	FBgn0039800	sterol traffic
Npc2d	FBgn0037782	sterol traffic
sug	FBgn0033782	transcription

Metabolism genes upregulated by lipid depletion relative to control: Posterior		
CG31075	FBgn0051075	aa catabolism
CG17597	FBgn0032715	b-oxidation
Amy-d	FBgn0000078	carb breakdown
Amy-p	FBgn0000079	carb breakdown
mt:ND3	FBgn0013681	electron transport
CG3523	FBgn0283427	fatty acid synthesis
CG1774	FBgn0039856	fatty acid synthesis
Pepck	FBgn0003067	gluconeogenesis
CG14205	FBgn0031034	glucose

CG11208	FBgn0034488	glyoxylate catabolism
ImpL2	FBgn0001257	insulin/TOR
Thor	FBgn0261560	insulin/TOR
Lip3	FBgn0023495	lipase
CG5966	FBgn0029831	lipase
mag	FBgn0036996	lipase
CG15531	FBgn0039755	lipid metabolism
CG3961	FBgn0036821	lipid metabolism
CG12512	FBgn0031703	lipid metabolism
Desat1	FBgn0086687	lipid metabolism
Desat2	FBgn0043043	lipid metabolism
CG3812	FBgn0030421	lipid synthesis
CG31414	FBgn0051414	sphingolipid metabolism
Npc2c	FBgn0037783	sterol traffic

Metabolism genes downregulated by lipid depletion relative to control: Posterior		
InR	FBgn0283499	insulin/TOR
Ilp3	FBgn0044050	insulin/TOR
CG31089	FBgn0051089	lipase
CG31091	FBgn0051091	lipase
CG3376	FBgn0034997	sphingolipid catabolism

Metabolism genes upregulated in *Hr96* mutant relative to control: Anterior		
levy	FBgn0034877	electron transport
CG8665	FBgn0032945	aa catabolism
CG9527	FBgn0031813	b-oxidation
CG17597	FBgn0032715	b-oxidation
tobi	FBgn0261575	carb breakdown
SdhC	FBgn0037873	citric acid cycle
CG3446	FBgn0029868	electron transport
RFeSP	FBgn0021906	electron transport
CG8680	FBgn0031684	electron transport
CG7712	FBgn0033570	electron transport
mt:ND3	FBgn0013681	electron transport

Pdsw	FBgn0021967	electron transport
CG14482	FBgn0034245	electron transport
mt:ND6	FBgn0013685	electron transport
emp	FBgn0010435	fatty acid synthesis
CG17108	FBgn0032285	fatty acid synthesis
CG14205	FBgn0031034	glucose
CG10960	FBgn0036316	glucose transport
Hex-C	FBgn0001187	glycolysis
CG11208	FBgn0034488	glyoxylate catabolism
Spat	FBgn0014031	glyoxylate catabolism
CG17292	FBgn0032029	lipase
CG3961	FBgn0036821	lipid metabolism
Desat1	FBgn0086687	lipid metabolism
CG17646	FBgn0264494	lipid metabolism
CG15531	FBgn0039755	lipid metabolism
Fad2	FBgn0029172	lipid metabolism
Desat2	FBgn0043043	lipid metabolism
LpR1	FBgn0066101	lipoprotein transport
Pect	FBgn0032482	sphingolipid metabolism
Npc2a	FBgn0031381	sterol traffic
Npc2f	FBgn0039154	sterol traffic
Npc2e	FBgn0051410	sterol traffic
sug	FBgn0033782	transcription
CG1315	FBgn0026565	urea cycle

Metabolism genes downregulated in *Hr96* mutant relative to control: Anterior		
GstZ1	FBgn0037696	aa catabolism
CG4594	FBgn0032161	b-oxidation
Mal-A4	FBgn0033294	carb breakdown
Mal-A3	FBgn0002571	carb breakdown
Men-b	FBgn0029155	citric acid cycle
ACC	FBgn0033246	fatty acid synthesis
CG1208	FBgn0037386	glucose transport
Pi3K21B	FBgn0020622	insulin/TOR

gig	FBgn0005198	insulin/TOR
SCOT	FBgn0035298	ketone body catabolism
inaE	FBgn0261244	lipase
Yp3	FBgn0004047	lipase
CG31089	FBgn0051089	lipase
laza	FBgn0037163	lipid synthesis
Mtp	FBgn0266369	lipid trafficking
LpR2	FBgn0051092	lipoprotein transport
CG31148	FBgn0051148	sphingolipid metabolism
lace	FBgn0002524	sphingolipid synthesis

Metabolism genes upregulated in *Hr96* mutant relative to control: Posterior		
CG8112	FBgn0037612	cholesterol metabolism
mt:ND6	FBgn0013685	electron transport
mt:ND3	FBgn0013681	electron transport
RFeSP	FBgn0021906	electron transport
CoVa	FBgn0019624	electron transport
emp	FBgn0010435	fatty acid synthesis
CG1774	FBgn0039856	fatty acid synthesis
CG17108	FBgn0032285	fatty acid synthesis
Pepck	FBgn0003067	gluconeogenesis
CG14205	FBgn0031034	glucose
CG7882	FBgn0033047	glucose transport
Hex-C	FBgn0001187	glycolysis
Spat	FBgn0014031	glyoxylate catabolism
CG11208	FBgn0034488	glyoxylate catabolism
CG8888	FBgn0033679	ketone body synthesis
Lip4	FBgn0032264	lipase
Lsd-1	FBgn0039114	lipid droplet
Lsd-2	FBgn0030608	lipid droplet
Desat2	FBgn0043043	lipid metabolism
Desat1	FBgn0086687	lipid metabolism
CG12512	FBgn0031703	lipid metabolism
CG15531	FBgn0039755	lipid metabolism

CG17646	FBgn0264494	lipid metabolism
CG9743	FBgn0039756	lipid metabolism
CG3812	FBgn0030421	lipid synthesis
Npc2c	FBgn0037783	sterol traffic
Npc2e	FBgn0051410	sterol traffic
Npc2a	FBgn0031381	sterol traffic
sug	FBgn0033782	transcription

Metabolism genes downregulated in *Hr96* Mutant relative to control: Posterior		
GstZ1	FBgn0037696	aa catabolism
CG4594	FBgn0032161	b-oxidation
CG17544	FBgn0032775	b-oxidation
CG14630	FBgn0014903	b-oxidation
Mal-A3	FBgn0002571	carb breakdown
Mal-A7	FBgn0033296	carb breakdown
Mal-A8	FBgn0033297	carb breakdown
Mal-A4	FBgn0033294	carb breakdown
Mal-A1	FBgn0002570	carb breakdown
Amy-p	FBgn0000079	carb breakdown
Amy-d	FBgn0000078	carb breakdown
Mal-A2	FBgn0002569	carb breakdown
crq	FBgn0015924	fatty acid synthesis
CG1208	FBgn0037386	glucose transport
CG6484	FBgn0034247	glucose transport
sut1	FBgn0028563	glucose transport
Yp3	FBgn0004047	lipase
mag	FBgn0036996	lipase
CG8093	FBgn0033999	lipase
CG6283	FBgn0039474	lipase
inaE	FBgn0261244	lipase
Yp2	FBgn0005391	lipase
CG3635	FBgn0032981	lipase
laza	FBgn0037163	lipid synthesis

fu12	FBgn0026718	lipid synthesis
Mtp	FBgn0266369	lipid trafficking
LpR2	FBgn0051092	lipoprotein transport
CG15534	FBgn0039769	sphingolipid catabolism
CDase	FBgn0039774	sphingolipid catabolism
CG31148	FBgn0051148	sphingolipid metabolism
lace	FBgn0002524	sphingolipid synthesis
Npc2d	FBgn0037782	sterol traffic
Npc2f	FBgn0039154	sterol traffic

Metabolism genes upregulated in Hr96 overexpression relative to control: Posterior		
CG9527	FBgn0031813	b-oxidation
tobi	FBgn0261575	carb breakdown
CG17374	FBgn0040001	fatty acid synthesis
CG1516	FBgn0027580	gluconeogenesis
Pepck	FBgn0003067	gluconeogenesis
CG14205	FBgn0031034	glucose
CG7882	FBgn0033047	glucose transport
CG4797	FBgn0034909	glucose transport
sut2	FBgn0028562	glucose transport
sut3	FBgn0028561	glucose transport
CG5966	FBgn0029831	lipase
Lip3	FBgn0023495	lipase
mag	FBgn0036996	lipase
Lsd-2	FBgn0030608	lipid droplet
Lsd-1	FBgn0039114	lipid droplet
CG3961	FBgn0036821	lipid metabolism
CG17646	FBgn0264494	lipid metabolism
Fad2	FBgn0029172	lipid metabolism
Cyp6a8	FBgn0013772	lipid metabolism
Pdk	FBgn0017558	pyruvate dehydrogenase
GlcAT-P	FBgn0036144	sphingolipid synthesis
Npc2b	FBgn0038198	sterol traffic
sug	FBgn0033782	transcription
CG1315	FBgn0026565	urea cycle

Metabolism genes downregulated in Hr96 overexpression relative to control: Posterior		
CG31075	FBgn0051075	aa catabolism
CG17544	FBgn0032775	b-oxidation
CG8925	FBgn0038404	b-oxidation
Amy-d	FBgn0000078	carb breakdown
Amy-p	FBgn0000079	carb breakdown
Mal-A2	FBgn0002569	carb breakdown
Mal-A1	FBgn0002570	carb breakdown
Mal-A3	FBgn0002571	carb breakdown
Mal-A4	FBgn0033294	carb breakdown
Men-b	FBgn0029155	citric acid cycle
crq	FBgn0015924	fatty acid synthesis
CG17108	FBgn0032285	fatty acid synthesis
sut1	FBgn0028563	glucose transport
CG6484	FBgn0034247	glucose transport
CG10960	FBgn0036316	glucose transport
CG1208	FBgn0037386	glucose transport
CG1213	FBgn0037387	glucose transport
Pgm	FBgn0003076	glycogenolysis
ImpL2	FBgn0001257	insulin/TOR
Ilp3	FBgn0044050	insulin/TOR
ImpL3	FBgn0001258	lactate synthesis
Yp1	FBgn0004045	lipase
Yp3	FBgn0004047	lipase
Yp2	FBgn0005391	lipase
CG3635	FBgn0032981	lipase
CG8093	FBgn0033999	lipase
CG31091	FBgn0051091	lipase
fu12	FBgn0026718	lipid synthesis
CG3812	FBgn0030421	lipid synthesis
Mtp	FBgn0266369	lipid trafficking
LpR2	FBgn0051092	lipoprotein transport
CG3376	FBgn0034997	sphingolipid catabolism
bwa	FBgn0045064	sphingolipid metabolism
GlcAT-S	FBgn0032135	sphingolipid synthesis
SMSr	FBgn0052380	sphingolipid synthesis
lace	FBgn0002524	sphingolipid synthesis
SCAP	FBgn0033052	SREBP pathway

Npc2g	FBgn0039800	sterol traffic

REFERENCE LIST: GENES INVOLVED IN METABOLISM IN DROSOPHILA MELANOGASTER

Gene Name	Fly-Base ID	**Metabolic Process**
brummer	FBgn0036449	lipase
CG1882	FBgn0033226	lipase
Doppelgän-ger of brummer	FBgn0030607	lipase
CG10357	FBgn0035453	lipase
CG11055	FBgn0034491	lipase
CG11406	FBgn0034990	lipase
CG11598	FBgn0038067	lipase
CG11600	FBgn0038068	lipase
CG11608	FBgn0038069	lipase
CG13282	FBgn0032612	lipase
CG17097	FBgn0265264	lipase
CG17191	FBgn0039473	lipase
CG17192	FBgn0039472	lipase
CG17292	FBgn0032029	lipase
CG18301	FBgn0032265	lipase
CG18530	FBgn0042207	lipase
CG2772	FBgn0031533	lipase
CG31089	FBgn0051089	lipase
CG31091	FBgn0051091	lipase
CG31684	FBgn0085477	lipase
CG31871	FBgn0051871	lipase
CG31872	FBgn0051872	lipase
CG33174	FBgn0261244	lipase
CG3635	FBgn0032981	lipase
CG5932	FBgn0036996	lipase
CG5966	FBgn0029831	lipase
CG6113	FBgn0032264	lipase
CG6271	FBgn0039476	lipase
CG6277	FBgn0039475	lipase
CG6283	FBgn0039474	lipase
CG6295	FBgn0039471	lipase
CG6296	FBgn0039470	lipase
CG6431	FBgn0032289	lipase
CG6472	FBgn0034166	lipase
CG6753	FBgn0038070	lipase
CG6847	FBgn0030884	lipase
CG7329	FBgn0032271	lipase
CG7367	FBgn0031976	lipase
CG8093	FBgn0033999	lipase
Lip1	FBgn0023496	lipase
Lip2	FBgn0024740	lipase
Lip3	FBgn0023495	lipase
Yp1	FBgn0004045	lipase
Yp2	FBgn0005391	lipase
Yp3	FBgn0004047	lipase
adipose	FBgn0000057	lipase
CG1583	FBgn0030013	lipase

SXE2	FBgn0038398	lipase
Lsd-1	FBgn0039114	lipid droplet
Lsd-2	FBgn0030608	lipid droplet
arg	FBgn0023535	aa catabolism
CG10184	FBgn0039094	aa catabolism
CG10474	FBgn0034427	aa catabolism
CG11251	FBgn0036346	aa catabolism
CG11796	FBgn0036992	aa catabolism
CG1461	FBgn0030558	aa catabolism
CG14681	FBgn0262717	aa catabolism
CG17896	FBgn0023537	aa catabolism
CG1827	FBgn0033431	aa catabolism
CG31075	FBgn0051075	aa catabolism
CG3267	FBgn0042083	aa catabolism
CG33092	FBgn0053092	aa catabolism
CG3626	FBgn0029706	aa catabolism
CG3999	FBgn0037801	aa catabolism
CG4372	FBgn0034665	aa catabolism
CG4434	FBgn0039071	aa catabolism
CG4685	FBgn0039349	aa catabolism
CG5235	FBgn0036565	aa catabolism
CG5241	FBgn0263602	aa catabolism
ade3	FBgn0000053	aa catabolism
CG11089	FBgn0039241	aa catabolism
CG1750	FBgn0039836	aa catabolism
CG3011	FBgn0029823	aa catabolism
CG8665	FBgn0032945	aa catabolism
hgo	FBgn0040211	aa catabolism
CG9362	FBgn0037696	aa catabolism
CG9363	FBgn0037697	aa catabolism
cn, cinnabar	FBgn0000337	aa catabolism
henna	FBgn0001208	aa catabolism
vermillion	FBgn0003965	aa catabolism
Gad1	FBgn0040740	aa catabolism
Gdh	FBgn0001098	aa catabolism
CG6385	FBgn0034276	aa catabolism
CG6415	FBgn0032287	aa catabolism
CG7430	FBgn0036762	aa catabolism
CG8043	FBgn0037610	aa catabolism
pumpless	FBgn0027945	aa catabolism
r, rudimentary	FBgn0003189	urea cycle*
CG1315	FBgn0026565	urea cycle
CG9510	FBgn0032076	urea cycle
arg	FBgn0023535	urea cycle
Glut1	FBgn0264574	glucose transport
Glut3	FBgn0015230	glucose transport
sugar transporter 1	FBgn0028563	glucose transport
sugar transporter 2	FBgn0028562	glucose transport
sugar transporter 3	FBgn0028561	glucose transport
sugar transporter 4	FBgn0028560	glucose transport
CG10960	FBgn0036316	glucose transport

CG1208	FBgn0037386	glucose transport
CG1213	FBgn0037387	glucose transport
CG30035	FBgn0050035	glucose transport
CG4797	FBgn0034909	glucose transport
CG6484	FBgn0034247	glucose transport
CG7882	FBgn0033047	glucose transport
CG8234	FBgn0033644	glucose transport
CG8249	FBgn0034045	glucose transport
CG11669	FBgn0033296	carb breakdown
tobi	FBgn0261575	carb breakdown
CG14476	FBgn0027588	carb breakdown
CG14934	FBgn0032381	carb breakdown
CG14935	FBgn0032382	carb breakdown
CG33080	FBgn0053080	carb breakdown
CG6453	FBgn0032643	carb breakdown
CG7685	FBgn0038619	carb breakdown
CG8690	FBgn0033297	carb breakdown
CG8693	FBgn0033294	carb breakdown
LvpD	FBgn0002569	carb breakdown
LvpH	FBgn0002570	carb breakdown
LvpL	FBgn0002571	carb breakdown
Amy-d	FBgn0000078	carb breakdown
Amy-p	FBgn0000079	carb breakdown
Hex-A	FBgn0001186	glycolysis
Hex-C	FBgn0001187	glycolysis
Hex-t1	FBgn0042711	glycolysis
Hex-t2	FBgn0042710	glycolysis
Pgi	FBgn0003074	glycolysis
Pfk	FBgn0003071	glycolysis
Ald	FBgn0000064	glycolysis
CG5432	FBgn0039425	glycolysis
Tpi	FBgn0086355	glycolysis
Gapdh1	FBgn0001091	glycolysis
Gapdh2	FBgn0001092	glycolysis
Pgk	FBgn0250906	glycolysis
Pglym78	FBgn0014869	glycolysis
Pglym87	FBgn0011270	glycolysis
CG7059	FBgn0038957	glycolysis
Eno	FBgn0000579	glycolysis
Pyk	FBgn0267385	glycolysis
Gpdh	FBgn0001128	glycolysis
ImpL3	FBgn0001258	lactate synthesis
GlyP	FBgn0004507	glycogenolysis
Pgm	FBgn0003076	glycogenolysis
CG9485	FBgn0034618	glycogenolysis
CG1516	FBgn0027580	gluconeogenesis
pepck	FBgn0003067	gluconeogenesis
Fbp	FBgn0032820	gluconeogenesis
CG15400	FBgn0031463	gluconeogenesis/glycogenolysis
CG9480	FBgn0265180	glycogen synthesis
UGP	FBgn0035978	glycogen synthesis

CG6904	FBgn0266064	glycogen synthesis
Zw, zwischenferment	FBgn0004057	pentose PO4 shunt*
Pgd	FBgn0004654	pentose PO4 shunt
Tal	FBgn0023477	pentose PO4 shunt
CG13369	FBgn0025640	pentose PO4 shunt
CG15093	FBgn0034390	pentose PO4 shunt
CG17333	FBgn0030239	pentose PO4 shunt
CG30410	FBgn0050410	pentose PO4 shunt
CG30499	FBgn0050499	pentose PO4 shunt
CG4747	FBgn0043456	pentose PO4 shunt
CG5103	FBgn0036784	pentose PO4 shunt
CG8036	FBgn0037607	pentose PO4 shunt
ATPCL	FBgn0020236	citric acid cycle
Acon	FBgn0010100	citric acid cycle
Idh	FBgn0001248	citric acid cycle/glyoxylate catabolism
CG7430	FBgn0036762	citric acid cycle
Scs	FBgn0004888	citric acid cycle
Scs-fp, SdhA	FBgn0261439	citric acid cycle
Sucb	FBgn0029118	citric acid cycle
CG6255	FBgn0038708	citric acid cycle
SdhB	FBgn0014028	citric acid cycle
CG10219	FBgn0039112	citric acid cycle
CG5718	FBgn0036222	citric acid cycle
CG6629	FBgn0037860	citric acid cycle
CG6666	FBgn0037873	citric acid cycle
CG7349	FBgn0030975	citric acid cycle
CG31874	FBgn0051874	citric acid cycle
CG4095	FBgn0029890	citric acid cycle
CG6140	FBgn0036162	citric acid cycle
(l(1)G0255)	FBgn0028336	citric acid cycle
CG10748	FBgn0036327	citric acid cycle
CG10749	FBgn0036328	citric acid cycle
CG5362	FBgn0262782	citric acid cycle
CG7998	FBgn0262559	citric acid cycle
Men	FBgn0002719	citric acid cycle
Mdh	FBgn0029155	citric acid cycle
Indy	FBgn0036816	citric acid cycle
AcCoAS	FBgn0012034	b-oxidation
CG6178	FBgn0039156	b-oxidation
CG6432	FBgn0039184	b-oxidation
CG8732	FBgn0263120	b-oxidation
CPTI	FBgn0261862	b-oxidation
CG2107	FBgn0035383	b-oxidation
Colt	FBgn0019830	b-oxidation
CG3476	FBgn0031881	b-oxidation
CG12201	FBgn0037970	b-oxidation
CG3790	FBgn0033778	b-oxidation
CG4630	FBgn0033809	b-oxidation
CG6006	FBgn0063649	b-oxidation
CG8925	FBgn0038404	b-oxidation
CG1041	FBgn0037440	b-oxidation

CG5122	FBgn0032471	b-oxidation
CG5265	FBgn0038486	b-oxidation
CG11637	FBgn0036822	b-oxidation
CG11667	FBgn0038743	b-oxidation
CG12262	FBgn0035811	b-oxidation
CG17544	FBgn0032775	b-oxidation
CG3902	FBgn0036824	b-oxidation
CG4586	FBgn0029924	b-oxidation
CG4860	FBgn0037999	b-oxidation
CG5009	FBgn0027572	b-oxidation
CG6638	FBgn0035911	b-oxidation
VLCAD	FBgn0034432	b-oxidation
CG9527	FBgn0031813	b-oxidation
CG9547	FBgn0031824	b-oxidation
Egm Enigma	FBgn0086712	b-oxidation
Acox57D-d	FBgn0034629	b-oxidation
CG6543	FBgn0033879	b-oxidation
CG6984	FBgn0034191	b-oxidation
CG18645	FBgn0033879	b-oxidation
CG8778	FBgn0033761	b-oxidation
CG9577	FBgn0031092	b-oxidation
CG4594	FBgn0032161	b-oxidation
CG4598	FBgn0032160	b-oxidation
CG13890	FBgn0035169	b-oxidation
CG5844	FBgn0038049	b-oxidation
CG5044	FBgn0038326	b-oxidation
CG5611	FBgn0039531	b-oxidation
Scu scully	FBgn0021765	b-oxidation
yip2	FBgn0040064	b-oxidation
CG4389	FBgn0028479	b-oxidation
CG17597	FBgn0032715	b-oxidation
thiolase	FBgn0025352	b-oxidation
CG10814	FBgn0033830	b-oxidation
CG14630	FBgn0014903	b-oxidation
CG4335	FBgn0038795	b-oxidation
CG5321	FBgn0030575	b-oxidation
Fatp	FBgn0267828	b-oxidation
CG11208	FBgn0034488	glyoxylate catabolism
Spat	FBgn0014031	glyoxylate catabolism
l(2)35Di	FBgn0001989	electron transport
ox (oxen)	FBgn0011227	electron transport
mtacp1	FBgn0011361	electron transport
l(3)neo18	FBgn0011455	electron transport
mt:CoI	FBgn0013674	electron transport
mt:CoII	FBgn0013675	electron transport
mt:CoIII	FBgn0013676	electron transport
mt:Cyt-b	FBgn0013678	electron transport
mt:ND1	FBgn0013679	electron transport
mt:ND2	FBgn0013680	electron transport
mt:ND3	FBgn0013681	electron transport
mt:ND4	FBgn0262952	electron transport

mt:ND4L	FBgn0013683	electron transport
mt:ND5	FBgn0013684	electron transport
mt:ND6	FBgn0013685	electron transport
SdhB	FBgn0014028	electron transport
cype cyclop	FBgn0015031	electron transport
Scs-fp	FBgn0261439	electron transport
ND75	FBgn0017566	electron transport
ND23	FBgn0017567	electron transport
CoVa	FBgn0019624	electron transport
ND42	FBgn0019957	electron transport
RFeSP	FBgn0021906	electron transport
Pdsw	FBgn0021967	electron transport
CG3621	FBgn0025839	electron transport
CG3446	FBgn0029868	electron transport
CG3192	FBgn0029888	electron transport
CG18624	FBgn0029971	electron transport
CG5548	FBgn0030605	electron transport
CG9172	FBgn0030718	electron transport
CG3560	FBgn0030733	electron transport
CG5703	FBgn0030853	electron transport
CG7349	FBgn0030975	electron transport
CG12203	FBgn0031021	electron transport
CG14235	FBgn0031066	electron transport
CG11455	FBgn0031228	electron transport
CG3214	FBgn0031436	electron transport
CG12400	FBgn0031505	electron transport
CG8680	FBgn0031684	electron transport
CG9140	FBgn0031771	electron transport
CG11015	FBgn0031830	electron transport
CG11043	FBgn0031831	electron transport
CG9306	FBgn0032511	electron transport
CG10664	FBgn0032833	electron transport
CG10396	FBgn0033020	electron transport
CG7712	FBgn0033570	electron transport
CG12859	FBgn0033961	electron transport
CG8102	FBgn0034007	electron transport
CG14482	FBgn0034245	electron transport
CG11423	FBgn0034251	electron transport
CG10320	FBgn0034645	electron transport
CG17280	FBgn0034877	electron transport
CG3683	FBgn0035046	electron transport
CG12079	FBgn0266582	electron transport
CG4769	FBgn0035600	electron transport
CG5718	FBgn0036222	electron transport
CG4169	FBgn0250814	electron transport
CG6485	FBgn0036706	electron transport
CG7580	FBgn0036728	electron transport
CG14077	FBgn0036830	electron transport
CG6020	FBgn0037001	electron transport
CG7181	FBgn0263911	electron transport
CG6914	FBgn0037172	electron transport

CG18193	FBgn0037579	electron transport
CG6629	FBgn0037860	electron transport
CG6666	FBgn0037873	electron transport
CG3731	FBgn0038271	electron transport
CG10219	FBgn0039112	electron transport
CG11913	FBgn0039331	electron transport
CG17856	FBgn0039576	electron transport
CG14508	FBgn0039651	electron transport
CG2014	FBgn0039669	electron transport
CG7598	FBgn0039689	electron transport
CG1970	FBgn0039909	electron transport
CG9603	FBgn0040529	electron transport
CG15434	FBgn0040705	electron transport
CG2249	FBgn0040773	electron transport
CG18809	FBgn0042132	electron transport
CG6463	FBgn0053493	electron transport
CG30354	FBgn0050354	electron transport
CG32230	FBgn0052230	electron transport
T-cp1	FBgn0003676	electron transport
ATPsyn-a	FBgn0010217	electron transport
l(2)06225	FBgn0010612	electron transport
blw	FBgn0011211	electron transport
mt:ATPase6	FBgn0013672	electron transport
mt:ATPase8	FBgn0013673	electron transport
sun	FBgn0014391	electron transport
ATPsyn-Cf6	FBgn0016119	electron transport
ATPsyn-d	FBgn0016120	electron transport
Oscp	FBgn0262509	electron transport
ATPsyn-b	FBgn0019644	electron transport
ATPsy	FBgn0020235	electron transport
l(1)G0230	FBgn0028342	electron transport
CG7211	FBgn0031941	electron transport
CG10731	FBgn0034081	electron transport
CG7813	FBgn0285943	electron transport
CG4692	FBgn0035032	electron transport
CG12027	FBgn0035585	electron transport
CG5389	FBgn0036568	electron transport
CG3321	FBgn0038224	electron transport
CG1746	FBgn0039830	electron transport
CG31477	FBgn0051477	electron transport
CG2857	FBgn0035078	uncoupling protein
CG9582	FBgn0032090	uncoupling protein
UCP4A	FBgn0030872	uncoupling protein
UCP4B	FBgn0031758	uncoupling protein
UCP4C	FBgn0031757	uncoupling protein
Bmcp; UCP5	FBgn0036199	uncoupling protein
catalase	FBgn0000261	peroxisome
CG10253	FBgn0033983	peroxisome
CG1041	FBgn0037440	peroxisome
CG11919	FBgn0033564	peroxisome
CG12428	FBgn0039543	peroxisome

CG12703	FBgn0031069	peroxisome
CG14778	FBgn0029580	peroxisome
CG1662	FBgn0030481	peroxisome
CG17544	FBgn0032775	peroxisome
CG2022	FBgn0037292	peroxisome
CG32103	FBgn0052103	peroxisome
CG32250	FBgn0052250	peroxisome
CG32262	FBgn0052262	peroxisome
CG33474	FBgn0053474	peroxisome
CG3639	FBgn0031282	peroxisome
CG4289	FBgn0037020	peroxisome
CG4586	FBgn0029924	peroxisome
CG4663	FBgn0033812	peroxisome
npc1a	FBgn0024320	sterol traffic
npc1b	FBgn0261675	sterol traffic
npc2a	FBgn0031381	sterol traffic
npc2b	FBgn0038198	sterol traffic
npc2c	FBgn0037783	sterol traffic
npc2d	FBgn0037782	sterol traffic
npc2e	FBgn0051410	sterol traffic
npc2f	FBgn0039154	sterol traffic
npc2g	FBgn0039800	sterol traffic
npc2h	FBgn0039801	sterol traffic
CG8112	FBgn0037612	cholesterol metabolism
CG3523	FBgn0283427	fatty acid synthesis
CG12170	FBgn0037356	fatty acid synthesis
CG17374	FBgn0040001	fatty acid synthesis
CG7842	FBgn0036691	fatty acid synthesis
CG3524	FBgn0042627	fatty acid synthesis
CG1774	FBgn0039856	fatty acid synthesis
CG8723	FBgn0033246	fatty acid synthesis
ACC	FBgn0033246	fatty acid synthesis
CG17108	FBgn0032285	fatty acid synthesis
emp	FBgn0010435	fatty acid synthesis
CG7422	FBgn0035815	fatty acid synthesis
crq	FBgn0015924	fatty acid synthesis
santa-maria	FBgn0025697	fatty acid synthesis
CG15531	FBgn0039755	lipid metabolism
CG9743	FBgn0039756	lipid metabolism
above three in cluster	FBgn0039754	lipid metabolism
CG8630	FBgn0038130	lipid metabolism
desat1	FBgn0086687	lipid metabolism
desat2	FBgn0043043	lipid metabolism
Fad2	FBgn0029172	lipid metabolism
Cyp4g1	FBgn0010019	lipid metabolism
Cyp6a8	FBgn0013772	lipid metabolism
bubblegum	FBgn0027348	lipid metabolism
CG12512	FBgn0031703	lipid metabolism
CG18155	FBgn0029945	lipid metabolism
CG3961	FBgn0036821	lipid metabolism
double bubble	FBgn0028519	lipid metabolism

CG6178	FBgn0039156	lipid metabolism
CG9009	FBgn0027601	lipid metabolism
CG32186	FBgn0261997	lipid metabolism
CG5853	FBgn0032167	lipid metabolism
CG31689	FBgn0031449	lipid metabolism
CG4822	FBgn0031220	lipid metabolism
CG17646	FBgn0264494	lipid metabolism
CG1718	FBgn0031170	lipid metabolism
CG6052	FBgn0036747	lipid metabolism
CG8534	FBgn0037761	lipid metabolism
CG18609	FBgn0034382	lipid metabolism
CG6261	FBgn0052072	lipid metabolism
CG31141	FBgn0051141	lipid metabolism
Elo68alpha	FBgn0052072	lipid metabolism
CG2781	FBgn0037534	lipid metabolism
noa, baldspot	FBgn0260960	lipid metabolism
eloF	FBgn0037762	lipid metabolism
CG8709	FBgn0263593	lipid metabolism
MTP	FBgn0266369	lipid trafficking
dnr1	FBgn0260866	lipid trafficking
pank	FBgn0011205	CoA biosynthesis
ppcs	FBgn0261285	CoA biosynthesis
ppcdc	FBgn0050290	CoA biosynthesis
ppat-dpck	FBgn0035632	CoA biosynthesis
dpck	FBgn0037469	CoA biosynthesis
CG15450	FBgn0031132	lipid synthesis
CG3209	FBgn0034971	lipid synthesis
CG3812	FBgn0030421	lipid synthesis
CG4729	FBgn0036623	lipid synthesis
CG4753	FBgn0036622	lipid synthesis
fu12	FBgn0026718	lipid synthesis
GPAT	FBgn0027579	lipid synthesis
CG11425	FBgn0037167	lipid synthesis
CG11426	FBgn0037166	lipid synthesis
CG11437	FBgn0037165	lipid synthesis
CG11438	FBgn0037164	lipid synthesis
CG11440	FBgn0037163	lipid synthesis
CG12746	FBgn0037341	lipid synthesis
mod(mdg4)	FBgn0002781	lipid synthesis
wun	FBgn0016078	lipid synthesis
wun-2	FBgn0041087	lipid synthesis
midway	FBgn0004797	lipid synthesis
LpR1	FBgn0066101	lipoprotein transport
LpR2	FBgn0051092	lipoprotein transport
RfaBg	FBgn0087002	lipoprotein transport
CG1140	FBgn0035298	ketone body catabolism
CG10932	FBgn0029969	ketone body synthesis
CG9149	FBgn0035203	ketone body synthesis
CG8888	FBgn0033679	ketone body synthesis
CG10399	FBgn0031877	ketone body synthesis
Hmgs	FBgn0010611	ketone body synthesis

HMG CoA reductase	FBgn0263782	isoprenoid biosynthesis
Fpps	FBgn0025373	isoprenoid biosynthesis
Pdk	FBgn0017558	pyruvate dehydrogenase
CG11876	FBgn0039635	pyruvate dehydrogenase
CG7010	FBgn0028325	pyruvate dehydrogenase
CG5261	FBgn0283658	pyruvate dehydrogenase
schlank	FBgn0040918	sphingolipid synthesis
SmSr	FBgn0052380	sphingolipid synthesis
GlcAT-P	FBgn0036144	sphingolipid synthesis
GlcAT-S	FBgn0032135	sphingolipid synthesis
brn	FBgn0000221	sphingolipid synthesis
CG9078	FBgn0001941	sphingolipid synthesis
Sply	FBgn0010591	sphingolipid catabolism
CG15533	FBgn0039768	sphingolipid catabolism
CG15534	FBgn0039769	sphingolipid catabolism
CG3376	FBgn0034997	sphingolipid catabolism
CDase	FBgn0039774	sphingolipid catabolism
bwa	FBgn0045064	sphingolipid metabolism
CG12034	FBgn0035421	sphingolipid metabolism
CG31148	FBgn0051148	sphingolipid metabolism
CG31413	FBgn0051413	sphingolipid metabolism
CG31414	FBgn0051414	sphingolipid metabolism
CG16708	FBgn0037315	sphingolipid metabolism
Sap-r	FBgn0000416	sphingolipid metabolism
Sk1	FBgn0030300	sphingolipid metabolism
Sk2	FBgn0052484	sphingolipid metabolism
Dhap-at	FBgn0040212	phospholipid biosynthesis
nessy	FBgn0026630	phospholipid biosynthesis
SREBP	FBgn0261283	SREBP pathway
SCAP	FBgn0033052	SREBP pathway
S1P	FBgn0037105	SREBP pathway
S2P	FBgn0033656	SREBP pathway
serine palmitoyltransferase I	FBgn0086532	sphingolipid synthesis
lace	FBgn0002524	sphingolipid synthesis
CG2159	FBgn0052484	sphingolipid catabolism
CG5547	FBgn0032482	sphingolipid metabolism
CG6016	FBgn0033844	sphingolipid metabolism
fatty aldehyde dehydrogenase	FBgn0010548	SREBP pathway
phosphocholine cytidylyltransferase	FBgn0041342	SREBP pathway
phosphatidylserine synthase	FBgn0037010	SREBP pathway
sug	FBgn0033782	transcription
glucose-ind.	FBgn0031034	glucose
bigmax	FBgn0039509	transcription
Mio	FBgn0032940	transcription
Sir2	FBgn0024291	transcription
ATF-2	FBgn0265182	transcription
dHNF4	FBgn0004914	transcription
DHR96	FBgn0015240	transcription

DHR38	FBgn0014859	transcription
ewg	FBgn0005427	transcription
dElg	FBgn0004510	transcription
spargel	FBgn0037248	transcription
CG8057	FBgn0260972	AMPK
SNF1A	FBgn0023169	AMPK
SNF4A	FBgn0264357	AMPK
IMP-L2	FBgn0001257	insulin/TOR
dALS	FBgn0261269	insulin/TOR
dilp1	FBgn0044051	insulin/TOR
dilp2	FBgn0036046	insulin/TOR
dilp3	FBgn0044050	insulin/TOR
dilp4	FBgn0044049	insulin/TOR
dilp5	FBgn0044048	insulin/TOR
dilp6	FBgn0044047	insulin/TOR
dilp7	FBgn0044046	insulin/TOR
chico, IGF1	FBgn0024248	insulin/TOR
dock; dreadlocks	FBgn0010583	insulin/TOR
InR	FBgn0283499	insulin/TOR
PI3K; p60	FBgn0020622	insulin/TOR
PI3K; Dp110	FBgn0015279	insulin/TOR
PTEN	FBgn0026379	insulin/TOR
PDK1	FBgn0020386	insulin/TOR
TOR	FBgn0021796	insulin/TOR
TSC1	FBgn0026317	insulin/TOR
TSC2, gigas	FBgn0005198	insulin/TOR
S6K	FBgn0283472	insulin/TOR
Thor	FBgn0261560	insulin/TOR
Akt	FBgn0010379	insulin/TOR
Lk6	FBgn0017581	insulin/TOR
melted	FBgn0023001	insulin/TOR
slimfast	FBgn0037203	insulin/TOR
Akh	FBgn0004552	Akh signaling
AKHR	FBgn0025595	Akh signaling

REFERENCES

Amcheslavsky, A., Song, W., Li, Q., Nie, Y., Bragatto, I., Ferrandon, D., Perrimon, N., and Ip, Y.T. (2014). Enteroendocrine cells support intestinal stem-cell-mediated homeostasis in *Drosphila*. Cell Rep. *9* : 32-39.

Baker, K.D., and Thummel, C.S. (2007). Diabetic larvae and obese flies-emerging studies of metabolism in *Drosophila*. Cell Metab. *6*: 257-66.

Barker, N., Ridgway, R.A., van Es, J.H., van de Wetering, M., Begthel, H., van den Born, M., Danenberg, E., Clarke, A.R., Sansom, O.J., and Clevers, H. (2009). Crypt stem cells as the cells-of-origin of intestinal cancer. Nature. *457*: 608-611.

Barthelme, D., Sauer, R.T. (2012). Identification of the Cdc48-20S proteasome as an ancient AAA+ proteolytic machine. Science. *337*, 843-846.

Bates, J.M., Mittge, E., Kuhlman, J., Baden, K.N., Cheesman, S.E., and Guillemin, K. (2006). Distinct signals from the microbiota promote different aspects of zebrafish gut differentiation. Dev. Biol. *297*, 374-386.

Beehler-Evans, R., and Micchelli, C. A. (2015). Generation of enteroendocrine cell diversity in midgut stem cell lineages. Development *142*, 654-664.

Bender, L.B., Kooh, P.J., and Muskavitch, M.A. (1993). Complex function and expression of Delta during Drosophila oogenesis. Genetics *133*, 967-978.

Beyaz, S., Mana, M.D., Roper, J., Kedrin, D., Saadatpour, A., Hong, S.J., Bauer-Rowe, K.E., Xifaras, M.E., Akkad, A., Arias, E., et al. (2016). High-fat diet enhances stemness and tumorigenicity of intestinal progenitors. Nature *531*, 53-58.

Bilder, D., and Fortini, M.E. (2009). Endocytic regulation of Notch signaling. Curr. Opin. Genet. Dev. *19*: 323-328.

Brown, M.S., and Goldstein, J.L. (1997). The SREBP pathway: regulation of cholesterol metabolism by proteolysis of a membrane-bound transcription factor. Cell *89*, 331-340.

Buchon, N., Broderick, N.A., Kuraishi, T., and Lemaitre, B. (2010). Drosophila EGFR pathway coordinates stem cell proliferation and gut remodeling following infection. BMC Biol. *8*, 152-171.

Buchon, N., Osman, D., David, F.P., Fang, H.Y., Boquete, J.P., Deplancke, B., and Lemaitre, B. (2013). Morphological and molecular characterization of adult midgut compartmentalization in Drosophila. Cell Rep. *3*, 1725-1738.

Buchon, N., and Osman, D. (2015). All for one and one for all: Regionalization of the Drosophila intestine. Insect Biochem Mol. Biol. *67*: 2-8.

Buffa, R., Capella, C., Fontana, P., Usellini, L., and Solcia, E. (1978). Types of endocrine cells in the human colon and rectum. Cell Tissue Res. *192* :227–240.

Bujold, M., Gopalakrishan, A., Nally, E., and King-Jones, K. (2010). Nuclear receptor DHR96 acts as a sentinel for low cholesterol concentrations in *Drosophila melanogaster*. Mol. Cell Bio. *30*, 793-805.

Campos-Ortega, J.A., and Hartenstein V. The Embryonic Development of Drosophila melanogaster. Springer-Verlag; Berlin: 1985.

Carulli, A.J., Samuelson, L.C., and Schnell, S. (2014). Unraveling intestinal stem cell behavior with models of crypt dynamics. Integr. Biol. (Camb.) *6*, 243-257.

Chen, J., Reiher, W., Hermann-Luibl, C., Sellami, A., Cognigni, P. Kondo, S., Helfrich-Förister, C., Veenstra, J.A., and Wegener, C. (2016). Allatostatin A signaling in Drosophila regulates feeding and sleep and is modulated by PDF. PloS Genet. *12*, e1006346.

Conner, S.D. (2016). Regulation of Notch signaling through intracellular transport. Int. Rev. Cell Mol. Biol. *323*, 107-27.

Cotte, A.K., Aires, V., Fredon, M., Limagne, E., Derangere, V., Thibaudin, M., Humblin, E., Scagliarini, A., de Barros, J-P.P., Hillon, P., Ghiringhelli, F., and Delmas, D. (2018). Lysophosphatidylcholine acyltransferase 2-mediated lipid droplet production supports olorectal cancer chemoresistance. Nature Comm. *9*: 322

Coumailleau, F., Furthauer, M., Knoblich, J.A., and Gonzalez-Gaitan, M. (2009). Directional Delta and Notch trafficking in Sara endosomes during asymmetric cell division. Nature *458*, 1051-1055.

Cox, J.E., Thummel, C.S., and Tennessen, J.M. (2017). Metabolic Studies in *Drosophila*. Genetics. *206*: 1169-1185.

DeBose-Boyd, R.A. (2008). Feedback regulation of cholesterol synthesis: sterol-accelerated ubiquitination and degradation of HMG CoA reductase. Cell Res. *18*, 609-621.

DeBose-Boyd, R.A., Brown, M.S., Li, W.P., Nohturfft, A., Goldstein, J.L., Espenshade, P.J., (2006). Transport-dependent proteolysis of SREBP: relocation of site-1 protease from Golgi to ER obviates the need for SREBP transport to Golgi. Cell. *99,* 703-12.

Demitrack, E.S., and Samuelson, L.C. (2016). Notch regulation of gastrointestinal stem cells. J. Physiol. *594*, 4791-803.

Ding, S., Chi, M.M., Scull, B.P., Rigby, R., Schwerbrock, N.M., Magness, S., Jobin, C., and Lund, P.K. (2010). High-fat diet: bacteria interactions promote intestinal inflammation which precedes and correlates with obesity and insulin resistance in mouse. PLoS One *5*, e12191.

Doane, W.W. (1960). Developmental physiology of the mutant female sterile(2)adipose of *Drosophila melanogaster*. I. Adult morphology, longevity, egg production, and egg lethality. J. Exp. Zool. *145*: 1-21.

Driver, I., and Ohlstein, B. (2014). Specification of regional intestinal stem cell identity during *Drosophila* metamorphosis. Development. *141:* 1848-1856.

Drummond-Barbosa, D., and Spradling, A.C. (2001). Stem cells and their progeny respond to nutritional changes during Drosophila oogenesis. Dev. Biol. *231*, 265-278.

D'Souza B., Meloty-Kapella L., and Weinmaster G. *(*2010*)*. Canonical and non-canonical Notch ligands. *Curr. Top. Dev. Biol. 92,* 73-129.

Dutta, D., Dobson, A.J., Houtz, P.L., Glaber, C., Revah, J., Korzelius, J., Patel, P.H., Edgar, B.A., Buchon, N. (2015). Regional cell-specific transcriptome mapping reveals regulatory complexity in the adult Drosophila midgut. Cell Rep. *12,* 346-58.

Egawa, J., Pearn, M. L., Lemkuil, B. P., Patel, P. M., Head, B. P. (2015). Membrane lipid rafts and neurobiology: age-related changes in membrane lipids and loss of neuronal function. J. Physiol. *594*, 4565–4579.

Elrick, H., and Stimmler, L. (1964). Plasma insulin response to oral and intravenous glucose administration. J. Clin. Endocrinol. Metab. *24*: 1076-82.

Evans, R.M., and Mangelsdorf, D.J. (2014). Nuclear Receptors, RXR, and the Big Bang. Cell *157*, 255-266.

Fang, S., Ferrone, M., Yang, C., Jensen, J.P., Tiwari, S., Weissman, A.M. (2001). The tumor autocrine motility factor receptor, gp78, is a ubiquitin protein ligase implicated in degradation from the endoplasmic reticulum. Proc. Natl. Acad. Sci. *98*, 14422-7.

Faulkner, R.A., Nguyen, A.D., Jo, Y., and DeBose-Boyd, R.A. (2013). Lipid-regulated degradation of HMG-Co reductase and Insig-1 through distinct mechanisms in insect cells. J. Lipid Res. *54*, 1011-1022.

Fluegel, M.L., Parker, T.J., and Pallank, L.J. (2006). Mutations of a drosophila NPC1 gene confer sterol and ecdysone metabolic defects. Genetics. *172:* 185-196.

Garcia-Sanz, P., Orgaz, L., Fuentes, J.M., Vicario, C. and Moratalla, R. (2018). Cholesterol and multilamellar bodies: Lysosomal dysfunction in GBA-Parkinson disease. Autophagy. *14:* 717-718

Garrison, W.D., Battle, M.A., Yang, C., Kaestner, K.H., Sladek, F.M., and Duncan, S.A. (2006). Hepatocyte nuclear factor 4alpha is essential for embryonic development of the mouse colon. Gastroenterology. *130*:1207-1220.

Gervais, L. and Bardin, A.J. (2017). Tissue homeostasis and aging : new insight from the fly intestine. Curr. Opin. Cell Biol. *48*, 97-105.

Gil, G., Faust, J.R., Chin, D.J., Goldstein, J.L., Brown, M.S., (1985). Membrane-bound domain of HMG CoA reductase is required for sterol-enhanced degradation of the enzyme. Cell. *41*, 249-58.

Gilbert, L.I., Rybczynski, R., and Warren, J.T. (2002). Control and biochemical nature of the ecdysteroidogenic pathway. Annual Review of Entomology, vol 47, pp. 883-916.

Goldstein, J. L., and Brown, M. S. (1990). Regulation of the mevalonate pathway. Nature *343*, 425-430.

Goldstein, J.L., DeBose-Boyd, R.A., Brown, M.S. (2006). Protein sensors for membrane sterols. Cell. *124*, 35-46.

Gong, Y., Lee, J.N., Lee, P.C., Goldstein, J.L., Brown, M.S., Ye, J. (2006). Sterol-regulated ubiquitination and degradation of Insig-1 creates a convergent mechanism for feedback control of cholesterol synthesis and uptake. Cell Metab. *3*,15-24.

Guo, Z. and Ohlstein, B. (2015). Stem cell regulation. Bidirectional Notch signaling regulates Drosophila intestinal stem cell multipotency. Science *350*, aab0988.

Gutierrez-Aguilar, R., and Woods, S.C. (2011). Nutrition and L and K-enteroendocrine cells. Curr. Opin. Endocrinol. Diabetes Obes. *18*: 35-41.

Habchi, J., Chia, S., Galvagnion, C., Michaels, T.C.T., Bellaiche, M.M.J., Ruggeri, F.S., Sanguanini, M., Idini, I., Kumita, J.R., Sparr, E., Linse, S., Dobson, C.M., Knowles, T.P.J., Vendruscolo, M. (2018). Cholesterol catalyses Aβ42 aggregation through a heterogeneous nucleation pathway in the presence of lipid membranes. Nat. Chem. *10:* 673-683

Harrop, T.W., Pearce, S.L., Daborn, P.J., and Batterham, P. (2014). Whole-genome expression analysis in the third instar larval midgut of *Drosophila melanogaster*. G3. *4*:2197-205.

Hartman, T.R., Strochlic, T.I., Ji, Y., Zinshteyn, D., and O'Reilly, A.M. (2009). Diet controls *Drosophila* follicle stem cell proliferation via Hedgehog sequestration and release. J. Cell Biol. *201*: 741-757.

Hentze, J.L., Carlsson, M.A., Kondo, S., Nässel, D.R, and Rewitz, K.F. (2015). The neuropeptide allatostatin A regulates metabolism and feeding decisions in Drosophila. Sci. Rep. *5*, 11680.

Hissa, B., Duarte, J.G., Kelles, L.F., Santos, F.P., del Puerto, H.L., Gazzinelli-Guimarães, P.H., de Paula, A.M., Agero, U., Mesquita, O.N., Guatimosim, C., Chiari, E., and Andrade, L.O. (2012). Membrane cholesterol regulates lysosome-plasma membrane fusion events and modulates Trypanosoma cruzi invasion of host cells. PLoS Negl. Trop. Dis. *6*: e1583

Hoey, T., Yen, W.C., Axelrod, F., Basi, J., Donigian, L., Dylla, S., Fitch-Bruhns, M., Lazetic, S., Park, I.K., Sato, A., et al. (2009). DLL4 blockade inhibits tumor growth and reduces tumor-initiating cell frequency. Cell Stem Cell *5*, 168-177.

Horner, M.A., Pardee, K., Liu, S., King-Jones, K., Lajoie, G., Edwards, A., Krause, H.M., and Thummel, C.S. (2009). The Drosophila DHR96 nuclear receptor binds cholesterol and regulates cholesterol homeostasis. Genes Dev. *23*, 2711-2716.

Hua, X., Nohturfft, A., Goldstein, J.L., Brown, M.S. (1996). Sterol resistance in CHO cells traced to point mutation in SREBP cleavage-activating protein. Cell. *87*, 415-26.

Huang, M., Narita, S., Numakura, K., Tsuruta, H., Saito, M., Inoue, T., Horikawa, Y., Tsuchiya, N., and Habuchi, T. (2012). A high-fat diet enhances proliferation of prostate cancer cells and activates MCP-1/CCR2 signaling. Prostate *72*, 1779-1788.

Huang, X., Suyama, K., Buchanan, J., Zhu, A.J., and Scott, M.P. (2005). A Drosophila model of the Niemann-Pick type C lysosome storage disease: dnpc1a is required for molting and sterol homeostasis. Development *132*, 5115-5124.

Huang, X., Warren, J.T., Buchanan, J.A., Gilbert, L.I., Scott, M.P. (2007). Drosophila Niemann-Pick Type C-2 genes control sterol homeostasis and steroid biosynthesis: a model of human neurodegenerative disease. Development *134*, 3733-3742.

Hudry, B., Khadayate, S., and Miguel-Aliaga, I. (2016). The sexual identity of adult intestinal stem cells controls organ size and plasticity. Nature *530*, 344-348.

Imbard, A., Benoist, J.-F. and Blom, H.J. (2013). Neural tube defects, folic acid and methylation. Int. J. Environ. Res. Public Health *10*, 4352-4389.

Janowski, B.A., Willy, P.J., Devi, T.R., Falck, J.R., and Mangelsdorf, D.J. (1996). An oxysterol signalling pathway mediated by the nuclear receptor LXR alpha. Nature. *383,* 728-731.

Jiang, H. and Edgar, B.A. (2009). EGFR signaling regulates the proliferation of *Drosophila* adult midgut progenitors. Development. *136:* 483-493.

Jiang, H., Patel, P.H., Kohlmaier, A., Grenley, M.O., McEwen, D.G., and Edgar, B.A. (2009). Cytokine/Jak/Stat signaling mediates regeneration and homeostasis in the Drosophila midgut. Cell *137*, 1343-1355.

Jones, M.W., de Jonge, M.D., James, S.A., Burke, R. (2015). Elemental mapping of the entire intact *Drosophila* gastrointestinal tract. J. Biol. Inorg. Chem. *20*: 979-87.

Kalaany, N.Y., and Mangelsdorf, D.J. (2006). LXRS and FXR: the yin and yang of cholesterol and fat metabolism. Annu. Rev. Physiol. *68*, 159-191.

Kloudova, A., Guengerich, F.P., Soucek P. (2017). The role of oxysterols in human cancer. Trends Endocrinol. Metab. *28*, 485-496.

Kuhnlein, R.P. (2010). Energy homeostasis regulation in *Drosophila*: a lipocentric perspective. Results Probl. Cell Differ. *52*: 159-73.

Kunte, A.S., Matthews, K.A., and Rawson, R.B. (2006). Fatty acid auxotrophy in Drosophila larvae lacking SREBP. Cell Metab. *3*, 439-448.

Lai, C.Q., Parnell, L.D., Arnett, D.K., Garcia-Bailo, B., Tsai, M.Y., Kabagambe, E.K., Straka, R.J., Province, M.A., An, P., Borecki, I.B., *et al.* (2009). WDTC1, the ortholog of Drosophila adipose gene, associates with human obesity, modulated by MUFA intake. Obesity (Silver Spring). *17:* 593-600.

Langmead, B., and Salzberg, S.L. (2012). Fast gapped-read alignment with Bowtie 2. Nat. Methods *4*, 357-359.

Lee, C.Y., Cooksey, B.A., and Baehrecke, E.H. (2002). Steroid regulation of midgut cell death during *Drosophila* development. Dev. Biol. *250:* 101-111.

Lingwood, D., and Simons, K. (2010). Lipid rafts as a membrane-organizing principle. Science. *327,* 46-50.

Lechtig, A., Yarbrough, C., Delgado, H., Habicht, J.P., Martorell, R., and Klein, R.E. (1975). Influence of maternal nutrition on birth weight. Am. J. Clin. Nutr. *28*, 1223-1233.

Lo Sasso, G., Murzilli, S., Salvatore, L., D'Errico, I., Petruzzelli, M., Conca, P., Jiang, Z.Y., Calabresi, L., Parini, P., and Moschetta, A. (2010). Intestinal specific LXR activation stimulates reverse cholesterol transport and protects from atherosclerosis. Cell Metab. *12* : 187-93.

Lipson, C., Alalouf, G., Bajorek, M., Rabinovich, E., Atir-Lande, A., Glickman, M., Bar-Nun, S. (2008). A proteasomal ATPase contributes to dislocation of endoplasmic reticulum-associated degradation (ERAD) substrates. J. Biol. Chem. *283*, 7166-75.

Lyman D. F., and Yedvobnick B. (1995). *Drosophila* Notch receptor activity suppresses Hairless function during adult external sensory organ development. Genetics *141*, 1491-1505.

Marianes, A., and Spradling, A.C. (2013). Physiological and stem cell compartmentalization within the Drosophila midgut. Elife *2*, e00886.

Micchelli, C.A., and Perrimon, N. (2006). Evidence that stem cells reside in the adult Drosophila midgut epithelium. Nature *439*, 475-479.

Micchelli, C.A., Sudmeier, L., Perrimon, N., Tang, S., and Beehler-Evans, R. (2011). Identification of adult midgut precursors in Drosophila. Gene Expr. Patterns. *11: 12-21.*

Millichap, J.G., Jones, J.D., Rudis, B.P. (1964). Mechanism of anticonvulsant action of ketogenic diet. Studies in animals with experimental seizures and in children with petit mal epilepsy. Am. J. Dis. Child. *107,* 593-604.

Miyagi, T., Takehara, T., Uemura, A., Nishio, K., Shimizu, S., Kodama, T., Hikita, H., Li, W., Sasakawa, A., Tatsumi, T., et al. (2010). Absence of invariant natural killer T cells deteriorates liver inflammation and fibrosis in mice fed high-fat diet. J. Gastroenterol. *45*, 1247-1254.

Miyawaki, K., Yamada, Y., Yano, H., Niwa, H., Ban, N., Ihara, Y., Kubota, A., Fujimoto, S., Kajikawa, M., Kuroe, A., Tsuda, K., Hashimoto, H., Yamashita, T., Jomori, T., Tashiro, F., Miyazaki, J., and Seino, Y. (1999). Glucose intolerance caused by a defect in the entero-insular axis: a study in gastric inhibitory polypeptide receptor knockout mice. Proc. Natl. Acad. Sci. *96* :14843–14847.

Mohr O. L. (1919). Character changes caused by mutation of an entire region of a chromosome in *Drosophila*. Genetics *4:* 1-18.

Moran, G.W., Leslie, F.C., Levison, S.E., and McLaughlin, J.T. (2008). Enteroendocrine cells: Neglected players in gastrointestinal disorders? Therapeutic Advances in Gastroenterology. *1*:51-60.

Morrisey, E.E., Tang, Z., Sigrist, K., Lu, M.M., Jiang, F., Ip, H.S., and Parmacek, M.S. (1998). GATA6 regulates HNF4 and is required for differentiation of visceral endoderm in the mouse embryo. Genes Dev. *12*: 3597-90.

Nakanishi, M., Goldstein, J.L., and Brown, M.S. (1988). Multivalent control of 3-hydroxy-3-methylglutaryl coenzyme A reductase. Mevalonate-derived product inhibits translation of mRNA and accelerates degradation of enzyme. J. Biol. Chem. *263*, 8929-8937.

Nation, J.L. (2002). Insect Physiology and Biochemistry. Boca Raton, FL: CRC Press. 485 pp.

de Navascues, J., Perdigoto, C.N., Bian, Y., Schneider, M.H., Bardin, A.J., nez-Arias, A.M.I. and Simons, B.D. (2012). Drosophila midgut homeostasis involves neutral competition between symmetrically dividing intestinal stem cells. EMBO J. *31*: 2473-2485.

O'Brien, L.E., Soliman, S.S., Li, X., and Bilder, D. (2011). Altered modes of stem cell division drive adaptive intestinal growth. Cell *14*, 603-14.

Ohlstein, B., and Spradling, A. (2006). The adult Drosophila posterior midgut is maintained by pluripotent stem cells. Nature *439*, 470-474.

Ohlstein, B., and Spradling, A. (2007). Multipotent Drosophila intestinal stem cells specify daughter cell fates by differential notch signaling. Science *315*, 988-992.

O'Neill, A.M., Burrington, C.M., Gillaspie, E.A., Lynch, D.T., Horsman, M.J., and Greene, M.W. (2016). High-fat Western diet-induced obesity contributes to increased tumor growth in mouse models of human colon cancer. Nutr. Res. *36*, 1325-1334.

Orho-Melander, M. (2015). Genetics of coronary heart disease: towards causal mechanisms, novel drug targets and more personalized prevention. J. Intern. Med. *278*, 433-446.

Osenkowski, P., Wenjuan, Y., Wang, R., Wolfe, M.S., and Selkoe, D. (2008). Direct and potent regulation of gamma-secretase by its lipid microenvironment. JBC. *283*: 2259-22540.

Palanker, L., Tennessen, J.M., Lam, G., and THummel, C.S. (2009). *Drosophila* HNF4 Regulates Lipid Mobilization and β-oxidation. Cell Metab. *9*: 228-239.

Park, J.H., Chen, J., Jang, S., Ahn, T.J., Kang, K., Choi, M.S., and Kwon J.Y. (2016). A subset of enteroendocrine cells is activated by amino acids in the *Drosophila* midgut. F.E.B.S. Letters. *590*: 493-500.

Parker, H.E., Habib, A.M., Rogers, G.J., Gribble, F.M., and Reimann, F. (2009). Nutrient-dependent secretion of glucose-dependent insulinotropic polypeptide from primary murine K cells. Diabetologia. *52*: 289-298.

Parks, A. L., Klueg, K. M., Stout J. R., and Muskavitch M. A. (2000). Ligand endocytosis drives receptor dissociation and activation in the Notch pathway. Development. *127*, 1373-1385.

Patel, P.H., Dutta, D., and Edgar, B.A. (2015). Niche appropriation by Drosophila intestinal stem cell tumours. Nat. Cell Biol. *17*, 1182-1192.

Pavlova, N. N., and Thompson, C. B., (2016). The emerging hallmarks of cancer metabolism. Cell. Metab. *23*, 27–47.

Phillips, M.D., and Thomas, G.H. (2006). Brush border spectrin in required for early endosome recycling in Drosophila. J. Cell Sci. *119*, 1361-1370.

Popp, J., Meichsner, S., Kolsch, H., Lewczuk, P., Maier, W., Kornhuber, J., Jessen, F., and Lutjohann, D. (2013). Cerebral and extracerebral cholesterol metabolism and CSF markers of Alzheimer's disease. Biochem. Pharmacol. *86*: 37-42.

Porter, J.A., Young, K.E., Beachy, P.A. (1996). Cholesterol modification of hedgehog signaling proteins in animal development. Science. *274*, 255-9.

Preston, J.D., Reynolds, L.J., and Pearson, K.J. (2018). Developmental origins of health span and life span: A Mini-Review. Gerontology. *64*, 237-245.

Rakoff-Nahoum, S., Kong, Y., Kleinstein, S.H., Subramanian, S., Ahern, P.P., Gordon, J.I., and Medzhitov, R. (2015). Analysis of gene-environment interactions in postnatal development of the mammalian intestine. Proc. Natl. Acad. Sci., USA *112*, 1929-1936.

Ramakrishnan, U. (2004). Nutrition and low birth weight: from research to practice. Am. J. Clin. Nutr. *79*, 17-21.

Raman, M., Sergeev, M., Garnaas, M., Lydeard, J.R., Huttlin, E.L., Goessling, W., Shah, J.V., Harper, J.W. (2015). Systemic proteomics of the VCP-UBXD adaptor network identifies a role for UBXN10 in regulating ciliogenesis. Nat. Cell Biol. *17*, 1356-1360.

Ravid, T., Doolman, R., Avner, R., Harats, D., Roitelman, J. (2000). The ubiquitin-proteasome pathway mediates the regulated degradation of mammalian 3-hydroxy-3-methylglutaryl-coenzyme A reductase. J. Biol. Chem. *275*, 35840-7.

Reiff, T., Jacobson, J., Cognigni, P., Antonello, Z., Ballesta, E., Tan, K.J., Yew, J.Y., Dominguez, M., and Miguel-Aliaga, I. (2015). Endocrine remodelling of the adult intestine sustains reproduction in Drosophila. Elife *4*, e06930.

Repa, J.J., Berge, K.E., Pomajzl, C., Richardson, J.A., Hobbs, H., and Mangelsdorf, D.J. (2002). Regulation of the ATP-binding cassette sterol transporters ABCG5 and ABCG8 by the liver X receptors alpha and beta. J. Biol. Chem. *227*, 18793-18800.

Reusens, B., Theys, N., Dumortier, O., Goosse, K., and Remacle, C. (2011). Maternal malnutrition programs the endocrine pancreas in progeny. Am. J. Clin. Nutr. *94*, 1824S-1829S.

Reynolds, C.M., Gray, C., Li, M., Segovia, S.A., and Vickers, M.H. (2015). Early life nutrition and energy balance disorders in offspring in later life. Nutrients *7*, 8090-111.

Rink, J., Ghigo, E., Kalaidzidis, Y. and Zerial, M. *(*2005*)*. Rab conversion as a mechanism of progression from early to late endosomes. *Cell. 122,* 735–749.

Saini, H.K., Arneja, A.S., and Dhalla, N.S. (2004). Role of cholesterol in cardiovascular dysfunction. Canadian Journal of Cardiology. *20*: 333-346.

Sang, J.H. (1956). The quantitative nutritional requirements of *Drosophila melanogaster*. The Journal of Experimental Biology. *33*, 45-72.

Schneider, C. A., Rasband, W. S. and Eliceiri, K. W. (2012). NIH Image to ImageJ: 25 years of image analysis. Nature Methods *9*, 671-675.

Seugnet, L., Simpson, P., and Haenlin, M. (1997). Requirement for dynamin during Notch signaling in Drosophila neurogenesis. Dev. Biol. *192*, 585-598.

Sieber, M.H., and Spradling, A.C. (2015). Steroid signaling establishes a female metabolic state and regulates SREBP to control oocyte lipid accumulation. Curr. Biol. *25*, 993-1004.

Sieber, M.H., and Thummel, C.S. (2009). The DHR96 nuclear receptor controls triacylglycerol homeostasis in Drosophila. Cell Metab. *10*, 481-490.

Sieber, M.H., and Thummel, C.S. (2012). Coordination of triacylglycerol and cholesterol homeostasis by DHR96 and the Drosophila LipA homolog magro. Cell Metab. *15*, 122-127.

Silvente-Poirot, S. and Poirot, M. (2014). Cancer. Cholesterol and cancer, in the balance. Science *343*, 1445-6.

Simons, K., and Toomre, D. 2000. Lipid rafts and signal transduction. Nat. Rev. Mol. Cell Biol. *1***:** 31–41.

Song, B.L., Sever, N., DeBose-Boyd, R.A. (2005). Gp78, a membrane-anchored ubiquitin ligase, associates with Insig-1 and couples sterol-regulated ubiquitination to degradation of HMG CoA reductase. Mol. Cell. *19*, 829-40.

Song, W., Veenstra, J.A., and Perrimon, N. (2014). Control of lipid metabolism by Tachykinin in *Drosophila*. Cell Rep. *9:* 40-47.

Suman, S., Das, T.P., Ankem, M.K., and Damodaran, C. (2014). Targeting Notch signaling in colorectal cancer. Curr. Colorectal Cancer Rep. *10*, 411-416.

Sun, J., and Deng, W.M. (2005). Notch-dependent downregulation of the homeodomain gene cut is required for the mitotic cycle/endocycle switch and cell differentiation in Drosophila follicle cells. Development *132*, 4299-4308.

Sun, J., and Deng, W.M. (2007). Hindsight mediates the role of Notch in suppressing hedgehog signaling and cell proliferation. Dev. Cell *12*, 431-442.

Tang, F.Y., Pai, M.H., and Chiang, E.P. (2012). Consumption of high-fat diet induces tumor progression and epithelial-mesenchymal transition of colorectal cancer in a mouse xenograft model. J Nutr Biochem *23*, 1302-1313.

Takashima, S., Adams, K.L., Ortiz, P.A., Ying, C.T., Moridzadeh, R., Younossi-Hartenstein, A., and Hartenstein, V. (2011). A novel tissue in an established model system: the *Drosophila* pupal midgut. Development. *353:* 161-172.

Takashima, S., Gold, D. and Hartenstein, V. (2013). Stem cells and lineages of the intestine: a developmental and evolutionary perspective. Dev. Genes Evol. *223*, 85-102.

Templeman, N.M. and Murphy, C.T. (2018). Regulation of reproduction and longevity by nutrient-sensing pathways. J. Cell Biol. *217*, 93-106.

Tepass, U., and Hartenstein, V. (1994). Epithelium formation in the Drosophila midgut depends on the interaction of endoderm and mesoderm. Development. *120*: 579-90.

van der Heijden, R.A., Bijzet, J., Meijers, W.C., Yakala, G.K., Kleemann, R., Nguyen, T.Q., de Boer, R.A., Schalkwijk, C.G., Hazenberg, B.P., Tietge, U.J., et al. (2015). Obesity-induced chronic inflammation in high fat diet challenged C57BL/6J mice is associated with acceleration of age-dependent renal amyloidosis. Sci. Rep. *5*, 16474.

van der Velde, A.E., Vrins, C.L., van den Oever, K., Kunne, C., Oude Elfernink, R.P., Kuipers, F., and Groen, A.K. (2007). Direct intestinal cholesterol secretion contributes significantly to total fecal neutral sterol excretion in mice. Gastroenterology. *133*, 967-975.

van der Wulp, M. Y., Verkade, H. J., Groen, A. K. (2013). Regulation of cholesterol homeostasis. Mol. Cell. Endocrinol. *368*, 1–16.

Veenstra, J.A., Agricola, H.J., and Sellami, A. (2008). Regulatory peptides in fruit fly midgut. Cell Tissue Res. *334*: 499-516.

Veenstra, J. A., and Ida, T. (2014). More Drosophila enteroendocrine peptides: Orcokinin B and the CCHamides 1 and 2. Cell Tissue Res. *357*, 607-621.

Vijendravarma, R.K., Narasimha, S., and Kawecki, T.J. (2013). Predatory cannibalism in *Drosophila melanogaster* larvae. Nature Comm. *4 :* 1789.

Voght, S.P., Fluegel, M.L., Andrews, L.A., and Pallanck, L.J. (2007). Drosophila NPC1b promotes an early step in sterol absorption from the midgut epithelium. Cell Metab. *5* : 195-205

Wang, B., and Tontonoz, P. (2018). Liver X receptors in lipid signaling and membrane homeostasis. Nature Reviews-Endocrinology. Doi:10.1038/s41574-018-0037-x.

Wang, M.L., Motamed, M., Infante, R.E., Abi-Mosleh, L., Kwon, H.J., Brown, M.S., and Goldstein, J.L. (2010). Identification of surface residues on Niemann-Pick C2 essential for hydrophobic handoff of cholesterol to NPC1 in lysosomes. Cell Metab. *12*: 166-173.

Wang, X., Sato, R., Brown, M.S., Hua, X., and Goldstein, J.L. (1994). SREBP-1, a membrane-bound transcription factor released by sterol-regulated proteolysis. Cell *77*, 53-62.

Weber, U., Eroglu, C. and Mlodzik, M. (2003). Phospholipid membrane composition affects EGF receptor and Notch signaling through effects on endocytosis during Drosophila development. Dev. Cell *5*, 559-570.

Wollmer, M.A. (2010). Cholesterol-related genes in Alzheimer's disease. Biochimica et Biophysica Acta. *1801*: 762-773.

Xiankun, Z., and Hou, S.X. (2015). Enteroendocrine cells are generated from stem cells through a distinct progenitor in the adult *Drosophila* posterior midgut. Development. *142:* 644-653.

Xie, C., Turley, S.D., Pentchev, P.G., and Dietschy, J.M. (1999). Cholesterol balance and metabolism in mice with loss of function of Niemann-Pick C protein. Am. J. Physiol. *276*: E336-344.

Ye, Y., Meyer, H.H., Rapoport, T.A. (2003). Function of the p97-Ufd1-Npl4 complex in retrotranslocation from the ER to the cytosol: dual recognition of nonubiquitinated polypeptide segments and polyubiquitin chains. J. Cell Biol. *162*, 71-84.

Zeng, X., Chauhan, C., and Hou, S.X. (2010). Characterization of midgut stem cell- and enteroblast-specific GAL4 lines in Drosophila. Genesis *48*, 607-611.

Zeng, X., and Hou, S.X. (2015). Enteroendocrine cells are generated from stem cells through a distinct progenitor in the adult *Drosophila* posterior midgut. *142:* 644-653.

BIOGRAPHY

Rebecca A. Obniski was born in 1989, and grew up in California, Maryland. She is a graduate of the College of William and Mary in Williamsburg, Virginia, where she studied music and chemistry, receiving dual Bachelor's degrees in May, 2011. As an undergraduate researcher she worked with William Starnes and Robert Pike to identify smoke suppressant and flame retardant additives for poly(vinyl) chloride. In 2010, she was invited by ExxonMobil Chemical to present a talk on her research at the annual conference of the SPI Flexible Vinyl Product Group in Chantilly, VA. She later went on to work with Matthew Wawersik on germ cell sex determination in *Drosophila,* and designed a budget fluorescent microscope that was adopted by James City County public school teachers.

In September, 2011, Rebecca began the Ph.D. program in Cellular, Molecular, and Developmental Biology and Biophysics at the Johns Hopkins University in Baltimore, MD. She worked as a teaching assistant for laboratory courses in Developmental Biology, Genetics, and Cancer Biology. Rebecca received a certificate from the Preparing Future Faculty Teaching Academy in 2016, and completed a Teaching as Research project studying the effect of pre-class videos on student perception and performance in a large lecture class. Rebecca completed three laboratory rotations during which she studied motor protein transport with Trina Schroer, the role of *Gas1* on enteric neuron migration with Chen-Ming Fan, and the effect of ethanol on blastocyst development with Yixian Zheng before joining Allan Spradling's laboratory in 2012.